Structure and Composition of Eisosomes in *Neurospora crassa*

Dissertation

in fulfillment of the requirements for the degree
Doctor rerum naturalium
of the Faculty of Mathematics and Natural Sciences at the
Christian Albrechts University of Kiel

Submitted by Qin Yang
Department of Botanical Genetics and Microbiology
Botanical Institute and Botanical Garden

Kiel, 2020

Referent: Prof. Dr. Frank Kempken
Korreferent: Prof. Dr. Thomas Roeder
Tag der mündlichen Prüfung: 03.06.2020
Zum Druck genehmigt: 03.06.2020

Der Dekan

Table of Contents

Summary

Diversely essential biochemical processes occur at the plasma membrane and require lateral separations. Eisosomes are protein containing microdomains at the plasma membrane in fungi and algae. They are spatially stable structures and are expected to have important function(s). However, the exact composition and the significant function(s) of eisosomes are still subjects of debate to date. This PhD thesis aims to improve the understanding about the composition, formation, and functions of eisosomes with the study in the model organism *Neurospora crassa*.

In this thesis, studies on eisosomes in *N. crassa* are systematically described and discussed: **(i)** Using the immunogold transmission electron microscope (TEM) and yeast complementary approaches, the eisosomal fundamental component LSP-1 was identified in *N. crassa* and was used as the eisosomal marker protein. **(ii)** The red fluorescent protein (RFP) tagged LSP-1 was employed to recognize the localization characteristics of eisosomes in *N. crassa*. By confocal laser scanning microscopy and fluorescence profile analysis, the distribution of eisosomes were found to be different in different type of cells of *N. crassa*. There was polar and restriction distribution of eisosomes in the hyphae germinating from macroconidia. **(iii)** After the liquid chromatography-tandem mass spectrometry (LC-MS) analysis of the LSP-1 coupled protein fragments, the initial composition of eisosomes in *N. crassa* was recognized and the structure of eisosomes was predicted. According to the eisosomal protein analysis, the multiple functions of eisosomes in *N. crassa* were proposed in the PhD thesis. **(iv)** In addition, eisosomes have stable fluorescence patterns similar to actin patches, combining with the data mentioned above, the relationships between eisosomes and the cytoskeleton were closely examined. It was first been described that the disassembly of microtubules or F-actins influences the distribution of eisosomes in *N. crassa*.

In conclusion, this PhD thesis systematically describes and discusses the composition and structure, functions, and the formation and regulation of eisosomes in the model fungus *N. crassa* for the first time. It bridges the studies of eisosomes in *N. crassa* and other fungi, and contributes to a better understanding about eisosomes.

Zusammenfassung

An der Plasmamembran finden diverse essentielle biochemische Prozesse statt, welche ein laterale Trennung benötigen. Eisosomen sind proteinhaltige Mikrodomänen an der Plasmamembran in Pilzen und Algen. Sie sind räumlich stabile Strukturen und man vermutet, dass sie wichtige Funktion(en) besitzen. Allerdings sind weder die exakte Zusammensetzung der Eisosomen noch ihre Funktion(en) zu diesem Zeitpunkt bekannt. Das Ziel dieser Arbeit ist es, das Verständnis der Zusammensetzung, Bildung und Funktionen von Eisosomen durch Studien an *Neurospora crassa* zu verbessern.

In dieser Arbeit werden die Untersuchungen an *N. crassa* systematisch beschrieben und diskutiert: **(i)** Mit Hilfe von Immunogold Transmissions-Elektronen-Mikroskopie (TEM) und Hefe-Komplementations-Analysen, wurde LSP-1 in *N. crassa* als eine fundamentale Eisosomen-Komponente identifiziert und als eisosomaler Protein-Marker verwendet. **(ii)** Ein an das rot fluoreszierende Protein (RFP) gekoppeltes LSP-1 wurde verwendet, um die Lokalisations-Charakteristika von Eisosomen in *N. crassa* zu analysieren. Unter Verwendung konfokaler Laser-Scanning Mikroskopie und einer Fluoreszenz-Profil-Analyse, wurde gezeigt, dass die Eisosomen eine unterschiedliche Verteilung in verschiedenen Zelltypen von *N. crassa* aufweisen. Eine polare und eingeschränkte Verteilung von Eisosomen wurde in aus Makrokonidien keimenden Hyphen beobachtet. **(iii)** Durch eine Flüssigchromatographie-Tandem Massen-Spektrometrie Analyse der an LSP-1 gebundenen Proteine wurde anfänglich die Komposition der Eisosomen in *N. crassa* identifiziert und damit die Struktur der Eisosomen vorhergesagt. Mit Hilfe dieser Analyse der eisosomalen Proteine wurden in dieser Arbeit mehrere Funktionen für Eisosomen in *N. crassa* vorgeschlagen. **(iv)** Zudem weisen Eisosomen ein stabiles Fluoreszenzmuster, ähnlich dem von Actin-Ansammlungen, auf. Aufgrund der zuvor erwähnten Daten wurden die Zusammenhänge zwischen Eisosomen und dem Zytoskelett näher untersucht. Es

wurde erstmalig beschrieben, dass der Abbau von Mikrotubuli oder F-Actin die Verteilung von Eisosomen in *N. crassa* beeinflussen.

Zusammenfassend werden in dieser Arbeit erstmalig systematisch die Zusammensetzung und Struktur, Funktionen, Bildung und die Regulierung von Eisosomen des Modelorganismuses *N. crassa* beschrieben und diskutiert. Sie verbindet Untersuchungen der Eisosomen in *N. crassa* mit denen in anderen Pilzen und trägt zum besseren Verständnis von Eisosomen bei.

General Introduction

1. What are Eisosomes?

The plasma membrane is composed of different subdomains including the membrane compartment PmaI (MCP), the membrane compartment TORC2 (MCT), and the membrane compartment Can1 (MCC) (Douglas & Konopka, 2014; Malínská *et al*, 2003). The MCC domains are immobile punctate patches at the plasma membrane (Douglas & Konopka, 2014), and eisosomes are complexes of cytoplasmic proteins that are associated with the MCC domains in fungi and algae (Douglas & Konopka, 2014; Walther *et al*, 2006; Kolláth-Leiβ & Kempken, 2017) (**Figure 1**).

Eisosomes were initially described in the yeast *Saccharomyces cerevisiae* (Moseley, 2018; Walther *et al*, 2006). The name comes from Greek, meaning portal body, because eisosomes were believed to mark sites of endocytosis at that time (Walther *et al*, 2006). Although later research has shown that they are distinct from sites of endocytosis (Douglas & Konopka, 2014; Grossmann *et al*, 2008; Seger *et al*, 2011), the name was retained. Earlier, furrow-like invaginations at the plasma membrane were already identified in *S. cerevisiae* (Moor & Mühlethaler, 1963). Nevertheless, the composition, formation, and functions of those invaginations were elusive for a long time (Kolláth-Leiβ & Kempken, 2017). Finally MCC/eisosomes were discovered to correspond with the invaginations (Young *et al*, 2002; Stradalova *et al*, 2009; Kolláth-Leiβ & Kempken, 2017; Moseley, 2018).

Eisosomes have a number of unique features including the stable distribution at the cell periphery (Douglas & Konopka, 2014), and the localization at the bottom of the MCC to stabilize unique invaginations (Malinsky & Opekarová, 2016) (**Figure 1**). The invaginations of MCC/eisosomes are about 50 nm deep and 300 nm long at the plasma membrane of *Saccharomyces cerevisiae* (Douglas & Konopka, 2014; Stradalova *et al*, 2009). In addition to proteins, eisosomes consist of membrane components: the core

proteins form half-pipe-shaped shells and bind to the plasma membrane (Moseley, 2018) (**Figure 1**). Eisosomes have been identified in fungi as well as in algae and in a ciliate (Douglas & Konopka, 2014; Walther *et al*, 2006; Kolláth-Leiβ & Kempken, 2017; Moseley, 2018), and in a typical *S. cerevisiae* cell there can be 20 – 50 eisosomes (Moseley, 2018). As large and complex domains that have spatially stable patterns at the cell periphery with distinct protein components (Athanasopoulos *et al*, 2015; Kabeche *et al*, 2011; Lacy *et al*, 2016; Babst, 2019; Moreira *et al*, 2009), they would be expected to have important function(s) matching these characteristics. According to the studies in *S. cerevisiae,* eisosomes are important for plasma membrane organization, sphingolipid homeostasis, and cell wall morphogenesis (Douglas & Konopka, 2014). However, the main function(s) of eisosomes remains unclear, and further studies are needed to solve the mystery. Currently, eisosomes have been examined in greatest detail in *S. cerevisiae* (Douglas & Konopka, 2014)*;* however*,* research on eisosomes in other fungi and algae should be intensified. The comparation of eisosomes in different species will help us understand their formation, structure, and functions.

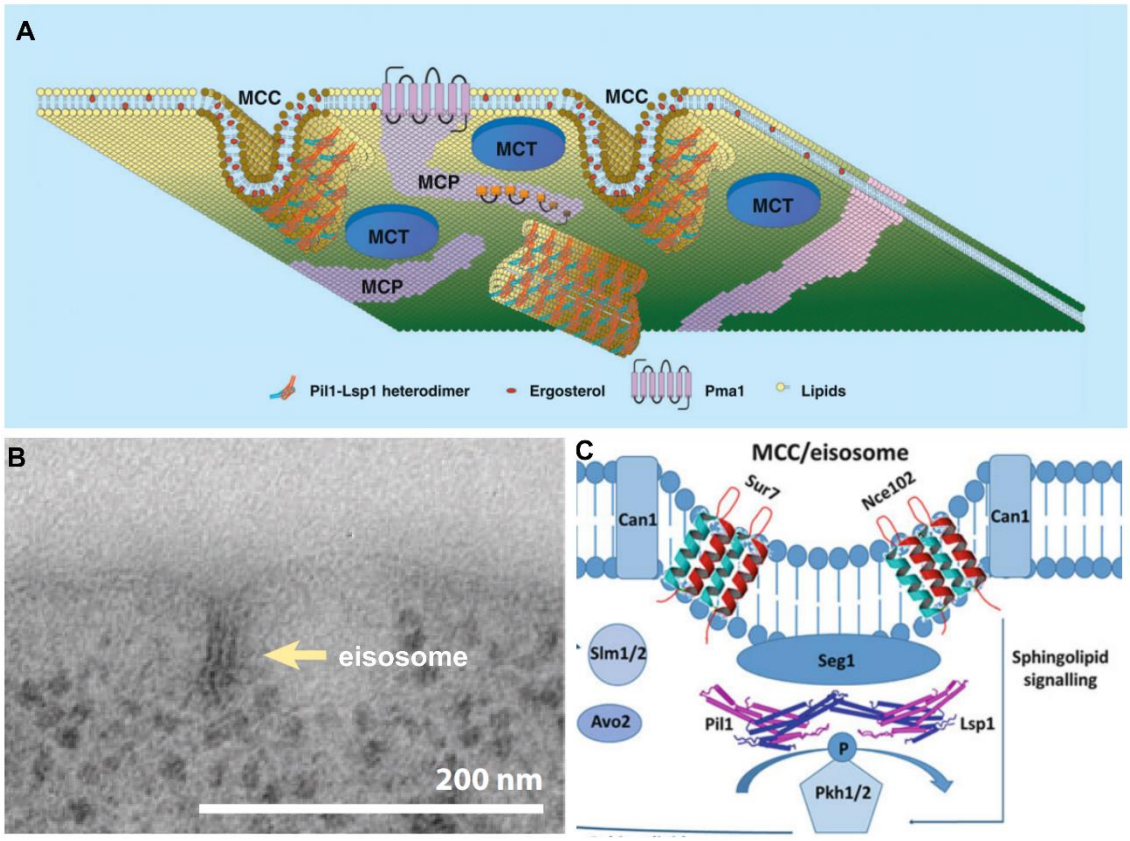

Figure 1. MCC/eisosome domains at the plasma membrane of *Saccharomyces cerevisiae*. A. Organization of the yeast plasma membrane into domains of distinct lipid and protein composition (Ziółkowska *et al*, 2012). **B.** Electron micrograph of an eisosome (Douglas & Konopka, 2014; Stradalova *et al*, 2009). **C.** Model for MCC/eisosome in *S. cerevisiae* (Kolláth-Leiß & Kempken, 2017).

2. Eisosome complexes in *Saccharomyces cerevisiae*

2.1 Composition of eisosomes

Eisosomes are complex structures and most of the eisosomal components were first identified in *S. cerevisiae.* To date, at least 19 proteins have been recognized to colocalize with eisosomes and some of them are key eisosomal components (**Table *1***).

Table 1 Selection of key eisosomal proteins in *Saccharomyces cerevisiae* (Douglas & Konopka, 2014)

Protein	Function	Copies
Pil1	BAR domain	115,000
Lsp1	BAR domain	104,000
Pkh1	Ser/Thr protein kinase	no data
Pkh2	Ser/Thr protein kinase	no data
Eis1	unknown	5,570
Slm1	BAR domain and PH domain	5,190
Slm2	BAR domain and PH domain	2,610
Seg1	unknown	no data
Mdg1	unknown	1,240
Ygr130c	unknown	10,300
Pst2	Similar to flavodoxin-like proteins	2,330
Rfs1	Similar to flavodoxin-like proteins	7,060
Ycp4	Similar to flavodoxin-like proteins	14,600
Msc3	unknown	131

Along with the recognition of eisosomes, Pil1 and Lsp1 were identified to be the primary components of eisosomes in *S. cerevisiae* (Walther *et al*, 2006) (**Figure 1**). These two proteins are paralogs, both carrying a BAR (Bin/Amphiphysin/Rvs) domain (Ziółkowska *et al*, 2011; Olivera-Couto *et al*, 2011; Murphy & Kim, 2012; Lacy *et al*, 2016). The BAR domain is a membrane-binding module. It is in banana shape and binds membranes electrostatically through its positively charged, concave surface (Zimmerberg & McLaughlin, 2004). The BAR domain has a significant function in the formation and detection of membrane curvatures, and plays a role in attracting other proteins (Zimmerberg & McLaughlin, 2004; Derkacheva *et al*, 2016). Proteins Pil1 and

Lsp1 form filamentous heterodimers and bind membranes through their BAR domains, then promote the formation of eisosomes (Douglas & Konopka, 2014). Eisosomes are composed of abundant of Pil1 and Lsp1 units (Olivera-Couto & Aguilar, 2012; Karotki *et al*, 2011). Pil1 has a banana-shaped central part (Malinsky & Opekarová, 2016; Olivera-Couto *et al*, 2011) and is significant for the formation of eisosomes (Zahumensky & Malinsky, 2019; Walther *et al*, 2006). It determines the size and location of eisosomes, and acts as the central regulator of eisosome biogenesis (Moreira *et al*, 2009). The absence of Pil1 prevents the formation of eisosomes and leads to a big decrease of the furrow-like structures at the plasma membrane (Stradalova *et al*, 2009; Zahumensky & Malinsky, 2019). It has been reported that eisosome assembly is regulated by phosphorylation of Pil1 (Ziółkowska *et al*, 2012; Walther *et al*, 2007). In addition, Pil1 was found to respond to the correct localization of Nce102 (Nce102 is a core component of MCC/eisosomes in *S. cerevisiae* (Kolláth-Leiβ & Kempken, 2017)) during the formation of MCC domains (Moreira *et al*, 2009). In contrast, the absence of Lsp1 did not have any obvious influence on the formation of eisosomes (Walther *et al*, 2006).

In addition to the primary eisosomal components, at least 17 additional eisosomal proteins have been identified to date in *S. cerevisiae* (Douglas & Konopka, 2014; Moseley, 2018; Douglas *et al*, 2011) (**Table *1***). Among them, Sur7 and Nce102 are two transmembrane proteins. They were found to colocalize with eisosome complexes at the furrow-like structure (Fröhlich *et al*, 2009; Walther *et al*, 2006; Moseley, 2018; Grossmann *et al*, 2007). Sur7 and the paralogous protein Fmp45, Pun1, and Ynl194c belong to a protein family of four membrane-spanning domains (tetraspanners) (Douglas *et al*, 2011). This protein family was identified to be associated with MCC/eisosome domains (Grossmann *et al*, 2008; Fröhlich *et al*, 2009; Alvarez *et al*, 2008), and the Sur7 protein was stably localized together with eisosomes (Douglas *et al*, 2011). Nce102 belongs to the other tetraspanner protein family which is included in

MCC/eisosome complexes (Grossmann *et al*, 2008; Fröhlich *et al*, 2009; Alvarez *et al*, 2008; Douglas *et al*, 2011). In contrast to Sur7, the Nce102 protein was not strictly localized at MCC/eisosomes. It has been detected away from MCC/eisosomes and to move into the invagination structures in response to sphingolipids (Douglas *et al*, 2011; Fröhlich *et al*, 2009). In addition to the primary eisosomal protein Pil1, Nce102 is another protein that is necessary for eisosome organization. The absence of Nce102 leads to an obvious reduction of eisosomes as well as the wider spacing of eisosome remnants (Kolláth-Leiβ & Kempken, 2017). The name of protein Seg1 is derived from "stability of eisosomes guaranteed" (Seger *et al*, 2011). It is another key component of eisosomes (Moreira *et al*, 2012). Studies have shown that Seg1 facilitates the assembly and controls the shapes of eisosomes (Moreira *et al*, 2012). Slm1 and Slm2 are eisosomal proteins that were predicted to contain a BAR domain (Olivera-Couto *et al*, 2011). They have been described to have roles in eisosome formation or stablility (Kamble *et al*, 2011; Douglas *et al*, 2011). The protein kinases Pkh1 and Pkh2 are another pair of eisosomal proteins (Walther *et al*, 2007; Luo *et al*, 2008). These two proteins have functions in diverse bioactivities and have been discovered to regulate the assembly and organization of eisosomes (Walther *et al*, 2007; Douglas *et al*, 2011).

2.2 Formation and regulation of eisosomes

The primary eisosomal proteins Pil1 and Lsp1 are significant for the assembly of eisosomes. They were estimated to have about 10^5 copies at each eisosome complex and to cover most of the surface area of the furrow-like structure (Douglas & Konopka, 2014; Ghaemmaghami *et al*, 2003). These two proteins were found to contain BAR-domains that could bind membranes and promote curvature for eisosome formation (Zimmerberg & McLaughlin, 2004; Douglas & Konopka, 2014). An important model of the formation of eisosomes is that Pil1 and Lsp1 assemble into filaments that align with the plasma membrane, and then promote the curvature to form the furrow-like

invaginations (Karotki *et al*, 2011). The foundation of this model is that Pil1 and Lsp1 have been recognized to be able to assemble into long filaments (Karotki *et al*, 2011). Additionally, Pil1 and Lsp1 were found to be regulated by Pkh1/2 through phosphorylation (Walther *et al*, 2007; Zhang *et al*, 2004). It has been proposed that the eisosomal protein Nce102 could be stimulated to colocalize with MCC/eisosomes by an elevated level of sphingolipids, and then prevents Pkh1/2 kinase from phosphorylating Pil1 and Lsp1, which promotes the formation of eisosomes (Fröhlich *et al*, 2009). Pil1 has been found to support formation of eisosomes, because eisosomal proteins cannot localize properly when Pil1 is absent (Grossmann *et al*, 2008; Loibl *et al*, 2010; Aguilar *et al*, 2010; Walther *et al*, 2006). The association of membrane and Pil1 is thought to be the limiting step during the formation of eisosomes (Douglas & Konopka, 2014). Nevertheless, other controls or regulations of eisosome assembly could presumably exist, because Slm1 and Slm2 have been discovered to be important for the formation or stability of the furrows (Kamble *et al*, 2011; Douglas *et al*, 2011), and Seg1 has been identified to precede Pil1 during the assembly of eisosomes (Moreira *et al*, 2012). Determining the detailed mechanisms/pathways for the formation of eisosomes will require further study.

2.3 Function(s) of eisosomes

Although the key components have been identified, the cellular functions of eisosomes remain unclear. It is intriguing that eisosomes have been found to play roles in a wide range of biological processes (Olivera-Couto & Aguilar, 2012; Bartlett *et al*, 2015); however, the massive disorganization of eisosomes caused by the deletion of one eisosomal protein does not lead to any obvious decrease in cellular fitness or growth fitness in *S. cerevisiae* (Moseley, 2018; Olivera-Couto & Aguilar, 2012). Currently, the discussion about the function(s) of eisosomes is mainly associated with the following aspects.

First, eisosomes have been identified to have functions for plasma membrane organization (Douglas *et al*, 2011; Douglas & Konopka, 2014). The deletion of Pil1 and Lsp1 caused broad defects in plasma membrane organization as well as in the cell wall (Walther *et al*, 2006; Foderaro *et al*, 2017). In addition, eisosome complexes appear to protect plasma membrane proteins from endocytosis, and to act as scaffolds for recruiting proteins to the furrow-like structures (Grossmann *et al*, 2008; Foderaro *et al*, 2017).

Second, eisosomes have been associated with a wide range of stress responses. For example, the eisosome components Pkh1/2 kinases regulate two important protein kinases,Pkc1 and Sch9, which affect the cell's response to heat stress (Douglas & Konopka, 2014). Eisosome domains also appear to be associated with responses to osmotic shock and dehydration (Douglas *et al*, 2011). The redistribution of the eisosomal protein Sur7 under hyperosmotic conditions suggests that eisosome reorganization is involved in the resistance process (Dupont *et al*, 2010). What is more, it has been recognized that the deletion of Sur7 leads to defects in osmotic stress response (Yoshikawa *et al*, 2009; Young *et al*, 2002).

In addition, eisosomes have been described to have functions in maintaining sphingolipid homeostasis, organizing proton flux, and cell signaling (Douglas & Konopka, 2014). Unfortunately the evidence supporting many of the proposed functions remains indirect or tenuous. More work is needed to gather the data that would answer the question posed at the beginning of this section.

3. Eisosomes in other fungi

After the discovery of eisosomes in *S. cerevisiae*, studies on other fungi such as *Aspergillus nidulans* (Vangelatos *et al*, 2010; Athanasopoulos *et al*, 2013)*, Candida albicans* (Douglas *et al*, 2013; Wang *et al*, 2016)*, Beauveria bassiana* (Zhang *et al*,

2017), and so on were performed and published. Although only a few eisosomal proteins have been discovered in these species, it appears that the eisosome composition exhibits differences within the analyzed fungi (Scazzocchio *et al*, 2011). The exact composition, formation and regulation mechanism, and functions of eisosomes still remain subjects of debate as too few critical data have been gathered thus far.

Eisosome domains are composed of fewer components in *Schizosaccharomyces pombe.* It has been reported that Pil1, Nce102, and Seg1 are eisosome associated proteins (Moreira *et al*, 2012; Kabeche *et al*, 2011). Not all orthologs of eisosomal proteins, e.g. Sur7 and Sim1, are localized at the invaginations (Kabeche *et al*, 2011). One explanation for Sur7 localization outside of eisosomes is that there is no actual ortholog of Sur7 in *S. pombe,* as the protein called Sur7 is more closely related to the eisosomal protein Pun1 of *S. cerevisiae* (Foderaro *et al*, 2017; Douglas & Konopka, 2014). Another unique feature is that *S. pombe* cells have longer eisosome complexes. Studies have shown that the eisosome patches at the plasma membrane were about 1 μm in *S. pombe* (Kabeche *et al*, 2011), which is about five times longer than the structures in *S. cerevisiae.* As for the function(s) of eisosomes in *S. pombe*, the deletion of Pil1 did not obviously cause any novel morphological phenotype (Kabeche *et al*, 2011). This reveals again that determining the function(s) of eisosomes is full of challenges.

Lsp1, Pil1, Sur7, Slm1, Seg1, and Fmp45 are components of eisosome complexes in *C. albicans* (Wang *et al*, 2011; Reijnst *et al*, 2011; Bernardo & Lee, 2010; Alvarez *et al*, 2008). The composition of eisosomes in *C. albicans* is similar to that of *S. cerevisiae,* and deletion of Sur7 does not influence colocalization of Lsp1 with eisosomes (Douglas & Konopka, 2014). Nevertheless, the functions and localizations of eisosomal proteins show differences in *C. albicans* compared to those in *S. cerevisiae.* First, the eisosomal protein Sur7 has more important functional roles than in *S. cerevisiae* (Alvarez *et al*,

2008). The absence of Sur7 leads to a strong virulence defect for infection (Douglas *et al*, 2012). It appears that Sur7 is necessary for the formation of hyphal filaments, and these hyphal filaments will penetrate host tissues during infections (Douglas *et al*, 2012; Bernardo & Lee, 2010; Alvarez *et al*, 2008; Wang *et al*, 2011). Additionally, the loss of Sur7 appears to make the fungus more sensitive to a wide range of stresses, such as high growth temperature and exposure to copper (Douglas *et al*, 2012). Sur7 is also associated with cell wall synthesis, because the deletion of this protein leads to long invaginations of the cell wall during growth (Alvarez *et al*, 2008), and to weaker cell walls (Wang *et al*, 2011). A cell wall composition analysis suggested that the defects were caused by the reduction of β-glucan (the major component of the cell wall) (Wang *et al*, 2011). This suggests that Sur7 plays a role in the β-glucan synthesis. Second, the localization of the eisosomal protein Nce102 is also distinct. It has been identified to partially localize at eisosome complexes during log phase, but to tightly congregate at the furrow structures during stationary phase in *C. albicans* (Douglas *et al*, 2013).

PilA, PilB, and SurG have been identified to be the components of eisosomes in *A. nidulans* (Vangelatos *et al*, 2010). PilA and PilB are two homologues of the *S. cerevisiae* Pil1/Lsp1, and they have been discovered to be the primary components of eisosomes in the filamentous fungal (Vangelatos *et al*, 2010). SurG is a strict Sur7 orthologue in *A. nidulans* (Vangelatos *et al*, 2010). In addition, the Nce102 homologue in *A. nidulans* is colocalized with eisosomes and has a crucial function in the density of PilA foci at the spore body of germlings (Athanasopoulos *et al*, 2015). The assembly and development of eisosome complexes differ between *A. nidulans* and *S. cerevisiae* (Scazzocchio *et al*, 2011), and the patches of eisosomes are different as well (Vangelatos *et al*, 2010). Eisosomes have packed punctate patches in *A. nidulans* conidiospores whereas they formed obvious distinct patches in *S. cerevisiae.* The intriguing aspect is that eisosomes have strict polar formations and distributions. For

example, the three core eisosomal proteins are expressed in mature ascospores but not in early ascospores (Athanasopoulos *et al*, 2013), and eisosomes do not localize in mycelia (Kolláth-Leiβ & Kempken, 2017). Furthermore, the core components of eisosomes have their distributional restrictions during different developmental stages. In the geminating hyphae of ascospores, eisosomes were found to be composed only of PilA, while PilB was diffused in the cytoplasm and SurG was localized in vacuoles (Athanasopoulos *et al*, 2013). This strongly suggests that the spatial formation/location of eisosomes is regulated. Nevertheless, the mechanism behind the regulation is poorly understood, even in *S. cerevisiae.* Currently there is no significant data on the function(s) of eisosomes. Deletion of each of the core eisosomal proteins did not lead to any clear modified growth phenotype (Vangelatos *et al*, 2010).

PilA and PilB have been found to be eisosomal proteins in *B. bassiana* (Zhang *et al*, 2017). They are homologous with the yeast eisosomal components Pil1/Lsp1 (Zhang *et al*, 2017). Eisosomes were found to exist at the periphery of hyphae and to form stable punctate patches (Zhang *et al*, 2017). The deletion of PilA, or PilB, or both together leads to a decrease of cell wall components in conidia. The β-GlcNAc and sialic acids decreased by 14% in the Δ*pil1A* mutant and by 25% in double mutant (Zhang *et al*, 2017). In addition, the absence of the eisosomal proteins leads to thicker cell walls in hyphae (Zhang *et al*, 2017). It appears that eisosomes have significant functions in secretion of proteases and pathogenicity, because the absence of these eisosomal proteins, singly or together, reduces the secretion of proteases for cuticle degradation, and leads to a loss of pathogenicity (Zhang *et al*, 2017).

The number of eisosomal proteins are reduced in *Ashbya gossypii*. The homologues of *S. cerevisiae* eisosome components Ycp4, Pst1, and Rfs1 (**Table *1***) were not found in *A. gossypii* (Seger *et al*, 2011). The orthologs of Pil1 and Lsp1, Slm1/2, Pkh1/2, Nce102, and Seg1 are all eisosomal proteins in *A. gossypii* (Seger *et al*, 2011; Douglas & Konopka, 2014). Among those proteins, Pil1 and Lsp1 are conserved, but the twin-

eisosomal-components Slm1 and Slm2, and Pkh1 and Pkh2 are each encoded by a single gene in *A. gossypii* (Seger *et al*, 2011). In contrast to *S. cerevisiae,* Pil1 is required for polarized growth, because the absence of Pil1 leads to obvious misshapen hyphal tips (Seger *et al*, 2011). Additionally, the deletion of Seg1 decreased the stability of eisosomes in hyphae (Seger *et al*, 2011). In contrast, the deletion of Nce102 did not have any clear influence on the formation and stability of eisosomes (Seger *et al*, 2011).

4. The model organism *Neurospora crassa*

Neurospora is a genus of ascomycete fungi. To date, 43 species have been recognized. Among them, 28 are homothallic, 13 are heterothallic, and two are pseudohomothallic (Roche *et al*, 2014). *Neurospora crassa* was first discovered in bakeries in France as an orange bread mold that produced luxuriant and conspicuous spores (Riquelme & Martínez-Núñez, 2016; Davis & Perkins, 2002). After Payen first described it as a bakeries contaminant (Galagan *et al*, 2003; Roche *et al*, 2014), it remained relatively obscure until about 80 years later, when Dodge began to develop it as an experimental organism (Shear & Dodge, 1927). In the 1940s Beadle and Tatum proposed the famous 'one-gene-one-enzyme' hypothesis based on their study of the linkage between genes and proteins in *N. crassa* (Beadle & Tatum, 1941; Galagan *et al*, 2003; Aramayo & Selker, 2013). The *N crassa* genome is somewhat larger than 40 megabases (Mb) containing about 10,082 protein-coding genes (Galagan *et al*, 2003). The *N. crassa* genome sequence was published in 2003, which makes it very convenient for genetic, biochemical, developmental, and subcellular studies (Galagan *et al*, 2003).

Neurospora has been well-established and studied as a model organism for genetics, biochemistry and molecular biology (Roche *et al*, 2014; Galagan *et al*, 2003). As a

multicellular filamentous fungus, *N. crassa* has sexual and asexual life cycles with a range of cell types (**Figure 2**). Currently there are at least 28 cell types having distinct recognized morphologies (Bistis *et al*, 2003). Remarkable differences between different cell types or different developmental stages have been reported for growth and intracellular organization (Riquelme & Martínez-Núñez, 2016). The vast variety of cell morphologies and the complex development stages make it an excellent model for multicellular microbes. For example, *N. crassa* exceeds the unicellular *Saccharomyces* as a model on cell differentiation, cellular developmental studies, polarized cell growth, differentiation and morphogenesis of structures, and many other aspects of eukaryotic biology (Galagan *et al*, 2003; Seale, 1973; Riquelme *et al*, 2011; Roche *et al*, 2014). In my thesis, the different features of eisosomes in different cell types during the different developmental stages of *N. crassa* are described and discussed. In addition, in *N. crassa*, there are many characteristic biological activities including hyphal fusion (Fleißner *et al*, 2008), and the establishment and maintenance of hyphal polarity (Riquelme *et al*, 2011), which are difficult or impossible to examine in unicellular yeasts. These considerations make *N. crassa* a better-suited model system for in-depth studies on the composition and function(s) of eisosomes.

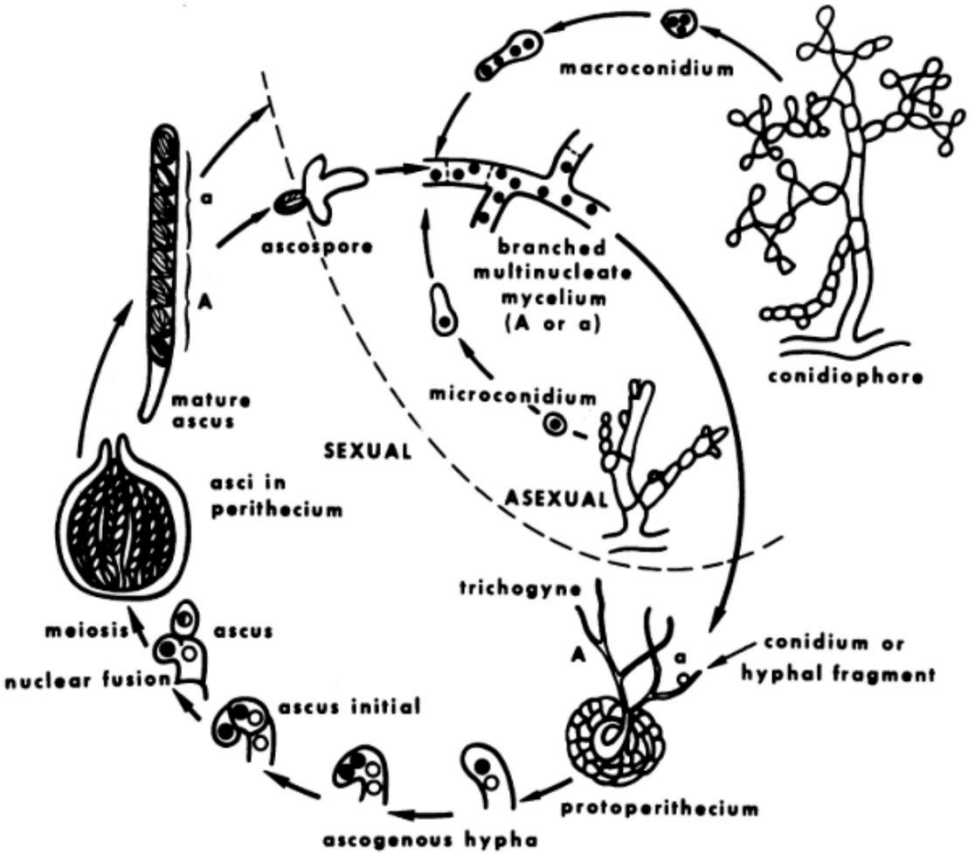

Figure 2. The life cycles in *N. crassa* (Seale, 1973)**.**

5. Aims and Outline of the Thesis

The plasma membrane is one of the most complicated components of a cell (Shi *et al*, 2018). It has various essential roles such as communications with surrounding matrix, cell adhesion and fusion, and material transport (Shi *et al*, 2018; Busto & Wedlich-Söldner, 2019; Li *et al*, 2016; Lombard, 2014; Goñi, 2014). In general, the plasma membrane organizes its lipid and protein components into lateral domains (Simons, 2016; Busto *et al*, 2018). Many plasma-membrane-associated biological processes require these spatiotemporal separations (Honigmann & Pralle, 2016). Nevertheless, the relationships between the domains and the functions at the plasma membrane remain unclear (Busto *et al*, 2018). We still lack a quantitative understanding of the molecular interactions between membrane domains (Honigmann & Pralle, 2016). The

studies on the functional domains and protein scaffolds at the plasma membrane are of increasing significance. Presently, eisosomes are known to be large protein complexes that are associated with the integral membrane area known as MCC (Zahumensky & Malinsky, 2019; Strádalová *et al*, 2009; Douglas & Konopka, 2014; Douglas *et al*, 2011). However, the composition of the eisosome is still poorly understood in *N. crassa.* Nor has the function(s) of eisosomes been reported in *N. crassa.* To date, only two proteins, the bud emergency 46 (BEM46) and the neutral amino acid transporter MTR, were discovered to co-localize with eisosomes in *N. crassa* (Kollath-Leiß *et al*, 2014; Kolláth-Leiβ & Kempken, 2017). Protein BEM46 is an $\alpha\beta$-hydrolase and is evolutionarily conserved in the eukaryotic kingdom (Mercker *et al*, 2009). It plays roles in type-specific hyphal polarity maintenance and in tryptophan-derived auxin pathway in *N. crassa* (Mercker *et al*, 2009; Kollath-Leiß *et al*, 2014). MTR is a putative tryptophan transporter in *N. crassa* (Kollath-Leiß *et al*, 2014). It is a homologue of the eisosomal localized transporter in *S. cerevisiae* (Kolláth-Leiβ & Kempken, 2017). As an important model organism, it would be a significant advance to study the composition, function, and formation of eisosomes in *N. crass.* With the comparation of eisosomes in different model organisms, we could get a better understanding and deepen our knowledge about eisosomes, as well as the connections between the domains and the functions at the plasma membrane.

Therefore, the aims of this doctoral thesis are to:

(1) identify the distribution and formation of eisosomes in different types of cells in *N. crassa*, in order to discover the general and unique characteristics of eisosomes;

(2) identify the composition of eisosomes and analyze the function(s) of eisosomes in *N. crassa*, in order to understand the role(s) of eisosomes in a living cell and hopefully to provide insights for applied research in the future; and

(3) study the regulation mechanism(s) of the formation and localization of eisosomes, in order to identify the interaction between eisosomes and other cellular structures or processes.

In **Chapter I**, LSP-1 protein in *N. crassa* is confirmed to be the core component of eisosomes. LSP-1 was then used as a marker protein of eisosome domains, which provided a base for further studies in the thesis.

Chapter II is organized as a research article. In this chapter, we systematically describe the polar distributions of eisosomes in *N. crassa*, discusses the different localization features of eisosomes in different cell types and different developmental stages. The observation that eisosomes were absent from the tips of hyphae originating from macroconidia but were located at the tips of hyphae emerging from ascospores in *N. crassa* gives new insights into cell type recognition at the subcellular scale.

Chapter III is generated as the second research article in this thesis. In this section, we discuss the composition, structure, and function(s) of eisosomes in *N. crassa*. We identified six eisosomal core components and some proteins that appear to be spatially associated with eisosomes in *N. crassa*. The structural and functional characteristics of the core eisosomal components in *N. crassa* are described. Eisosomes were recognized to have multiple roles in *N. crassa*. In addition, a model of eisosomal structure in *N. crassa* was constructed. In *N. crassa*, this is the first time that the composition and functions were systematically described.

Chapter IV is formed as a research report in the thesis. In this section, we describe our discovery that the cytoskeleton influences the formation and distribution of eisosomes in *N. crassa*. We have found that the distribution characteristics and fluorescence patterns of eisosomes were similar to those of the cytoskeleton, and that eisosomes were functionally associated with actin organization in *N. crassa*. We

separately inhibited microtubule and F-actin to identify the relationships between them and eisosomes. In *N. crassa,* microtubules influence the assembly and the distribution of eisosomes, and F-actins influence the localization of eisosomes. It was novel to find that the intact cytoskeleton is necessary for the normal localization of eisosomes.

References

Aguilar PS, Fröhlich F, Rehman M, Shales M, Ulitsky I, Olivera-Couto A, Braberg H, Shamir R, Walter P, Mann M, Ejsing CS, Krogan NJ & Walther TC (2010) A plasma-membrane E-MAP reveals links of the eisosome with sphingolipid metabolism and endosomal trafficking. *Nat. Struct. Mol. Biol.* **17:** 901–908

Alvarez FJ, Douglas LM, Rosebrock A & Konopka JB (2008) The Sur7 protein regulates plasma membrane organization and prevents intracellular cell wall growth in *Candida albicans*. **19:** 5214–5225

Aramayo R & Selker EU (2013) *Neurospora crassa*, a model system for epigenetics research. *Cold Spring Harb. Perspect. Biol.* **5:** a017921–a017921

Athanasopoulos A, Boleti H, Scazzocchio C & Sophianopoulou V (2013) Eisosome distribution and localization in the meiotic progeny of *Aspergillus nidulans*. *Fungal Genet. Biol.* **53:** 84–96

Athanasopoulos A, Gournas C, Amillis S & Sophianopoulou V (2015) Characterization of AnNce102 and its role in eisosome stability and sphingolipid biosynthesis. *Sci. Rep.* **5:** 15200

Babst M (2019) Eisosomes at the intersection of TORC1 and TORC2 regulation. *Traffic*. **20:** 543–551

Bartlett K, Gadila SKG, Tenay B, Mcdermott H, Alcox B & Kim K (2015) TORC2 and eisosomes are spatially interdependent, requiring optimal level of phosphatidylinositol 4, 5-bisphosphate for their integrity. *J. Biosci.* **40:** 299–311

Beadle GW & Tatum EL (1941) Genetic control of biochemical reactions in *Neurospora*. *Proc. Natl. Acad. Sci.* **27:** 499–506

Bernardo SM & Lee SA (2010) *Candida albicans* SUR7 contributes to secretion, biofilm formation, and macrophage killing. *BMC Microbiol.* **10:** 133

Bistis GN, Perkins DD & Read ND (2003) Different cell types in *Neurospora crassa*. *Fungal Genet. Rep.* **50:** 17–19

Busto J V., Elting A, Haase D, Spira F, Kuhlman J, Schäfer-Herte M & Wedlich-Söldner R (2018) Lateral plasma membrane compartmentalization links protein function and turnover. *EMBO J.***:** e99473

Busto J V. & Wedlich-Söldner R (2019) Integration through separation - The role of lateral membrane segregation in nutrient uptake. *Front. Cell Dev. Biol.* **7:** 1–6

Davis RH & Perkins DD (2002) *Neurospora*: a model of model microbes. *Nat. Rev. Genet.* **3:** 397–403

Derkacheva NI, Polevova S V & Sokolova OS (2016) The role of BAR domain proteins in the regulation of membrane dynamics. **8:** 60–69

Douglas LM & Konopka JB (2014) Fungal membrane organization: the eisosome concept. *Annu. Rev. Microbiol.* **68:** 377–393

Douglas LM, Wang HX, Keppler-ross S, Dean N & Konopka JB (2012) Sur7 promotes plasma membrane organization and is needed for resistance to stressful conditions and to the invasive growth and virulence of *Candida albicans*. *MBio* **3:** 1–12

Douglas LM, Wang HX & Konopka JB (2013) The MARVEL domain protein Nce102 regulates actin organization and invasive growth of *Candida*. *MBio* **4:** 1–12

Douglas LM, Wang HX, Li L & Konopka JB (2011) Membrane compartment occupied by Can1 (MCC) and eisosome subdomains of the fungal plasma membrane. *Membranes (Basel).* **1:** 394–411

Dupont S, Beney L, Ritt JF, Lherminier J & Gervais P (2010) Lateral reorganization of plasma membrane is involved in the yeast resistance to severe dehydration. *Biochim. Biophys. Acta - Biomembr.* **1798:** 975–985

Fleißner A, Simonin AR & Glass NL (2008) Cell fusion in the filamentous fungus, *Neurospora crassa*. *Methods Mol. Biol.* **475:** 21–38

Foderaro JE, Douglas LM & Konopka JB (2017) MCC / eisosomes regulate cell wall synthesis and stress responses in fungi. *J. Fungi* **1:** 1–18

Fröhlich F, Moreira K, Aguilar PS, Hubner NC, Mann M, Walter P & Walther TC (2009) A genome-wide screen for genes affecting eisosomes reveals Nce102 function in sphingolipid signaling. *J. Cell Biol.* **185:** 1227–1242

Galagan JE, Calvo SE, Borkovich KA, Selker EU, Read NO, Jaffe D, FitzHugh W, Ma LJ, Smirnov S, Purcell S, Rehman B, Elkins T, Engels R, Wang S, Nielsen CB, Butler J, Endrizzi M, Qui D, Ianakiev P, Bell-Pedersen D, et al (2003) The genome sequence of the filamentous fungus *Neurospora crassa*. *Nature* **422:** 859–868

Ghaemmaghami S, Huh WK, Bower K, Howson RW, Belle A, Dephoure N, O'Shea EK & Weissman JS (2003) Global analysis of protein expression in yeast. *Nature* **425:** 737–741

Goñi FM (2014) The basic structure and dynamics of cell membranes: An update of the Singer–Nicolson model. *Biochim. Biophys. Acta - Biomembr.* **1838:** 1467–1476

Grossmann G, Malinsky J, Stahlschmidt W, Loibl M, Weig-Meckl I, Frommer WB, Opekarová M & Tanner W (2008) Plasma membrane microdomains regulate turnover of transport proteins in yeast. *J. Cell Biol.* **183:** 1075–1088

Grossmann G, Opekarová M, Malinsky J, Weig-Meckl I & Tanner W (2007) Membrane potential governs lateral segregation of plasma membrane proteins and lipids in yeast. *EMBO J.* **26:** 1–8

Honigmann A & Pralle A (2016) Compartmentalization of the cell membrane. *J. Mol. Biol.* **428:** 4739–4748

Kabeche R, Baldissard S, Hammond J, Howard L & Moseley JB (2011) The filament-forming protein Pil1 assembles linear eisosomes in fission yeast. *Mol. Biol. Cell* **22:** 4059–4067

Kamble C, Jain S, Murphy E & Kim K (2011) Requirements of Slm proteins for proper eisosome organization, endocytic trafficking and recycling in the yeast Saccharomyces cerevisiae. *J. Biosci.* **36:** 79–96

Karotki L, Huiskonen JT, Stefan CJ, Ziółkowska NE, Roth R, Surma MA, Krogan NJ, Emr SD, Heuser J, Grünewald K & Walther TC (2011) Eisosome proteins assemble into a membrane scaffold. *J. Cell Biol.* **195:** 889–902

Kollath-Leiß K, Bönniger C, Sardar P & Kempken F (2014) BEM46 shows eisosomal localization and association with tryptophan-derived auxin pathway in *Neurospora crassa*. *Eukaryot. Cell.* **13:** 1051–1063

Kolláth-Leiß K & Kempken F (2017) The fungal MCC / eisosome complex : an unfolding story. In *The Mycota XV*, Anke T & Schüffler A (eds) pp 119–130. Springer International Publishing AG 2018

Lacy MM, Baddeley D & Berro J (2017) Single-molecule imaging of the BAR domain protein Pil1p reveals filament-end dynamics. *Mol Biol Cell.* **17:** *2251*–2259

Li ZL, Ding HM & Ma YQ (2016) Interaction of peptides with cell membranes: Insights from molecular modeling. *J. Phys. Condens. Matter* **28:** 83001

Loibl M, Grossmann G, Stradalova V, Klingl A, Rachel R, Tanner W, Malinsky J & Opekarová M (2010) C terminus of Nce 102 determines the structure and function of microdomains in the *Saccharomyces cerevisiae* plasma membrane. *Eukaryot. Cell* **9:** 1184–1192

Lombard J (2014) Once upon a time the cell membranes: 175 years of cell boundary research. *Biol. Direct* **9:** 32

Luo G, Gruhler A, Liu Y, Jensen ON & Dickson RC (2008) The sphingolipid long-chain base-Pkh1/2-Ypk1/2 signaling pathway regulates eisosome assembly and turnover. *J. Biol. Chem.* **283:** 10433–10444

Malínská K, Malínský J, Opekarová M & Tanner W (2003) Visualization of protein compartmentation within the plasma membrane of living yeast cells. *Mol. Biol. Cell* **14:** 4427–4436

Malinsky J & Opekarová M (2016) New insight into the roles of membrane microdomains in physiological activities of fungal cells. In *International Review of Cell and Molecular Biology* pp 119–180. Academic Press

Mercker M, Kollath-Leiß K, Allgaier S, Weiland N & Kempken F (2009) The BEM46-like protein appears to be essential for hyphal development upon ascospore germination in *Neurospora crassa* and is targeted to the endoplasmic reticulum. *Curr. Genet.* **55:** 151–161

Moor H & Mühlethaler K (1963) Fine structure frozen-etched in yeast cells. *J Cell Biol* **1:** 609–628

Moreira KE, Schuck S, Schrul B, Fröhlich F, Moseley JB, Walther TC & Walter P (2012) Seg 1 controls eisosome assembly and shape. *J. Cell Biol.* **198:** 405–420

Moreira KE, Walther TC, Aguilar PS & Walter P (2009) Pil1 controls eisosome biogenesis. *Mol. Biol. Cell* **20:** 809–818

Moseley JB (2018) Eisosomes. *Curr. Biol.* **28:** R376–R378

Murphy ER & Kim KT (2012) Insights into eisosome assembly and organization. *J. Biosci.* **37:** 295–300

Olivera-Couto A & Aguilar PS (2012) Eisosomes and plasma membrane organization. *Mol. Genet. Genomics* **287:** 607–620

Olivera-Couto A, Grana M, Harispe L & Aguilar PS (2011) The eisosome core is composed of BAR domain proteins. *Mol. Biol. Cell* **22:** 2360–2372

Reijnst P, Walther A & Wendland J (2011) Dual-colour fluorescence microscopy using yEmCherry-/GFP-tagging of eisosome components Pil1and Lsp1 in *Candida albicans*. *Yeast.* **28:** 331–338

Riquelme M & Martínez-Núñez L (2016) Hyphal ontogeny in *Neurospora crassa*: a model organism for all seasons. *F1000Research* **5:** 2801

Riquelme M, Yarden O, Bartnicki-Garcia S, Bowman B, Castro-Longoria E, Free SJ, Fleißner A, Freitag M, Lew RR, Mouriño-Pérez R, Plamann M, Rasmussen C, Richthammer C, Roberson RW, Sanchez-Leon E, Seiler S & Watters MK (2011) Architecture and development of the *Neurospora crassa* hypha - a model cell for polarized growth. *Fungal Biol.* **115:** 446–474

Roche CM, Loros JJ, McCluskey K & Glass NL (2014) *Neurospora crassa*: Looking back and looking forward at a model microbe. *Am. J. Bot.* **101:** 2022–2035

Scazzocchio C, Vangelatos I & Sophianopoulou V (2011) Eisosomes and membrane compartments in the ascomycetes : A view from *Aspergillus nidulans*. **4:** 64–68

Seale T (1973) Life cycle of *Neurospora crassa* viewed by scanning electron microscopy. *J. Bacteriol.* **113:** 1015–1025

Seger S, Rischatsch R & Philippsen P (2011) Formation and stability of eisosomes in the filamentous fungus *Ashbya gossypii*. *J. Cell Sci.* **124:** 1629–1634

Shear CL & Dodge BO (1927) Life histories and heterothallism of the red bread-mold fungi of the *Monilia sitophila* group. *J. Agric. Res.* **34:** 1019–1042

Shi Y, Cai M, Zhou L & Wang H (2018) The structure and function of cell membranes studied by atomic force microscopy. *Semin. Cell Dev. Biol.* **73:** 31–44

Simons K (2016) Cell membranes: A subjective perspective. *Biochim. Biophys. Acta - Biomembr.* **1858:** 2569–2572

Stradalova V, Stahlschmidt W, Grossmann G, Blazikova M, Rachel R, Tanner W & Malinsky J (2009) Furrow-like invaginations of the yeast plasma membrane correspond to membrane compartment of Can1. *J. Cell Sci.* **122:** 2887–2894

Strádalová V, Stahlschmidt W, Grossmann G, Blazíková M, Rachel R, Tanner W & Malinsky J (2009) Furrow-like invaginations of the yeast plasma membrane correspond to membrane compartment of Can1. *J. Cell Sci.* **122:** 2887–2894

Vangelatos I, Roumelioti K, Gournas C, Suarez T, Scazzocchio C & Sophianopoulou V (2010) Eisosome organization in the filamentous ascomycete *Aspergillus nidulans*. *Eukaryot. Cell* **9:** 1441–1454

Walther TC, Aguilar PS, Fröhlich F, Chu F, Moreira K, Burlingame AL & Walter P (2007) Pkh-kinases control eisosome assembly and organization. *EMBO J.* **26:** 4946–4955

Walther TC, Brickner JH, Aguilar PS, Bernales S & Walter P (2006) Eisosomes mark static sites of endocytosis. *Nature* **439:** 998–1003

Wang HX, Douglas LM, Aimanianda V, Latgé JP & Konopka JB (2011) The *Candida albicans* Sur7 protein is needed for proper synthesis of the fibrillar component of the cell wall that confers strength. *Eukaryot. Cell* **10:** 72–80

Wang HX, Douglas LM, Veselá P, Rachel R, Malinsky J & Konopka JB (2016) Eisosomes promote the ability of Sur7 to regulate plasma membrane organization in *Candida albicans*. *Mol Biol Cell* ***10*****:** 1663–1675

Yoshikawa K, Tanaka T, Furusawa C, Nagahisa K, Hirasawa T & Shimizu H (2009) Comprehensive phenotypic analysis for identification of genes affecting growth under ethanol stress in *Saccharomyces cerevisiae*. *FEMS Yeast Res.* **9:** 32–44

Young ME, Karpova TS, Brügger B, Moschenross DM, Wang GK, Schneiter R, Wieland FT & Cooper JA (2002) The Sur7p family defines novel cortical domains in *Saccharomyces cerevisiae*, affects sphingolipid metabolism, and is involved in sporulation. *Mol. Cell. Biol.* **22:** 927–934

Zahumensky J & Malinsky J (2019) Role of MCC/Eisosome in fungal lipid homeostasis. *Biomolecules* **9:** 305

Zhang LB, Tang L, Ying SH & Feng MG (2017) Two eisosome proteins play opposite roles in autophagic control and sustain cell integrity, function and pathogenicity in *Beauveria bassiana*. *Environ. Microbiol.* **19:** 2037–2052

Zhang X, Lester RL & Dickson RC (2004) Pil1p and Lsp1p negatively regulate the 3-phosphoinositide-dependent protein kinase-like kinase Pkh1p and downstream signaling pathways Pkc1p and Ypk1p. *J. Biol. Chem.* **279:** 22030–22038

Zimmerberg J & McLaughlin S (2004) Membrane curvature: How BAR domains bend bilayers. *Curr. Biol.* **14:** 250–252

Ziółkowska NE, Christiano R & Walther TC (2012) Organized living: formation mechanisms and functions of plasma membrane domains in yeast. *Trends Cell Biol.* **22:** 151–158

Ziółkowska NE, Karotki L, Rehman M, Huiskonen JT & Walther TC (2011) Eisosome-driven plasma membrane organization is mediated by BAR domains. *Nat. Struct. Mol. Biol.* **18:** 854–856

Publications and Contributions of Authors

This doctoral thesis was generated as a combination dissertation. Parts of this doctoral thesis have been submitted or manuscripts for publication:

Chapter II

Yang Q, Kollath-Leiß K, Kempken F. (**submitted to Microbiological Research**). Eisosomes show different features in morphologically identical hyphae germinating from sexual and asexual spores in *Neurospora crassa.*

F.K. and K.K. conceived the project, with some contributions of Q.Y. during the project. Q.Y. performed the experiments, analyzed the data, and wrote the manuscript. K.K. created the Supplementary Fig. *S2* and Q.Y. created all the other figures in the manuscript.

Chapter III

Yang Q, Kempken F. (**ready for submission**). Multiple bioactivities of eisosomes and interspecific differences in *Neurospora crassa.*

F.K. conceived the study. Q.Y. carried out the experiments, analyzed the data and drafted the paper.

Chapter IV

Yang Q, Kempken F. (**ready for submission**). The cytoskeleton regulates the formation and distribution of eisosomes in *Neurospora crassa.*

F.K. conceived the project. Q.Y. prepared the samples, performed the experiments, analyzed the data, and wrote the manuscript.

Chapter I

The eisosomal marker protein in *Neurospora crassa*

Results

LSP-1, the first confirmed eisosome component in *Neurospora crassa*

Firstly, the LSP-1 protein in *N. crassa* was detected as a functional and core component of the eisosome by our research. This was a basis of the further research and LSP-1 was then used as an eisosomal marker.

Eisosomes are protein complexes associated to furrow-like invagination domains at the plasma membrane. In our study, transmission electron microscopic analysis was performed and confirms the existence of the eisosome complexes at the plasma membrane of *N. crassa* cells (**Figure 1 A - C**). The outline and the depth (28.8-44.0 nm) of the invaginations correspond to the reported characteristics of yeast eisosomes (Douglas & Konopka, 2014; Strádalová *et al*, 2009). LSP-1 protein in *N. crassa* is a homologue of the *A. nidulans* PilA, which is a core component of eisosomes. Immunogold labeling against LSP-1::GFP was carried out to determine the exact localization of LSP-1 protein in *N. crassa* (**Figure 1 B - C).** The gold particles mainly accumulate close to the plasma membrane at eisosome-like invaginations and are rarely observed in the cytoplasm.

The TEM captures confirmed that there were no eisosome-similar invaginations at hyphal tips (**Figure 1 D**). Although there were a few furrows at some of the hyphal tip sections (**Figure 1 D ii**), they were not eisosomes because they were clearly smaller (8.3 – 12.9 nm, shown in **Figure 1 D ii**) than expected; The yeast eisosomes were reported to be around 50 nm in depth (Douglas & Konopka, 2014) and in our study the approximate depth of eisosomal invaginations was 40 nm.

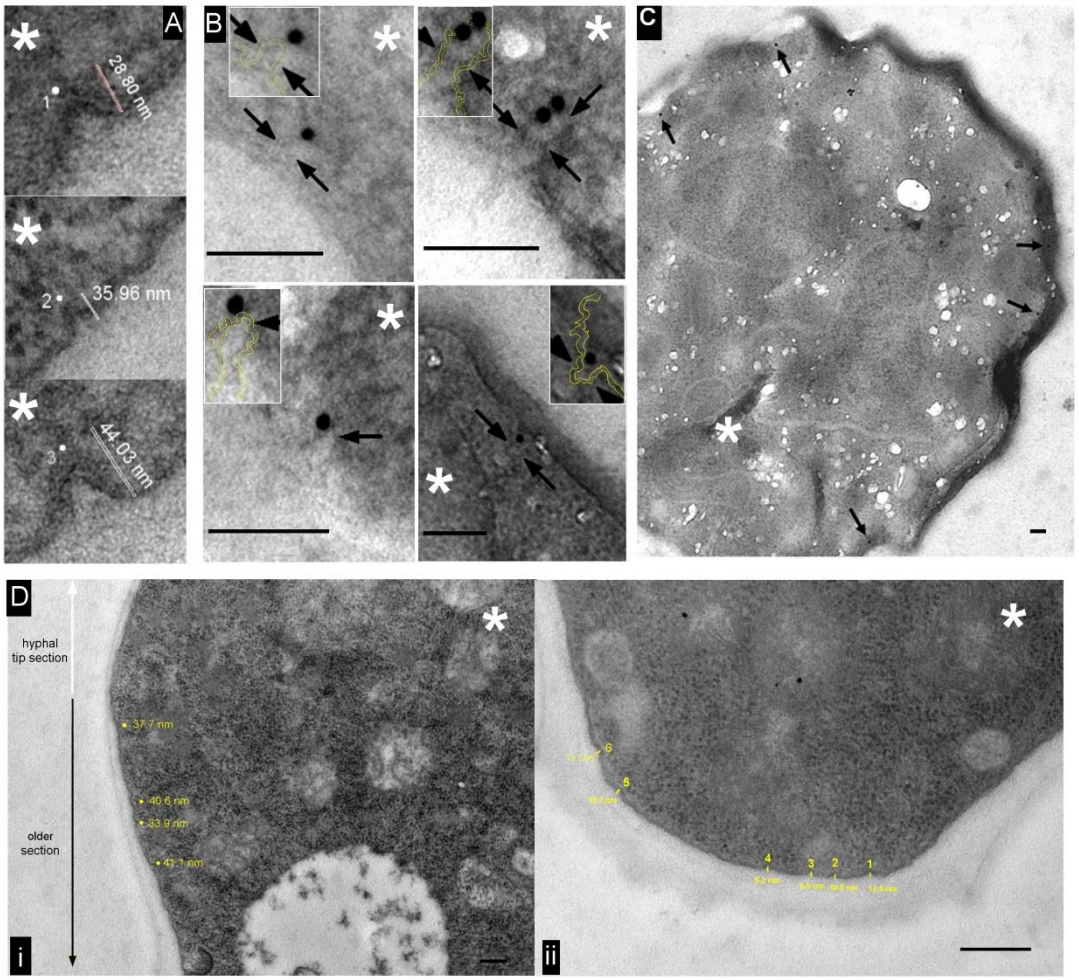

Figure 1. Ultrastructure of invaginations/eisosomes at the plasma membrane. A. Eisosome ultra-structures shown in TEM. Depth measurements of three eisosomes were shown (1–3). **B.** High magnification examples of immunogold-labeled eisosomes shown in TEM. Arrows point to the invaginations (eisosomes) at the cell membrane. Black spots are gold particles. The yellow lines in white frames highlight the cell membranes at the invaginations. **C**. A low magnification example with labeling of gold particles at the cell membrane. Asterisks marked the cell interior. Arrows point to the invaginations (eisosomes) at the cell membrane. Black spots are gold particles. **D**. Eisosomes are absent from hyphal tips. **i**. There was no obvious invagination at the hyphal tip section while many furrows around 40 nm were observed at the older section of the hypha. The depth of some of these furrows were measured and shown in the image. **ii**. Some non-eisosomal, small invaginations (less than 12.9 nm in depth, not eisosomes) were detected at the hyphal tip. For all images, asterisks marked the cell interior. Scale bars on **A - C**: 100 nm, Scale bars on **D**: 200nm.

LSP-1 is highly expressed in *Neurospora crassa*

Once LSP-1 was used as an eisosomal marker in the study, the dual fluorescence localization analysis became to convenient and efficient method to investigate or confirm eisosome components. The gene fragment expressing fluorescent protein(s) tagged LSP-1 was constructed and insert to *N. crassa* genome (**Figure 2**). Then the fusion protein successfully expressed and report localizations of eisosomes at the cell membrane. The native promoter of *N. crassa lsp-1* gene was found (**Figure 2**) in the research. The expressions of LSP-1::RFP promoted by the native promoter and by the strong promoter used in the research were equally strong (As shown in **Figure 3**, no obviously difference was observed.). The data showed LSP-1 is a highly expressed protein in *N. crassa,* and the overexpression of the construction did not influence the native formation/distribution of eisosomes. In addition, the green fluorescent protein (GFP) and the red fluorescent protein (RFP) were separately fused to LSP-1 in *N. crassa* and act as the positive control to check the efficiency of the dual fluorescence localization analysis in the thesis (**Figure 4**). The method was confirmed to be highly confident and efficient in the research.

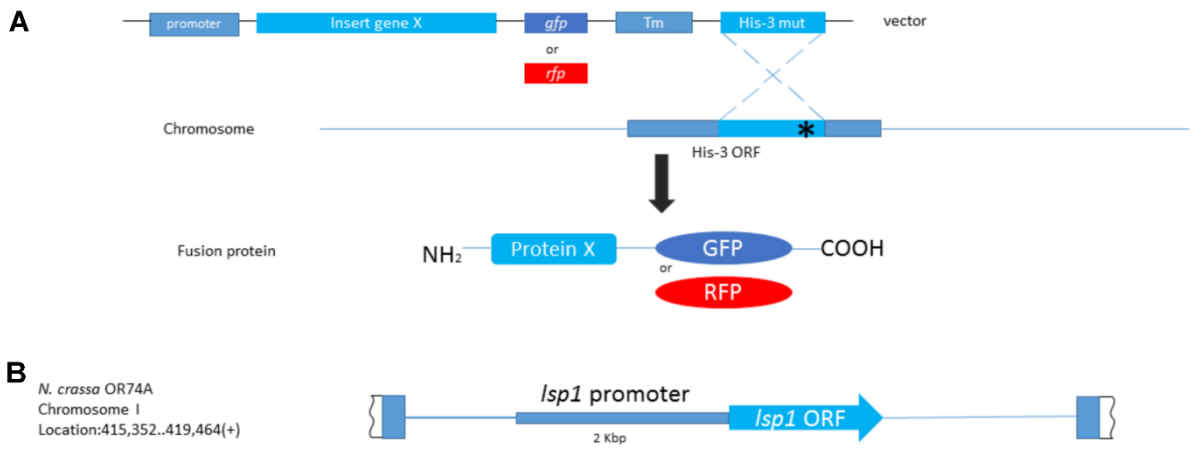

Figure 2. A. The strategy to express fluorescent protein(s) tagged LSP-1 in *N. crassa*. B. The location of the LSP-1 native promoter on chromosome I of *N. crassa*.

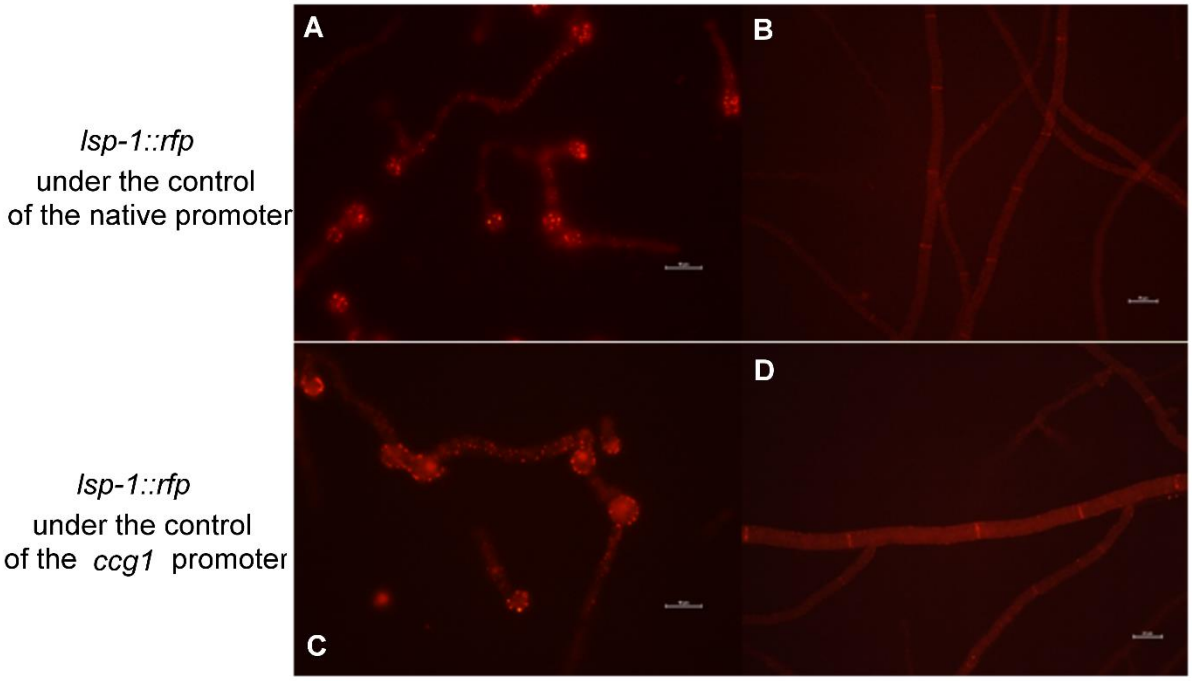

Figure 3. A. The expression of LSP-1::RFP under the control of the *lsp-1* promoter and the strong promoter *ccg1* in *N. crassa*. There are no obvious differences observed. Scale bars in A, C = 10 µm; scale bars in B, D = 20 µm.

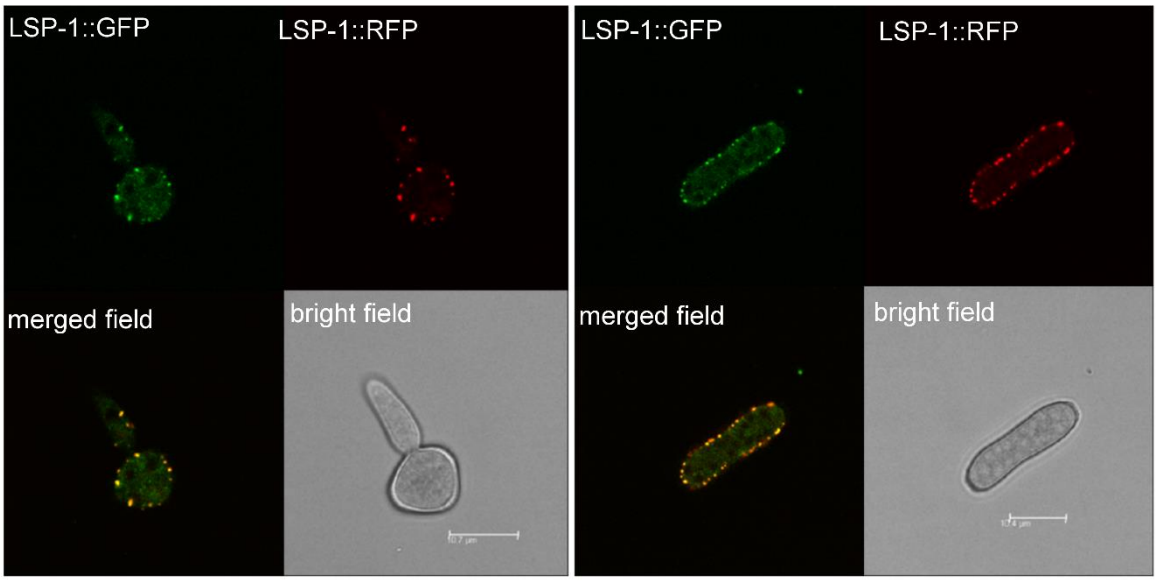

Figure 4. The LSP-1::GFP and LSP-1::RFP dual fluorescence profile analysis in *N. crassa*. Scale bar in on the left panel = 10 µm; scale bar on the right = 20 µm.

Material and Method

Strains and growth conditions

Vogel's minimal medium with 2% sucrose (4621.1, ROTH) (VMM + S) was used cultivation of *N. crassa* and Vogel's minimal medium with 1% sorbose (4028.1, ROTH), 0.05% glucose (6887.1, ROTH), 0.05% fructose (4981.1, ROTH) (VMM + SGF) was used for single colony selection on plates. Thin agar plates of the media mentioned above were used for microscope analysis. *N. crassa* were cultivated at 25°C.

The *N. crassa* strains NcT475: *ccg1 promoter::lsp-1::rfp* mat A, NcT507: *lsp-1 promoter::lsp-1::rfp* mat A, and NcT467: *cfp promoter::lsp-1::gfp* mat A were used in this chapter.

Molecular experiments

DNA amplifications were performed with a PCR machine (LabCycler, SensoQuest). MolTaq polymerase (P-010-1000, Molzym) and *Pwo*-DNA-Polymerase (732-3262, PeqLab) were used for DNA amplifications. Primers QY2942 5'-CCTTAATTAAGGTGAGGACGGATGAATAAGAC-3', and QY2943 5'-TTGGCGCGCCGGTGGATTAGGTAGTATTTATCGATTG-3' were used to amplified *N. crassa lsp-1* promoter fragment.

USER enzyme (M5505S, New England BioLabs) was employed for fusion fragment ligation constructions while CloneJET PCR cloning Kit (K1231, Thermo scientific) and T4 ligase (M0202S, New England BioLabs) was used for other ligations.

Microscopy

Microscope analysis was performed with a fluorescence microscope (ECLIPSE Ci system plus INTENSILIGHT C-HGFI 130w lamp, Nikon). 40×/NA0.75 (plan fluor), 100×/NA1.30 oil (plan fluor) objective lenses were used to acquire images. Immersion oil (Type N, Nikon) was used with the oil objective lens for observation and image acquisition. Epi-Fluorescence filter G-2E/C (TRITC), EX 540/25, DM 565, BA 605/55

was used for red fluorescence. A GigE camera (DFK 23U274, Imaging Source) was used to capture photos. The acquisition software is NIS elements D basic (Nikon). Images were captured at room temperature (22 - 25°C).

Confocal fluorescence analysis was performed using a confocal laser scanning microscope (Leica, TCS SP5) and images ware captured with the Leica LAS AF Lite Software. GFP was excited with 488 nm and emission was detected at 500-550 nm, while RFP was excited with 543nm and emission was detected at 590-610 nm.

EM and immunogold EM

N. crassa strains were cultivated at 25°C for 2 weeks, and then macroconidia were washed and harvested with 1M sorbitol (6213.1, ROTH) and incubated at 28°C and 120 rpm for 4 h. Germinating conidiospores were isolated by centrifugation at 4000 rpm for 5 min (Allegra X-30, Beckman Coulter). For transmission electron microscopy of membrane structures, the pellet was fixed at 4°C overnight in 2.5% (v/v) glutardialdehyde, 1% (w/v) formaldehyde (freshly prepared from paraformaldehyde), and 5% ethanol (v/v) in 0.1 M sodium cacodylate buffer, pH 7.3. After washing in sodium cacodylate buffer, the sample was mixed with 50°C warm and 2% noble agar and cut into small pieces. Subsequently, the small segments were fixed at room temperature for 4 h in 2.5% (v/v) glutardialdehyde and 1% (w/v) formaldehyde (freshly prepared from paraformaldehyde) in 0.1 M sodium cacodylate buffer, pH 7.3. After washing in buffer, the samples were postfixed at 4°C in 1% (w/v) OsO_4 in buffer for 4 h, washed again, dehydrated in a graded series of ethanol, and embedded in LR white resin (Plano, Marburg, Germany) with subsequent polymerisation at 60°C. Ultrathin sections were prepared by a diamond knife in a Leica Ultracut UCT Ultramicrotome (Leica Microsystems GmbH). Sections were viewed under a transmission electron microscope (TEM) (CM10, Philips Scientifics) with a CCD camera (MegaView III, EMSIS) and Olympus Soft Imaging System (version 5.0, build 1233).

For immunogold labeling, the pellet was fixed at 4°C for 2 h in 0.2% (v/v) glutardialdehyde, 4% (w/v) formaldehyde (freshly prepared from paraformaldehyde), and 5% ethanol (v/v) in phosphate buffered saline solution (PBS), pH 7.4. After washing in PBS, the sample was mixed with 50°C warm, 2% noble agar and cut into small pieces. Subsequently, the small segments were fixed at 4°C for 2 h in 4% (w/v) formaldehyde (freshly prepared from paraformaldehyde) in PBS buffer. After washing in buffer at 4°C, samples were dehydrated in a graded series of ethanol and embedded in LR white resin (Plano, Marburg, Germany) with subsequent polymerization at 50°C for two days. Ultrathin sections were prepared by a diamond knife in a Leica Ultracut UCT Ultramicrotome (Leica Microsystems GmbH). Ultrathin sections were collected on Au-grids. Samples were incubated at room temperature for 30 min in blocking buffer (0.2% (w/v) bovine serum albumin (BSA) and 0.2% (w/v) fish gelatin in PBS, pH7.4). Anti-GFP (NB 600-308, Novus Biologicals) diluted 1:100 in blocking buffer was used as primary antibody. Samples were incubated at 4°C overnight. After washing with 0.1% BSA in PBS buffer, pH 7.4, sections were incubated with the corresponding anti-rabbit IgG secondary antibody, diluted 1:50 in blocking buffer, conjugated to 10 nm gold particles (British BioCell International Ltd.). Finally, after washing with PBS and Millipore water, sections were poststained for 10 min with saturated uranyl acetate in water and viewed with a TEM (Tecnai G2 BioTWIN, FEI Company). A bottom-mounted High-Sensitive 4K Eagle camera (FEI Company), TEM user interface (version 4.2, build 6173; FEI Company), and TEM imaging and analysis software (version 4.2 SP1, build 816; FEI Company) were used for image acquisition.

References

Douglas LM & Konopka JB (2014) Fungal membrane organization: the eisosome concept. *Annu. Rev. Microbiol.* **68:** 377–393

Strádalová V, Stahlschmidt W, Grossmann G, Blazíková M, Rachel R, Tanner W & Malinsky J (2009) Furrow-like invaginations of the yeast plasma membrane correspond to membrane compartment of Can1. *J. Cell Sci.* **122:** 2887–2894

CHAPTER II

Eisosomes Show Different Features in Morphologically Identical Hyphae Germinating from Sexual and Asexual Spores in *Neurospora crassa*

Qin Yang, Krisztina Kollath-Leiß, Frank Kempken*

Department of Botanical Genetics and Molecular Biology

Botanical Institute and Botanic Gardens

Olshausenstr. 40

24098 Kiel

Germany

Phone: +49 431 880 4274

Fax: +49 431 880 4248

* author for correspondence: fkempken@bot.uni-kiel.de

Abstract

Eisosomes are complex protein structures which play roles in various cellular processes but so far were rarely reported in the model fungus *Neurospora crassa.* Here we show that LSP-1 in *N. crassa* is a functional and core eisosomal component, and we give a systematical description about the distributional characteristics of eisosomes in different developmental stages. In *N. crassa*, hyphae germinated from sexual and asexual spores are identical in morphology and have been historically recognized as the same type of cells. Here we demonstrate the structural differences between hyphae germinated from sexual and asexual spores on the cellular level. Eisosomes are found to be absent from the tips of hyphae germinated from macroconidia but are located at the tips of hyphae emerged from ascospores in *N. crassa*. The observations in our study suggest the necessity of the distinction of hyphae germinating from sexual and asexual spores. Our research data bring new insights on eisosome formation and cell type recognition and deserve further investigation.

Keywords: eisosome; distribution; *Neurospora crassa*; hypha; fluorescence.

1. Introduction

The plasma membrane of fungal cells is of lateral heterogeneity (Malinsky and Opekarová, 2016) and allow spatial segregation of different domains with various functions (Olivera-Couto and Aguilar, 2012). Among them, MCCs (membrane compartment occupied by Can1) are nanoscale furrow-like invaginations at the plasma membrane, associated with spatially stable protein complexes called eisosomes (Strádalová et al., 2009). Eisosomes were first proposed and described in detail in the yeast *Saccharomyces cerevisiae* (Moseley, 2018; Walther et al., 2006). Later on,

studies on *Aspergillus nidulans* (Athanasopoulos et al., 2013; Vangelatos et al., 2010), *Candida albicans* (Douglas et al., 2013; Wang et al., 2016), and *Beauveria bassiana* (Zhang et al., 2017) were performed and published.

The main proteins components of eisosomes in yeast are Pil1 and Lsp1 (Walther et al., 2006). At the furrow site, the transmembrane protein Sur7 and Nce102 were found to colocalize with the MCC/eisosome complex (Fröhlich et al., 2009; Moseley, 2018; Walther et al., 2006). Pil1 and Lsp1 are paralogs, both carrying a BAR (Bin/Amphiphysin/Rvs) domain (Olivera-Couto et al., 2011). The absence of Pil1 reduces the formation of eisosomes in yeast (Walther et al., 2006; Ziółkowska et al., 2012). Pil1 appears to be regulated by VPS15 (Moreira et al., 2009; Moseley, 2018), which is critical for the fast internalization of extracellular vesicles (Stein et al., 2017). A large coiled-coil peripheral membrane protein without recognizable functional domains, SEG1 (stability of eisosomes guaranteed), is required for efficient incorporation of Pil1 into eisosomes (Moreira et al., 2012; Moseley, 2018; Seger et al., 2011). In addition, Pkh-kinases are reported to localize to eisosomes and are associated with Pil1 protein phosphorylation (Walther et al., 2007).

In filamentous fungi, eisosome composition seems to be similar, but not identical with their *Saccharomyces cerevisiae* counterparts. In *Aspergillus nidulans* and *Aspergillus fumigatus*, there are two orthologs (PILA and PILB) of Pil1 and Lsp1, which arose from a duplication event that is distinct from the evolution of Pil1 and Lsp1 in *Saccharomyces cerevisiae (S. cerevisiae)* (Douglas et al., 2011; Douglas and Konopka, 2014). In *A. nidulans,* PILA, PILB, and SURG were found to be the core components of eisosomes (Vangelatos et al., 2010). They colocalize at the cell cortex and form tightly packed punctate structures. The three core constituents were not observed in early ascospores of *A. nidulans,* but they exist in mature ascospores, and only PILA was observed in hyphae germinating from ascospores and conidia. In *Ashbya gossypii,* Pil1 and Lsp1 were reported to be the main components of

eisosomes; however, in contrast to *S. cerevisiae*, the *Ashbya gossypii* homologue of Pil1 is very important for polar growth, whereas the homologue of Nce102, which colocalizes with eisosomes, is not needed for eisosome stability (Seger et al., 2011). In *Candida albicans*, the components of eisosomes are highly similar to that of *S. cerevisiae*. Sur7, Fmp45, Lsp1, Pil1, Slm1, and Seg1 are all eisosomal components (Douglas and Konopka, 2014). Among them, Pil1 and Lsp1 are the core components and are required for eisosomal formation (Wang et al., 2016). Nevertheless, interesting differences were reported, such as Sur7 plays a more important functional role in *C. albicans* than in *S. cerevisiae* (Alvarez et al., 2008), Nce102 is only partially enriched to MCC/eisosome domains in log phase cells, but it becomes tightly localized to these domains as cells enter stationary phase (Douglas et al., 2013), and deletion of the only ortholog of PKH1/2 does not obviously affect MCC/eisosome organization (Douglas et al., 2013).

The functional properties of eisosomes are not yet well understood (Kolláth-Leiβ and Kempken, 2017). Eisosomes play a role in a variety of cellular processes, such as plasma membrane organization, cell wall synthesis and morphogenesis, sphingolipid homeostasis (Douglas and Konopka, 2014; Foderaro et al., 2017), and stress response (Douglas and Konopka, 2014). Furthermore, eisosomes are functionally associated with membrane domain formation (Bartlett et al., 2015), nutrient transporter regulation (Moharir et al., 2018), cellular signaling (Olivera-Couto and Aguilar, 2012), proton flux organization, and scaffold protein formation (Douglas and Konopka, 2014). Eisosomes may also be functional on the transcript regulation level. It was reported that properly assembled eisosomes are necessary for the regulation of Xrn1 (the main 5'-3' mRNA exoribonuclease), which mediates mRNA degradation in *S. cerevisiae* (Vaškovičová et al., 2017). In the human pathogen *C. albicans,* eisosomes are involved in plasma membrane organization, as well as cell wall synthesis and organization (Alvarez et al., 2009). In this fungus, eisosomes also mediate fungal pathogen

virulence as they are important for actin organization and invasive hyphal elongation (Douglas and Konopka, 2014).

The functional properties of eisosomes in filamentous fungi are even more elusive. For the insect pathogenic fungus *Beauveria bassiana,* eisosomal core proteins PILA and PILB were found to be associated with the target of rapamycin signaling pathway. Deletions of PILA/PILB or both of them led to the loss of pathogenicity (Zhang et al., 2017). Eisosomes are important for polarized growth in *Ashbya gossypii* as deletion of the eisosomal protein Pil1 had a strong effect on hyphal tip development (Douglas and Konopka, 2014; Seger et al., 2011). On the contrary, in *A. nidulans,* eisosomes only seem to play a role in the stress resistance of spores as deletions of the three core eisosomal proteins did not result in any other obvious defects (Vangelatos et al., 2010). In *Neurospora crassa*, the protein, annotated as LSP-1 (encoded by the gene NCU07495), is in fact the ortholog of the *A. nidulans* PILA protein (Kollath-Leiß et al., 2014). In this fungus, the general amino acid transporter MTR and the alpha-beta-hydrolase domain containing protein BEM46 are reported to localize to eisosomes.

In our study, LSP-1 of *N. crassa* was shown to be a marker protein of eisosomes and was fused to fluorescent protein to establish the locational characteristics of eisosomes in different developmental stages of the *N. crassa* life cycle.

2. Materials and methods

2.1. Media and growth conditions

Vogel's minimal medium with 2% sucrose (4621.1, ROTH) (VMM + S) was used for cultivation of *N. crassa*, and Vogel's minimal medium with 1% sorbose (4028.1, ROTH), 0.05% glucose (6887.1, ROTH), and 0.05% fructose (4981.1, ROTH) (VMM + SGF) was used for single colony selection on plates. *His*-3^{-} *N. crassa* FGSC strains 6103 and 9716 were grown on Vogel's minimal medium with sucrose (4621.1, ROTH)

and 0.02% histidine (H5659-25G, SIGMA-ALDRICH) (VMM + S + His) and used as transformation host. *N. crassa* microconidia production was induced on microconidia medium, which contains 1% sucrose (4621.1, ROTH), 0.06% iodoacetate (I2512-25G, SIGMA-ALDRICH), 5% synthetic cross medium (2 × strength stock) (Westergaard and Mitchell, 1947), and 2% agar (5210.2, ROTH). Cellophane was cooked and put on the surface of microconidia medium plates to induce microconidia production to obtain homozygous strains. Westergaard's medium was used for *N. crassa* crossing experiments to get ascospores (Westergaard and Mitchell, 1947). Thin agar plates of the media mentioned above were used for microscopy analysis. *N. crassa* were cultivated at 25°C in light. For germination analysis, conidia were inoculated on thin agar plates and cultivated at 30°C for 3–5h.

For *S. cerevisiae,* if not stated otherwise, cells were grown in YPD medium (2% peptone, 1% yeast extrat, and 2% glucose) at 30°C.

2.2. Strains

The *N. crassa* strains used in our study are listed in Supplementary Table S1. Plasmids carrying fusion constructs were transformed into the histidine auxotrophic strains FGSC 6103 and 9716 (Fungal Genetics Stock Center; Kansas City, MO, USA). The chromosomal integrations were introduced by homologous recombination. To make LSP-1::RFP expressed from *his-3* locus, the coding fusion fragments with 1618 base pairs of *his-3* sequence were inserted in the vectors (Margolin et al., 1997).

The *S. cerevisiae* strain (*ade2-1, can1-100, his3-11,15 leu2-3,112 trp1-1, ura3-1, LSP1-GFP:HIS, pil1Δ:Kan*) used for the yeast complement experiment in our study was provided by Farese & Walther Lab (Walther et al., 2006). *S. cerevisiae* Y187 (*MATα, ura3-52, his3-200, ade2-101, trp1-901, leu2-3, 112, gal4Δ, met–, gal80Δ,*

*URA3::GAL1*UAS -*GAL1*TATA-*lacZ*) (Clontech, Mountain View) was used as a non-fluorescent control.

The bacterial strain *E. coli* XL1-Blue [*recA1, endA1, gyrA96, thi-1, hsdR17, supE44, relA1, lac F'proAB lacIqZΔM15 Tn10 (Tetr)*] (200249, Stratagene) was used for electroporation and chemical transformations.

2.3. Molecular experiments in the study

For DNA isolation, *N. crassa* strains were cultivated at 25°C for 3–4 days, mycelium was ground under liquid nitrogen and transferred into lysis buffer (10 mM Tris-HCl, 1 mM EDTA, 100 mM NaCl, 2% SDS, pH 8.0), and phenol extraction was performed. Subsequently, the aqueous phase was incubated with 100 µg RNase A, followed by an additional phenol extraction and ethanol precipitation. Bacterial plasmids were isolated using NucleoSpin Plasmid Easypure (740727.250, Macherey-Nagel).

DNA amplifications were performed with a PCR machine (LabCycler, SensoQuest). MolTaq polymerase (P-010-1000, Molzym) and *Pwo*-DNA-Polymerase (732-3262, PeqLab) were used for DNA amplifications. Primers used in our study were synthesized by Eurofins MWG Operon (Ebersberg, Germany) and are listed in Supplementary Table S2.

Gel electrophoresis were normally performed with 1% agarose at 20 V for 20 min and then raise to 100–120 V for 1 h (Mercker et al., 2009). Markers for DNA from MBBL (Bielefeld) were used to determine size in DNA gel electrophoresis.

Gel elution was carried out with NucleoSpin Gel and PCR Clean-up kit (740609.50, Macherey-Nagel).

Restriction endonuclease enzymes from New England BioLabs were used according to the manufacturer's recommendation.

USER enzyme (M5505S, New England BioLabs) was employed for fusion fragment ligation constructions, while CloneJET PCR Cloning Kit (K1231, Thermo scientific) and T4 ligase (M0202S, New England BioLabs) were used for other ligations.

2.4. Plasmid construction

Construction of plasmid pJQ771 (Supplementary **Fig.** *S1*) has been previously described (Kollath-Leiß et al., 2014). Plasmid pQY868 (Supplementary **Fig.** *S1*) carries the *N. crassa lsp-1* promoter (amplified with primers QY2492 and QY2493). The promoter controls the expression of the sequence coding for the *N. crassa lsp*-1 gene fused to the coding sequence of tRFP, which was amplified as described (Kollath-Leiß et al., 2014). The final open reading frame was verified by sequencing.

For the yeast complementation experiment, plasmid pQY878 was used in our study. It was generated by cloning *N. crassa lsp*-1*::rfp* into the yeast expression vector pYES2/NT A (V8252-20, Invitrogen). The *lsp*-1*::rfp* fragment was amplified by QY3213 and QY3214 using the pQY868 plasmid as a template. The final product was verified by DNA sequencing.

2.5. Electroporation and selection of transformants

Electroporation of *N. crassa* conidia was carried out by an electroporation system (Gene Pulser II Apparatus, Pulse Controller Plus, Cap Extender plus; BioRad) using 1.5 kV/cm, 25 µF, and 600 Ω (Kumar et al., 2013). Immediately after electroporation, *N. crassa* conidia were plated on VMM + SGF plates. Transformant strains were selected on VMM+S plates without histidine. Single colonies were inoculated on VMM + S slants and were checked under an epi-fluorescence microscope. Single colonies exhibiting the desired fluorescence were inoculated on microconidia medium plates covered by cooked cellophanes to induce microconidia production.

Microconidiospores were diluted and inoculated on VMM + SGF plates to get homozygous single colonies which would be inoculated into VMM + S slants. Then the colonies were checked by epi-fluorescence, and fluorescent homokaryons were conserved and used in this research. All cloning and transformation experiments were conducted in accordance with the requirements of the German gene technology law (GenTG).

Transformation of yeast was performed by electroporation, similar to methods published (Kollath-Leiß et al., 2014). 50 µl of electrocompetent *Saccharomyces cerevisia* cell suspension was mixed with 100 ng DNA and kept for 5 min on ice. Subsequently, the cells were transferred into a cold electroporation cuvette (Gene Pulser Cuvette, BioRad, Munich), and transformation was realized in a Gene PulserTM (BioRad, Munich) at 200 Ω and 25 µF with 1.5 kV. Directly after transformation, 1 ml of 4°C cold 1 M sorbitol was added, and after incubation for 5 min at room temperature, 100 µl of the samples was plated on solid medium. Plates were incubated at 30°C until colony development. Then single colonies were inoculated into induction medium and incubated at 30°C for some days. The fluorescence was monitored microscopically. Putative positive colonies were identified on selective minimal medium (SC /-Ura) containing 0.67% yeast nitrogen base; 2% glucose; 0.01% of the following amino acids: adenine, arginine, cysteine, leucine, lysine, threonine, and tryptophan; 0.05% of the following amino acids: aspartic acid, histidine, isoleucine, methionine, phenylalanine, proline, serine, tyrosine, and valine; and 2% agar. The expression of the desired protein was induced by using the same medium, except for the following modifications: usage of 2% galactose instead of glucose.

2.6. Crossing experiments of *N. crassa*

Fluorescent strains of different mating types were crossed on Westergaard's medium. Perithecia were picked by a needle and squashed on an optical slide in

distilled water prior to microscope. Mature ascospores were collected and could then be observed directly under the microscope. After a heat shock at 65°C for 30 min, the ascospores could germinate on VMM + S agar plates, and then the germinating hyphae of ascospores could be investigated by microscope.

2.7. Viability test

Viability tests of yeast cells were performed using Evans blue (E2129, SIGMA-ALDRICH) stain. Yeast cell samples were mixed 1:1 (v/v) with 1% (w/v) Evans blue stock solution in PBS buffer and incubated at room temperature for 3 minutes. The stained samples were centrifuged at 200 × g for 2 min (Allegra X-30, Beckman Coulter), then the supernatants were removed. The pellets were washed three times by resuspendation in PBS buffer and subsequent centrifugation at 200 × g for 2 min to remove the residual Evans blue. The resulting pellet was used for microscopic analysis.

2.8. Microscopy

Fungi were incubated on thin agar plates. At different time points, fungi in different developmental stages were cut out of the plates. The thin agar sections with fungi were transferred to optical slides and investigated by microscope. The analysis could get clear captures when the spores were covered with sterile water. Perithecia were collected with a needle and squashed on slides by cover glass before microscopic analysis.

Microscopic analysis was performed with an epi-fluorescence microscope (ECLIPSE Ci system plus INTENSILIGHT C-HGFI 130w lamp, Nikon). 40×/NA0.75 (plan fluor), 100×/NA1.30 oil (plan fluor) objective lenses were used to acquire images. Immersion oil (Type N, Nikon) was used with the oil objective lens for observation and image acquisition. Epi-Fluorescence filter G-2E/C (TRITC), EX 540/25, DM 565, BA

605/55 was used for red fluorescence. A GigE camera (DFK 23U274, Imaging Source) was used to capture photos. The acquisition software is NIS elements D basic (Nikon). Images were captured at room temperature (22°C –25°C).

Confocal fluorescence analysis was performed using a confocal laser scanning microscope (Leica, TCS SP5), and images ware captured with the Leica LAS AF Lite. GFP was excited with 488 nm, and emission was detected at 500–550 nm, while RFP was excited with 543 nm, and emission was detected at 590–610 nm.

2.9. Fluorescence and localization analysis

Analysis of the localization and quantity of fluorescent spots, the length of hyphae, and the perimeter of conidia (include germinating conidia) was performed by the ImageJ software. The lengths of hyphae were a half perimeter of the hyphae including the conidia part. The fluorescence intensity of the conidia and hyphae, which were captured under the same epi-fluorescence setting, was valid and was compared with each other. The mycelium of different developmental phases was divided into 5 μm fragments from tips to conidia parts, and fluorescent spots were quantitatively analyzed in each fragment by ImageJ.

2.10. Time lapse

The geminating spores on thin agar plates were cut and checked under the epi-fluorescence microscope (Eclipse Ci system, Nikon). The spores and hyphae were carefully covered by glass covers to ensure that they were alive and not damaged. The slides with agar were put on the microscope table without any movement during the whole time-lapse analysis process. The lens of the microscope was not changed, and the focus was locked. The hyphae were captured after a certain elongation. The laser

lamp was turned off during the capture interphase to avoid fluorescence blenching as much as possible. The hyphae were growing at room temperature during the analysis.

3. Results

3.1. LSP-1 is an eisosomal marker protein in *N. crassa*

LSP-1 protein in *N. crassa* is a homologue of the *A. nidulans* PilA, which is a core component of eisosomes (Supplementary **Fig.** *S2*). Both *A. nidulans* PilA and *N. crassa* LSP-1 are homologous to the yeast core eisosomal proteins Pil1 and Lsp1 (Supplementary **Fig.** *S2*). In *S. cerevisiae*, the absence of Pil1, but not Lsp1, leads to reduced eisosome formation with fewer and bigger eisosomes, which demonstrates that Pil1 is the fundamental component of eisosomes and is required for proper formation or maintenance of eisosomes (Walther et al., 2006). We transferred *N. crassa lsp-1::rfp* into a *Δ pil1* yeast strain (Lsp1:GFP:HIS, *Δpil1::kan*^{R}) (Walther et al., 2006) and found that *N. crassa* LSP-1 is a functional core eisosome component (**Fig. 1**). An additional viability staining was performed to ensure, that the detected fluorescence signals were not artificially produced by dead cells (**Fig. 1**). The GFP and RFP fluorescences in the complemented cells show high positional coincidence, indicating *N. crassa* LSP-1 is highly collocated with eisosomes in yeast cells. Yeast cells complemented with *N. crassa* LSP-1 exhibit phenotypically normal eisosomal fluorescent patches at the plasma membrane, while the cells without *N. crassa* LSP-1 complementation show the mutant phenotype with the formation of fewer and bigger eisosomes; thus, the defect by the deletion of the *S. cerevisiae pil1* gene was successfully recovered by the heterologous expression of *N. crassa* LSP-1, which provides conclusive proof that LSP-1 in *N. crassa* is a functional eisosomal core protein. Together with the microscopic results, the complementation experiment demonstrates clearly that LSP-1 is a suitable eisosomal marker protein.

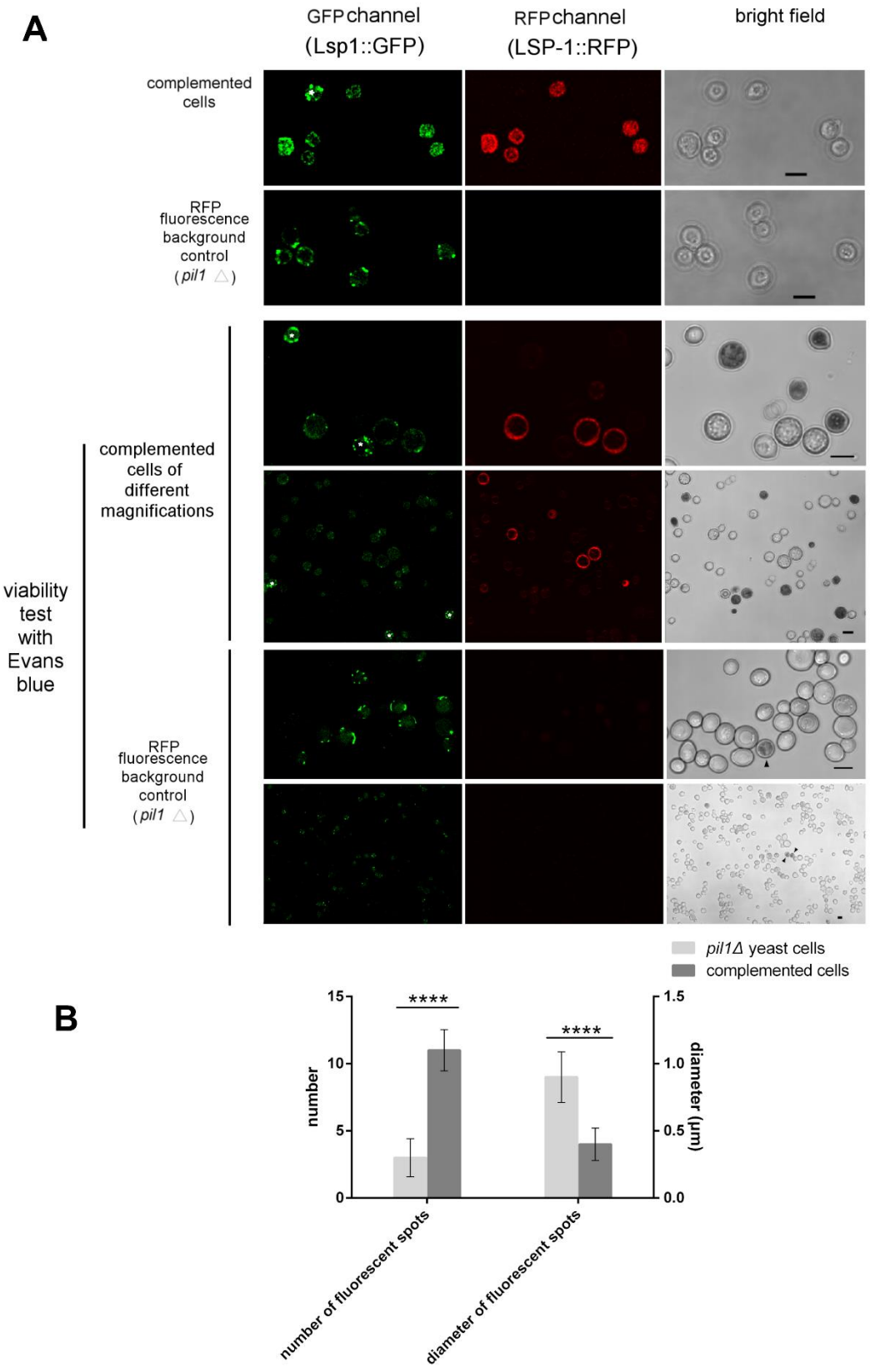

Fig. 1. The yeast complementation result. The loss of Pil1 in the yeast leads to fewer but bigger eisosome fluorescence patches. These cells expressed only Lsp1::GFP and

could be seen only in the GFP channel (no signals in the RFP channel). The heterologous *N. crassa lsp-1::rfp* was transferred into these *pil1Δ* yeast cells and complemented the absence of the yeast Pil1. Thus, only the successfully complemented cells exhibited dual fluorescences in both RFP and GFP channels. **A.** The complemented cells show phenotypically normal eisosome formation at the cell membrane and the dual fluorescences are coincided. The fluorescence background control panels show the *pil1Δ* yeast cells which were cultivated under the same condition as the complemented yeast cells. It confirmed that the fluorescence background in our research was negligible. In the viability test with Evans blue, the dead cells were stained and could be obviously distinguished from the living cells by their darker color in the bright field. The viability test shows that the dead cells did not produce any significant additional fluorescent signal. The stains used for viability tests usually introduced fluorescence contaminations. The RFP fluorescence background control confirmed that the background caused by Evans blue was negligible in the viability test. The arrow heads pointed out the dead cells in the viability test. The asterisks indicate uninduced cells in the complemented experiments. These cells had abnormal eisosomal patches and had no signals in the RFP channel. All the cells were cultivated under the same condition. All the images within each channel were captured with the same settings. Scale bars: 5 µm. **B.** The quantitative data: numbers and sizes (measured by diameters of the fluorescent spots) of eisosomes in *pil1Δ* yeast cells and complemented cells. mean ± SD, n = 7 experiments, statistical analysis using one-way analysis of variance, **** means $P \leq 0.0001$.

3.2. Localization of eisosomes during the asexual life cycle

N. crassa is a heterothallic fungus with both sexual and asexual propagation (Roche et al., 2014). During the asexual life cycle, multinuclear spores, called macroconidia, are produced and germinated to a branched, multinucleated mycelium. The eisosomal protein LSP-1 in *N. crassa* was fused to the tRFP fluorescent protein to analyze the localization of eisosomes in conidia and hyphae. Importantly, there were no significant cross-contaminations of fluorescence signals from GFP and RFP and the fluorescence background was negligible in our setup.

3.3. LSP-1 is restricted at the cell membrane

Our results show that eisosomes are distributed at the cell membrane rather than in the cytoplasm of macroconidia as well as of hyphae germinating from macroconidia, and there is no significant LSP-1 cytoplasmic pool (**Fig. 2**). Different sections of macroconidia were examined. As it is showed in **Fig. 2 A i**, there is a large number of fluorescent spots at the plasma membrane in the middle of the top cell plane and at the periphery of the equatorial cell plane of the cells. It demonstrates that LSP-1 is specifically distributed at the cell membrane of macroconidia in *N. crassa*. **Fig. 2** shows the distribution of eisosomes/LSP-1 during the germination of macroconidia. In macroconidial spore bodies as well as in hyphae, the distribution of eisosomes/LSP-1 is restricted at the cell membrane.

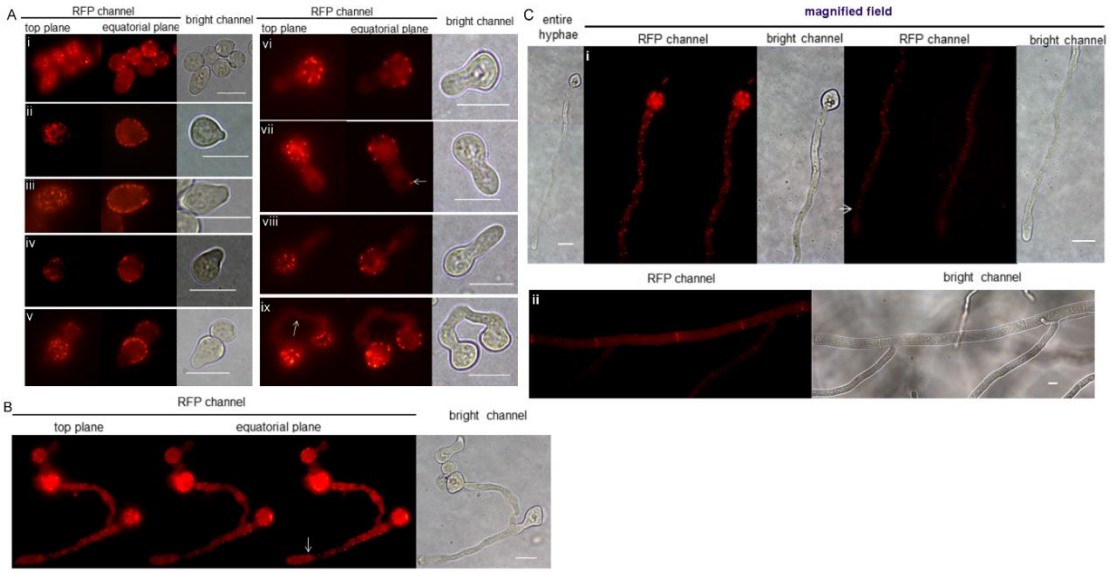

Fig. 2. Eisosomes in macroconidia and different developmental stages of hyphae germinating from macroconidia. A. **i**. Mature conidia. Top and equatorial plane captures are arranged to show the localization of eisosomes. **ii–ix.** The developmental phases of the geminating buds growing out of conidia. Fluorescent spots distributed at the buds/germinating tubes are missing; however, rare exceptions are detected (with arrows). **B.** The elongation phase of the germinating hyphae (< 100 µm). Fluorescent spots reappear at the hyphae, along the direction from conidial parts

to hyphal tips. The density of fluorescent spots is higher in parts of older hyphae than in younger ones. Fluorescent spots are absent at hyphal tips. The white arrows indicate the fluorescence signal closest to the hyphal tips. **C.** Fluorescent spot distribution characteristics in long hyphae (> 100 μm). The fluorescence channels show parts of the hyphae. The entire germinating hyphae are shown in the bright field. Fluorescent spots are present at most parts of those hyphae, except for the tip parts. **ii.** LSP-1::RFP enriched at septa of mature hyphae. Scale bars: 10 μm.

3.4. The density of eisosomes in conidia is higher than that in hyphae

When comparing macroconidia with hyphae, the density (density values in our study are all expressed by spot quantity per unit length) of fluorescent spots in conidia was much higher than that in hyphae. Furthermore, the density of spots in hyphae was different depending on their developmental stage (**Fig. 3 B**). The density of spots in conidia is about 0.90 ± 0.10 spots/μm ($P < 0.05$), while the spot densities in hyphae of different developmental stages (without conidia basis) differ from 0.08 ± 0.08 spots/μm ($P < 0.05$) (5–10 μm long hyphae) to 0.26 ± 0.04 spots/μm ($P < 0.05$) (25–35 μm long hyphae). The density of eisosomes in early hyphae, which are below 35 μm in length, is obviously increasing as hyphae grow longer and stronger, but when the hyphae are longer than 35 μm, the density divergence becomes less obvious (**Fig. 3 B**). The comparisons of fluorescence intensity between conidia and hyphae are shown in Supplementary **Fig.** *S3*. Under the settings where spots were visible, the fluorescence in conidia was too strong to see any details. Likewise, when spots in conidia were visible, the fluorescence from the hyphae was too weak that only a few fluorescent spots could be observed (shown on the left of Supplementary **Fig.** *S3*). After analyzing the single spot fluorescence intensity and the total fluorescence intensity in conidia and hyphae, we found that spots in conidia showed a somewhat stronger fluorescence than spots in hyphae, while their integrated fluorescence intensity was much more different (shown on the right of Supplementary **Fig.** *S3*), which indicates that the

different fluorescence intensities between conidia and hyphae are mainly caused by the different quantity/density of eisosomes (LSP-1::RFP) in conidia and hyphae.

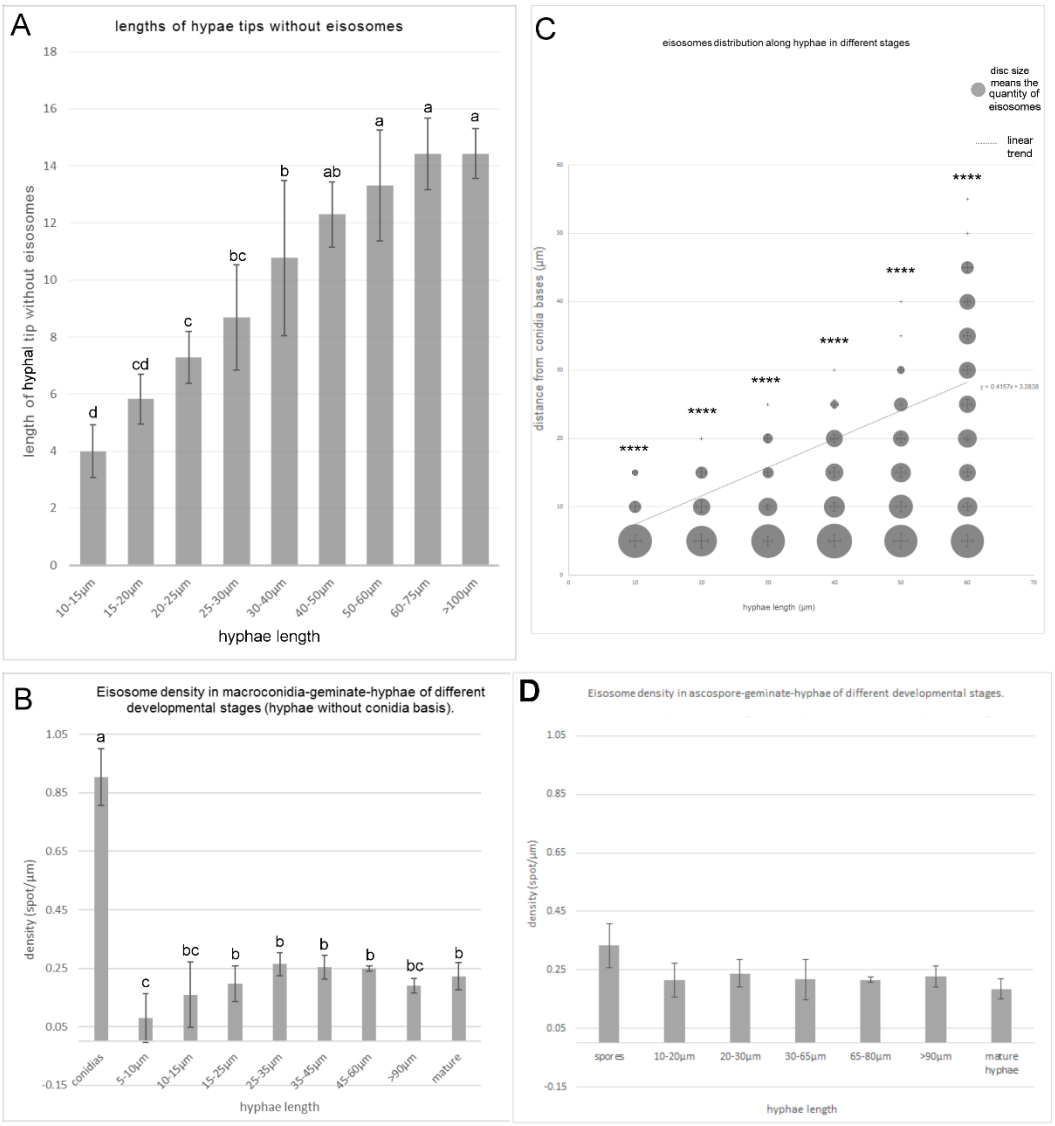

Fig. 3. **Statistical analysis of eisosomes distributions in macroconidia and hyphae germinating from macroconidia. A.** The length of hyphal tips without eisosome distributions in hyphae of different developmental stages. Mean ± SD, n ≥ 3 experiments, statistical analysis using one-way analysis of variance on ranks ($P = 3.03 \times 10^{-11}$) with Fisher LSD multiple comparisons test. We mark significant differences between bars with different letters ($P \leq 0.05$), If there is no significant difference between two bars, they get the same letter. For example, the bar marked with “ab” means it is not significant to each bar marked by either “a” or “b” but is significant to each group marked with other letters. **B.** The densities of eisosomes distributed in hyphae of different developmental stages (The density means the eisosomes quantity

per µm.). Mean ± SD, n ≥ 3 experiments, statistical analysis using one-way analysis of variance on ranks ($P = 1.30 \times 10^{-10}$) with Fisher LSD multiple comparisons test. We mark the significant differences by the same method as described above. **C.** Eisosome distribution in different areas of hyphae at different developmental stages. The quantity of eisosomes (number/5µm) was calculated and expressed by the area of the discs, which are independent in size from both axes. They show the different relative eisosome quantities along hyphae at different developmental stages. The corresponding standard deviations are presented as horizontal and vertical bars. The error bars are independent from both x and y axes and correspond to the size of the discs. For each group, mean ± SD, n ≥ 3 experiments, statistical analysis using one-way analysis of variance, ****, $P \leq 0.0001$ ($P_{10\mu m} = 4.55 \times 10^{-7}$, $P_{20\mu m} = 2.50 \times 10^{-7}$, $P_{30\mu m} = 1.16 \times 10^{-7}$, $P_{40\mu m} = 2.05 \times 10^{-6}$, $P_{50\mu m} = 1.46 \times 10^{-6}$, $P_{60\mu m} = 6.31 \times 10^{-9}$). **D**. The densities of eisosomes distributed in ascospore-germinate-hyphae of different developmental stages (The density means the eisosome quantity per µm.). Mean ± SD, n ≥ 3 experiments, statistical analysis using one-way analysis of variance on ranks (P = 0.076, not significant).

3.5. Eisosomes are absent from the tips of hyphae germinating from macroconidia

Intriguingly, eisosomes were found to be absent from the tips of hyphae germinating from macroconidia. As the hyphae grew longer, the older parts of the hyphae started to be covered by eisosomes. (**Fig. 2**, Supplementary **Fig.** *S4* **A**). **Fig. 2** sequentially shows the elongation of hyphae from macroconidia. Among them, **Fig. 2 A i–v** show the early stages of hyphae germination. The buds tended to germinate from areas of conidiospores where there was no visible LSP-1 accumulation. Fluorescent spots were clearly present at the junctions of the buds and in the conidiospores, but not at the tips. As the buds grew bigger during this period, there was no fluorescence detected in the tiny germination tubes. **Fig. 2 B–C** show the later stages of hyphal elongation. It appears that there is still no LSP-1 accumulation at the tips of the hyphae. However, occasionally single spots may be observed as shown in **Fig. 2 A vii**, where one fluorescent spot was detected near the tip on a newly

germinated hypha. The fluorescence intensity of the spot was as strong as that of spots in conidia, but spots like these were rarely detected in our study. In **Fig.** *S4*, time-lapse captures and spectra of a germinating hypha are shown. The intensity profiles show no fluorescence spots at the hyphal tip during the 210 minutes of elongation. To confirm that there was no LSP-1 accumulation at the hyphal tips, the length of the hyphal tips without fluorescent spots was examined (**Fig. 3 A**). These data confirm the observations we report above and reveal that there is a correlation between the developmental stages and the length of hyphal tip areas without eisosomes. Hyphae length in our study is defined as the half perimeter of the whole hyphae including the conidial base. The length of eisosome-free hyphal sections depends on the length of the entire germinated hyphae. The tip length without detectable eisosomes was 4.0 ± 0.9 µm ($P < 0.05$) with a total hyphal length range of 10–15 µm. As hyphae grew further, the eisosome-free areas increased in length (from 5.8 ± 0.9 µm to 13.3 ± 1.9 µm, $P < 0.05$). After hyphae grew up to 60–75 µm in length, the eisosome-free tip region increased to a maximum length of 14.4 ±1.3 µm ($P < 0.05$). It indicates that there may be some correlations between eisosome distribution and hyphal elongation. The results of the time-lapse analysis to eisosome neogenesis and hyphae elongation are shown in Supplementary **Fig.** *S4* **B**. For instance, the hypha shown in Supplementary **Fig.** *S4* **A i** exhibited an elongation from 53.4 µm to 76.3 µm in 210 minutes, and the eisosomes were exclusively found in the range from 39.5 µm to 62.9 µm, while the hyphal tip contained no eisosomes. We observed the longest area (2.3 µm) without eisosomes at the hyphal tip during hyphal elongation from 70.3 µm to 76.3 µm, while the smallest (0.2 µm) occurred when the hypha elongated from 59.5 µm to 68.0 µm. Corresponding to hyphal elongation, eisosomes are being established. This may indicate that during the early germinating phase, hyphal elongation exceeds eisosomal formation, which results in a longer eisosome-free section at the hyphal tip. Once hyphae are at least 60 µm in length, hyphal elongation and eisosome formation appear to reach a balance. Nevertheless, the spreading of eisosomes exhibits hysteresis

compared with the elongation of hyphae during the germination of macroconida in *N. crassa*. The mechanism of the hysteresis is not yet clear. It seems, that the formation of eisosomes is inhibited in the hyphal tip germinated from macroconidia. This inhibition is maintained, as the hyphae grow longer. The inhibitory mechanism is still elusive and needs further investigation.

Interestingly, the distribution of eisosomes is heterogeneous along the germinating hyphae (**Fig. 3 C**). The longer the hyphae, the more fluorescent spots tend to be close to the conidia basis; however, once hyphae are longer than 60 µm, the differences become insignificant (for hyphae of 60–75 µm, 4 ± 1 spots and hyphae more than 100 µm 3.5 ± 2.12 spots near the conidia basis). Moreover, especially in young hyphae, the sections closer to the conidia basis normally have more eisosomes (**Fig. 3 C**). In hyphae of *N. crassa*, new eisosomes mostly begin to form at the older sections of germinating hyphae, which are close to the conidial basis (**Fig. 2**). In addition, the formation of new eisosomes takes time, and the intensity of fluorescence is weaker compared with that in conidia.

In mature hyphae that were observed 24 hours after germination, the distribution of eisosomes was stable, and their quantity and location did not change within 20 min (Supplementary **Fig.** *S4* **A v**). Eisosomes are evenly distributed at the periphery of mature hyphae, their density is not significantly different from that of the germinating hyphae from 25 µm to 60 µm in length (**Fig. 3 B**). Furthermore, fluorescence was strong at septa of mature hyphae, indicating LSP-1 enrichment at those sites (**Fig. 2 C ii**).

3.6. Distribution of eisosomes during the sexual life cycle

During the sexual life cycle, spores or hyphae of different mating types fuse, and nuclear fusion occurs in the ascus prior to meiosis. In *N. crassa*, finally, eight

ascospores are formed in each ascus (Raju, 1992). Mature ascospores are thick-walled spores, and the young ascospores accumulate pigment during the maturation process and emerge hyphae to form new colonies (Bistis et al., 2003; Raju, 1992; Seale, 1973).

3.7. LSP-1 forms a significant cytoplasmic pool in immature ascospores

In young ascospores (Supplementary **Fig.** *S5* **A i**), LSP-1 was found to be distributed at the plasma membrane as well as in the cytoplasm, which was confirmed by fluorescence intensity profile analysis (Supplementary **Fig.** *S6* **A, B**). Many bright fluorescent spots were observed at the periphery of the ascospores, which was similar to the distribution of those in macroconidia. Nevertheless, the density of fluorescent spots at the periphery of ascospores is lower compared with conidiospores (**Fig. 3 B, D**). In ascospores, the eisosome density at the plasma membrane is 0.33 ± 0.074 spots/µm ($P < 0.05$), in contrast to 0.90 ± 0.097 spots/µm ($P < 0.05$) in macroconidia. In significant contrast to macroconidia (Supplementary **Fig.** *S6* **C**), LSP-1 is not only located at the plasma membrane but also in the cytoplasm of ascospores. In the equatorial plane of the ascospore, details of fluorescence in the cytoplasm is visible (Supplementary **Fig.** *S5* **A. i**). The fluorescence in the cytoplasm is almost as strong as that at the plasma membrane and much stronger than that in the cytoplasm of macroconidia (Supplementary **Fig.** *S6*). Hence, it is not just the background from LSP-1::RFP in the ER or vesicles, but more likely, LSP-1 is evenly distributed in the cytoplasm. This is the first example reported of a difference in LSP-1 distribution between sexual and asexual life cycle in *N. crassa*.

3.8. Eisosomes exist at the tips of hyphae germinating from ascospores

LSP-1 distribution in different stages of hyphal growth on ascospore germination was examined in our study (see Supplementary **Fig.** *S5*). At the first germination phase (Supplementary **Fig.** *S5* **A ii**), one or two round buds grew out of an ascospore at the poles. No fluorescence could be detected in the mature ascospore body because of the thick cell wall and the melanin accumulation. However, fluorescent spots were observed in the buds. The spots located at the plasma membrane and the fluorescence in the cytoplasm were evenly distributed and strong. As the buds grew longer (Supplementary **Fig.** *S5* **A iii**), the fluorescence in the cytoplasm became much weaker, and more fluorescent spots were observed at the periphery of the whole germinating tubes. In contrast to conidiospores, LSP-1 is also present at the tips of hyphae germinated from ascospores as confirmed by fluorescence intensity profile analysis (**Fig. 4**). Eisosomes were detected at the tips of hyphae in different developmental stages. As the hyphae grew longer (Supplementary **Fig.** *S5*), fluorescent spots were observed at the periphery as well as at the tips of hyphae. Among the germinating hyphae of different growth stages (hyphae length from 10 µm to 300 µm), the fluorescent spot densities, which are from 0.22 ± 0.06 spots/µm (of 10–20 µm hyphae length) to 0.24 ± 0.05 spots/µm (of 20–30 µm hyphae length) are not significantly different, whereas in mature hyphae, it is reduced to 0.19 ± 0.03 spots/µm (**Fig. 3 D**). Interestingly, in mature hyphae germinated from both asco- and conidiospores, the eisosome density is lower than that in the germinating hyphae (**Fig. 3 B**, **D**). But in contrast to hyphae germinated from macroconidia, there is no increase of eisosome density during the germination of hyphae from ascospores (**Fig. 3 B, D**). In addition to that, eisosomes are randomly distributed in hyphae (there is no polar distribution of LSP-1 in the mycelium germinated from ascospores). This is in strong contrast to hyphae germinating from macrocoidia. When the hyphae grew stronger and started to get branches (Supplementary **Fig.** *S7*), still, no polar distribution of eisosomes was

detectable. Moreover, hyphal tips of the main hyphae and their branches were examined, and eisosomes were found to be located at the tips (Supplementary **Fig.** *S7*).

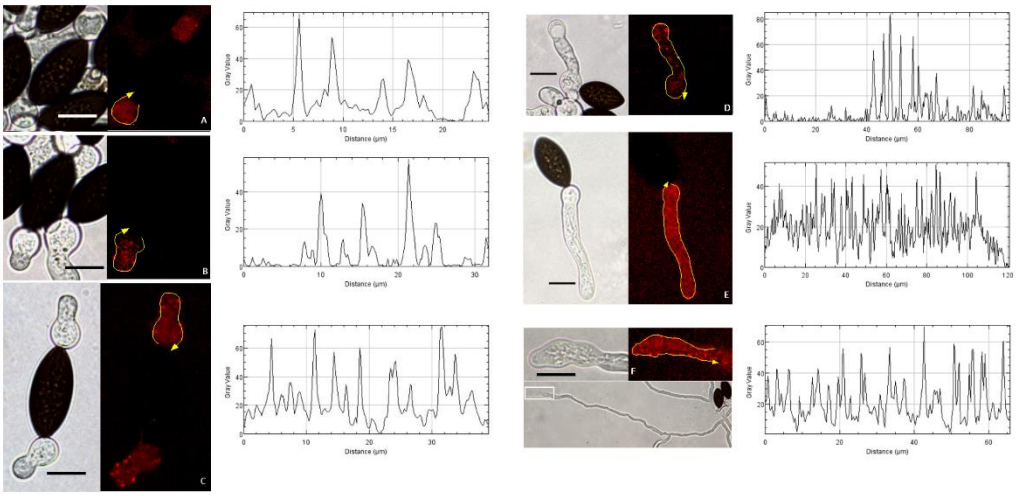

Fig. 4. Ascospore-hyphal-tip fluorescence intensity profile analysis. Fluorescent microscope captures and fluorescence intensity profile analysis of LSP-1::RFP localizations in hyphae germinated from ascospores. **A–F** sequentially show hyphae under different growth stages. Arrow lines show routes of fluorescence intensity profile analysis in hyphae, and the distance of intensity profiles is consistent to that of the epi-fluorescence captures. Scale bars: 10 μm.

In summary, we show that *Neurospora crassa* LSP-1 is an eisosomal protein. Further, we demonstrate that *N. crassa* eisosomes have a rather different distribution in hyphae germinating from sexual and asexual spores and systematically describe eisosomal distribution characteristics in different types of fungal hyphae.

4. Discussion

In *S. cerevisiae,* the Lsp1 and Pil1 proteins share 74% of their amino acid sequences and consist mostly of an evolutionarily conserved BAR domain, which are able to bind to cell membranes and have an important role for membrane bending

(Ziółkowska et al., 2011). To form an eisosome, Pil1 assembles into a membrane scaffold which is about 60 nm from the cell membrane (Bianchi et al., 2018; Karotki et al., 2011b). LSP-1 in *N. crassa* is a homolog of Lsp1 and Pil1 in *S. cerevisiae* and belongs to the Pil1 super family and can assemble into a scaffold at the base of eisosomes. The microscopic captures in our study show that fluorescent spots of LSP-1::RFP in *N. crassa* are of different sizes, indicating different quantities of LSP-1 in eisosomes in *N. crassa*. The reason for this uneven distribution remains elusive.

N. crassa is a model organism with an asexual and a sexual life cycle. The distribution and localization of eisosomes in *N. crassa* in both life cycles were examined and compared in our study. Eisosomes in *N. crassa* form stable punctate patches at the periphery of spores and hyphae during both life cycles, which are similar to that in *A. nidulans* and *S. cerevisiae* (Vangelatos et al., 2010; Walther et al., 2006). Notwithstanding, here we point out some differences. In *N. crassa* ascospores, LSP-1 is distributed at the plasma membrane as well as in the cytoplasm and form punctate patterns similar to those at the plasma membrane, while in macroconidia, it is exclusively located at the cell periphery. In *A. nidulans*, the eisosomal core component PILA has been reported to form discrete spots in the cytoplasm of germinating hyphae but not in conidia or ascospores (Athanasopoulos et al., 2013; Vangelatos et al., 2010). Furthermore, in *A. nidulans*, three eisosomal proteins (PILA, PILB, and SURG) were only found in mature ascospores and not in hülle cells or in young ascospores (Athanasopoulos et al., 2013). Those differences may indicate that eisosomes may have different functions in different fungi and different life cycles in *N. crassa*.

Another discovery is that the density of eisosomes in spores is higher than that in hyphae of *N. crassa*. The difference is especially remarkable between macroconidia and hyphae, and the germination tubes of macroconidia tend to emerge from areas where there are no eisosomes. It indicates that eisosomes have polar distribution in asexual life cycle. It has been reported that, in *N. crassa*, there may be microscale and

macroscale polarity existing in hyphae (Lew, 2011). Actin, mitochondria, and ion transporters are enriched at the hyphal tips. The apex invades new territory, while the hyphal net behind uptakes nutrients, which results in pressure gradients in the cytoplasm to promote mass flow to the hyphal tips. Conversely, the pressure facilitates the elongation of hyphae (Lew, 2011).

The fungal hypha is a complex system with different distinct regions, and each region has its own characteristics concerning structure and function (Riquelme et al., 2011). The hyphal tips are significantly important as they are associated with polarized growth, stress response, fungal colony growth, and the formation of the characteristic filamentous shape of the mycelium (Lew, 2011; Riquelme et al., 2011; Riquelme and Martínez-Núñez, 2016). Secretory vesicles are actively being transported to the growing tips and play roles in the growing process (Lew, 2011), which requires a high degree of plasticity of the growing tip. Eisosomes are stable protein complexes with a scaffold protein base rivet at the cytoplasmic surface of the cell membrane (Karotki et al., 2011a; Moseley, 2018; Vaskovicova et al., 2015), which play a role in a variety of cellular processes, such as cell wall synthesis and morphogenesis, sphingolipid homeostasis (Douglas and Konopka, 2014; Foderaro et al., 2017), and stress response (Douglas and Konopka, 2014). Furthermore, eisosomes are functionally associated with membrane domain formation (Bartlett et al., 2015), nutrient transporter regulation (Moharir et al., 2018), cellular signaling (Olivera-Couto and Aguilar, 2012), and proton flux organization, and they are important for actin organization and invasive hyphal elongation (Douglas and Konopka, 2014). Our study shows that, in *N. crassa,* eisosomes are distributed at the tips of hyphae germinated from ascospores, while they are completely absent from the tips of the germinating hyphae of macroconidia, even though these hyphae are identical in morphology (Bistis et al., 2003). Hyphae germinated from macroconidia and ascospores are distinct on the cellular level, especially at the hyphal tips, which indicates that physiological processes, such as

elongation, polarized growth, and stress response, could also be different in these hyphae. As eisosomes reportedly play role in pathogenicity (Douglas and Konopka, 2014; Zhang et al., 2017), if the differences discovered in *N. crassa* exist also in pathogenic fungi, the mechanism of virulence may also be distinct in hyphae germinated from sexual and asexual spores, which could provide new strategies for the development of antifungal therapies (Moseley, 2018). Besides, we propose that in *N. crassa*, the localization of eisosomes is not randomly established at the cell cortex; in other words, an unknown regulatory mechanism is responsible for the formation and localization of eisosomes.

Remarkable differences in growth and intracellular organization between germ tubes and mature hyphae in *N. crassa* are reported at the apex (Riquelme and Martínez-Núñez, 2016). However, the differences between hyphae germinated from ascospores and macroconidia are rarely reported. In our study, we discover structural differences between hyphae germinated from ascospores and macroconidia and firstly distinguish these hyphae as two diffident type of cells.

Author Contributions

Frank Kempken and Krisztina Kollath-Leiß conceived the project, with some contributions of Qin Yang during the project. Qin Yang prepared the sample preparations, performed the experiments, analyzed the data, and wrote the manuscript. Krisztina Kollath-Leiß created the Supplementary Fig. *S2* and Qin Yang created all the other figures in the manuscript. Frank Kempken and Krisztina Kollath-Leiß revised the manuscript.

Declaration of Competing Interests

The authors declare no additional competing financial and nonfinancial interests.

Acknowledgments

We want to express our gratitude to Tobias Walter from Harvard Medical School for providing us the yeast strain. We thank Karin Krupinska and Christine Desel from the Botanical Institute of Kiel University for providing us the yeast expression vector and the Evans blue stain. We are grateful to Vicky Sophianopoulou from the National Center for Scientific Research “Demokritos” and to Marcel Austenfeld from the Computing Centre of Kiel University for the assistance with the use of the ImageJ software.

Qin Yang is financially supported by the China Scholarship Council and is appreciated for it.

References

Alvarez, F.J., Douglas, L.M., Konopka, J.B., 2009. The Sur7 protein resides in punctate membrane subdomains and mediates spatial regulation of cell wall synthesis in *Candida albicans*. Commun. Integr. Biol. 2, 76–77. https://doi.org/10.1091/mbc.E08-05-0479.76

Alvarez, F.J., Douglas, L.M., Rosebrock, A., Konopka, J.B., 2008. The Sur7 protein regulates plasma membrane organization and prevents intracellular cell wall growth in *Candida albicans* 19, 5214–5225. https://doi.org/10.1091/mbc.E08

Athanasopoulos, A., Boleti, H., Scazzocchio, C., Sophianopoulou, V., 2013. Eisosome distribution and localization in the meiotic progeny of *Aspergillus nidulans*. Fungal Genet. Biol. 53, 84–96. https://doi.org/10.1016/j.fgb.2013.01.002

Bartlett, K., Gadila, S.K.G., Tenay, B., Mcdermott, H., Alcox, B., Kim, K., 2015. TORC2 and eisosomes are spatially interdependent, requiring optimal level of phosphatidylinositol 4, 5-bisphosphate for their integrity. J. Biosci. 40, 299–311. https://doi.org/10.1007/s12038-015-9526-4

Bianchi, F., Syga, L., Moiset, G., Spakman, D., Schavemaker, P.E., Punter, C.M., Seinen, A.B., Van Oijen, A.M., Robinson, A., Poolman, B., 2018. Steric exclusion and protein conformation determine the localization of plasma membrane transporters. Nat. Commun. 9. https://doi.org/10.1038/s41467-018-02864-2

Bistis, G.N., Perkins, D.D., Read, N.D., 2003. Different cell types in *Neurospora crassa*. Fungal Genet. Rep. 50, 17–19. https://doi.org/10.4148/1941-4765.1154

Douglas, L.M., Konopka, J.B., 2014. Fungal membrane organization: the eisosome concept. Annu. Rev. Microbiol. 68, 377–393. https://doi.org/doi:10.1146/annurev-micro-091313-103507

Douglas, L.M., Wang, H.X., Konopka, J.B., 2013. The MARVEL domain protein Nce102 regulates actin organization and invasive growth of *Candida*. MBio 4, 1–12. https://doi.org/10.1128/mBio.00723-13

Douglas, L.M., Wang, H.X., Li, L., Konopka, J.B., 2011. Membrane compartment occupied by Can1 (MCC) and eisosome subdomains of the fungal plasma membrane. Membranes (Basel). 1, 394–411. https://doi.org/10.3390/membranes1040394

Foderaro, J.E., Douglas, L.M., Konopka, J.B., 2017. MCC / eisosomes regulate cell wall synthesis and stress responses in fungi. J. Fungi 1, 1–18. https://doi.org/10.3390/jof3040061

Fröhlich, F., Moreira, K., Aguilar, P.S., Hubner, N.C., Mann, M., Walter, P., Walther, T.C., 2009. A genome-wide screen for genes affecting eisosomes reveals Nce102 function in sphingolipid signaling. J. Cell Biol. 185, 1227–1242. https://doi.org/10.1083/jcb.200811081

Karotki, L., Huiskonen, J.T., Stefan, C.J., Ziółkowska, N.E., Roth, R., Surma, M.A., Krogan, N.J., Emr, S.D., Heuser, J., Grünnewald, K., Walther, T.C., 2011a. Eisosome proteins assemble into a membrane scaffold. J. Cell Biol. 195, 889–902. https://doi.org/10.1083/jcb.201104040

Karotki, L., Huiskonen, J.T., Stefan, C.J., Ziółkowska, N.E., Roth, R., Surma, M.A., Krogan, N.J., Emr, S.D., Heuser, J., Grünewald, K., Walther, T.C., 2011b. Eisosome proteins assemble into a membrane scaffold. J. Cell Biol. 195, 889–902. https://doi.org/10.1083/jcb.201104040

Kollath-Leiß, K., Bönniger, C., Sardar, P., Kempken, F., 2014. BEM46 shows eisosomal localization and association with tryptophan-derived auxin pathway in *Neurospora crassa*. Eukaryot. Cell 13, 1051–1063. https://doi.org/10.1128/EC.00061-14

Kolláth-Leiβ, K., Kempken, F., 2017. The fungal MCC / eisosome complex : an unfolding story, in: Anke, T., Schüffler, A. (Eds.), The Mycota XV. Springer International Publishing AG 2018, pp. 119–130.

Kumar, A., Kollath-Leiß, K., Kempken, F., 2013. Characterization of bud emergence 46 (BEM46) protein: Sequence, structural, phylogenetic and subcellular localization analyses. Biochem. Biophys. Res. Commun. 438, 526–532. https://doi.org/10.1016/j.bbrc.2013.07.103

Lew, R.R., 2011. How does a hypha grow? The biophysics of pressurized growth in fungi. Nat. Rev. Microbiol. 9, 509–518. https://doi.org/10.1038/nrmicro2591

Malinsky, J., Opekarová, M., 2016. New insight into the roles of membrane microdomains in physiological activities of fungal cells, in: International Review of Cell and Molecular Biology. Academic Press, pp. 119–180. https://doi.org/10.1016/bs.ircmb.2016.02.005

Margolin, B.S., Freitag, M., Selker, E.U., 1997. Improved plasmids for gene targeting at the *his-3* locus of *Neurospora crassa* by electroporation. Fungal Genet. Reports Vol. 44.

Mercker, M., Kollath-Leiß, K., Allgaier, S., Weiland, N., Kempken, F., 2009. The BEM46-like protein appears to be essential for hyphal development upon ascospore germination in *Neurospora crassa* and is targeted to the endoplasmic reticulum. Curr. Genet. 55, 151–161. https://doi.org/10.1007/s00294-009-0232-3

Moharir, A., Gay, L., Appadurai, D., Keener, J., Babst, M., 2018. Eisosomes are metabolically regulated storage compartments for APC-type nutrient transporters. Mol. Biol. Cell 29, 2113–2127. https://doi.org/10.1091/mbc.E17-11-0691

Moreira, K.E., Schuck, S., Schrul, B., Fröhlich, F., Moseley, J.B., Walther, T.C., Walter, P., 2012. Seg 1 controls eisosome assembly and shape. J. Cell Biol. 198, 405–420. https://doi.org/10.1083/jcb.201202097

Moreira, K.E., Walther, T.C., Aguilar, P.S., Walter, P., 2009. Pil1 controls eisosome biogenesis. Mol. Biol. Cell 20, 809–818. https://doi.org/10.1091/mbc.E08

Moseley, J.B., 2018. Eisosomes. Curr. Biol. 28, R376–R378. https://doi.org/10.1016/j.cub.2017.11.073

Olivera-Couto, A., Aguilar, P.S., 2012. Eisosomes and plasma membrane organization. Mol. Genet. Genomics 287, 607–620. https://doi.org/10.1007/s00438-012-0706-8

Olivera-Couto, A., Grana, M., Harispe, L., Aguilar, P.S., 2011. The eisosome core is composed of BAR domain proteins. Mol. Biol. Cell 22, 2360–2372. https://doi.org/10.1091/mbc.E10-12-1021

Raju, N.B., 1992. Genetic control of the sexual cycle in *Neurospora*. Mycol. Res. 96, 241–262. https://doi.org/10.1016/S0953-7562(09)80934-9

Riquelme, M., Martínez-Núñez, L., 2016. Hyphal ontogeny in *Neurospora crassa*: a model organism for all seasons. F1000Research 5, 2801. https://doi.org/10.12688/f1000research.9679.1

Riquelme, M., Yarden, O., Bartnicki-Garcia, S., Bowman, B., Castro-Longoria, E., Free, S.J., Fleißner, A., Freitag, M., Lew, R.R., Mouriño-Pérez, R., Plamann, M., Rasmussen, C., Richthammer, C., Roberson, R.W., Sanchez-Leon, E., Seiler, S., Watters, M.K., 2011. Architecture and development of the *Neurospora crassa* hypha - a model cell for polarized growth. Fungal Biol. 115, 446–474. https://doi.org/10.1016/j.funbio.2011.02.008

Roche, C.M., Loros, J.J., McCluskey, K., Glass, N.L., 2014. *Neurospora crassa*: Looking back and looking forward at a model microbe. Am. J. Bot. 101, 2022–2035. https://doi.org/10.3732/ajb.1400377

Seale, T., 1973. Life cycle of *Neurospora crassa* viewed by scanning electron microscopy. J. Bacteriol. 113, 1015–1025.

Seger, S., Rischatsch, R., Philippsen, P., 2011. Formation and stability of eisosomes in the filamentous fungus *Ashbya gossypii*. J. Cell Sci. 124, 1629–1634. https://doi.org/10.1242/jcs.082487

Stein, K., Winters, C., Chiang, H.L., 2017. Vps15p regulates the distribution of cup-shaped organelles containing the major eisosome protein Pil1p to the extracellular fraction required for endocytosis of extracellular vesicles carrying metabolic enzymes. Biol. Cell 109, 190–209. https://doi.org/10.1111/boc.201600060

Strádalová, V., Stahlschmidt, W., Grossmann, G., Blazíková, M., Rachel, R., Tanner, W., Malinsky, J., 2009. Furrow-like invaginations of the yeast plasma membrane correspond to membrane compartment of Can1. J. Cell Sci. 122, 2887–2894. https://doi.org/10.1242/jcs.051227

Vangelatos, I., Roumelioti, K., Gournas, C., Suarez, T., Scazzocchio, C., Sophianopoulou, V., 2010. Eisosome organization in the filamentous ascomycete *Aspergillus nidulans*. Eukaryot. Cell 9, 1441–1454. https://doi.org/10.1128/EC.00087-10

Vaškovičová, K., Awadová, T., Veselá, P., Balážová, M., Opekarová, M., Malinsky, J., 2017. mRNA decay is regulated via sequestration of the conserved 5′-3′ exoribonuclease Xrn1 at eisosome in yeast. Eur. J. Cell Biol. 96, 591–599. https://doi.org/10.1016/j.ejcb.2017.05.001

Vaskovicova, K., Stradalova, V., Efenberk, A., Opekarova, M., Malinsky, J., 2015. Assembly of fission yeast eisosomes in the plasma membrane of budding yeast: import of foreign membrane microdomains. Eur. J. Cell Biol. 94, 1–11. https://doi.org/10.1016/j.ejcb.2014.10.003

Walther, T.C., Aguilar, P.S., Fröhlich, F., Chu, F., Moreira, K., Burlingame, A.L., Walter, P., 2007. Pkh-kinases control eisosome assembly and organization. EMBO J. 26, 4946–4955. https://doi.org/10.1038/sj.emboj.7601933

Walther, T.C., Brickner, J.H., Aguilar, P.S., Bernales, S., Walter, P., 2006. Eisosomes mark static sites of endocytosis. Nature 439, 998–1003. https://doi.org/Doi 10.1038/Nature04472

Wang, H.X., Douglas, L.M., Veselá, P., Rachel, R., Malinsky, J., Konopka, J.B., 2016. Eisosomes promote the ability of Sur7 to regulate plasma membrane organization in *Candida albicans*. Mol Biol Cell 1–46. https://doi.org/10.1091/mbc.E16-01-0065

Westergaard, M., Mitchell, K.H., 1947. *Neurospora V.* A synthetic medium favoring sexual reproduction 573–577. https://doi.org/10.1002/j.1537-2197.1947.tb13032.x

Zhang, L.B., Tang, L., Ying, S.H., Feng, M.G., 2017. Two eisosome proteins play opposite roles in autophagic control and sustain cell integrity, function and pathogenicity in *Beauveria bassiana*. Environ. Microbiol. 19, 2037–2052. https://doi.org/10.1111/1462-2920.13727

Ziółkowska, N.E., Christiano, R., Walther, T.C., 2012. Organized living: formation mechanisms and functions of plasma membrane domains in yeast. Trends Cell Biol. 22, 151–158. https://doi.org/10.1016/j.tcb.2011.12.002

Ziółkowska, N.E., Karotki, L., Rehman, M., Huiskonen, J.T., Walther, T.C., 2011. Eisosome-driven plasma membrane organization is mediated by BAR domains. Nat. Struct. Mol. Biol. 18, 854–856. https://doi.org/10.1038/nsmb.2080

Appendix A. Supplementary data

Supplementary Fig. S1 – S7, Table S1 – S2.

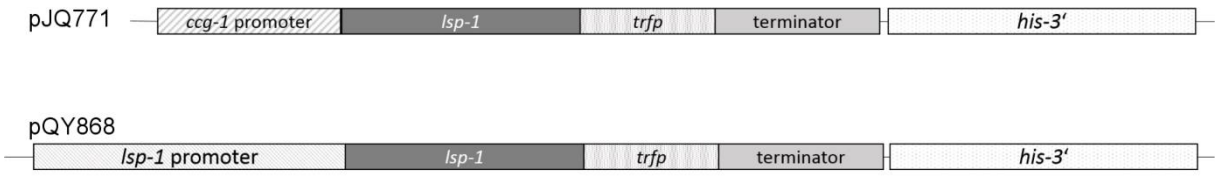

Supplementary Fig. S1. Schematic representation of vectors pJQ771, pQY868. Vector components are indicated within the drawings. The His-3 gene fragment was used as a selection marker. Only the main parts of plasmids are shown.

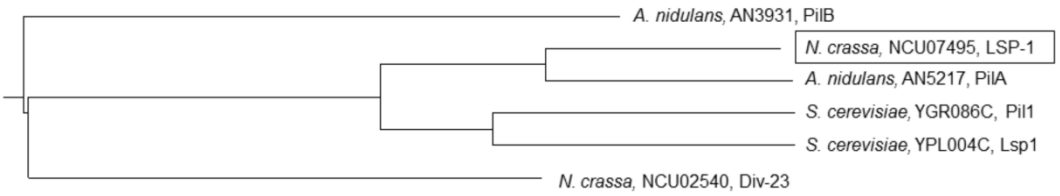

Supplementary Fig. S2. Phylogenetic analysis results. LSP-1 protein in *N. crassa* is a homologue of the *A. nidulans* PilA, which is a core component of eisosomes. Both *A. nidulans* PilA and *N. crassa* LSP-1 are homologous to the yeast core eisosomal proteins Pil1 and Lsp1. Analyzed with Clone Manager, Multiway Alignment, Scoring matrix: BLOSUM62, Similarity significance value set to 60%.

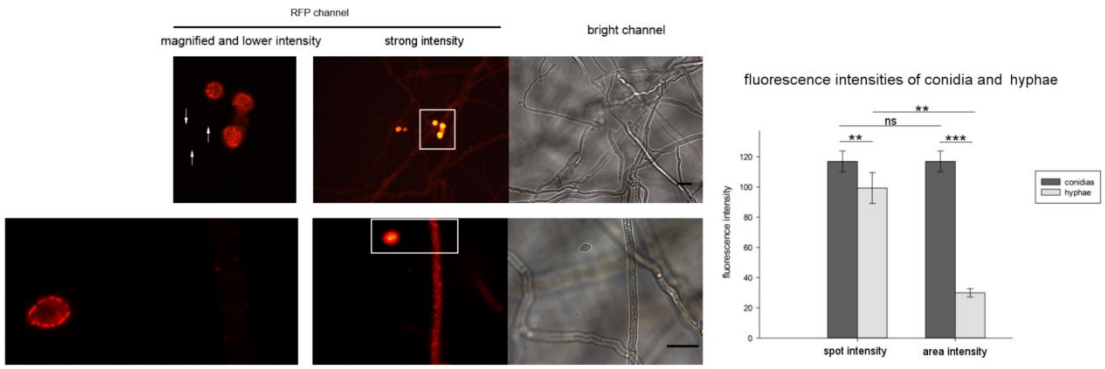

Supplementary Fig. S3. Comparison of LSP-1::RFP fluorescence in conidiospores and mature hyphae. The captures show distributions of LSP-1 in hyphae and conidia. The fluorescence in conidia was much stronger than it was in hyphae. Magnifications of each box region are shown on the left sides. They were captured under a lower excitation light intensity. The distribution of LSP-1 in conidia were shown while the fluorescence in hyphae was too weak that only a few fluorescent spots could be observed under the same setting. The arrow points out several of the fluorescent spots in hyphae. The column graph shows the result of the fluorescence intensity analysis of conidia and hyphae in the same captures. Spot intensity means the fluorescence intensity of each spot, while area intensity means the average intensity of the cell/hypha. Mean ± SD, n = seven experiments, statistical analysis using t-test, **, P ≤ 0.01, ***, P ≤ 0.001, ns, not significant. Scale bars: 20 μm.

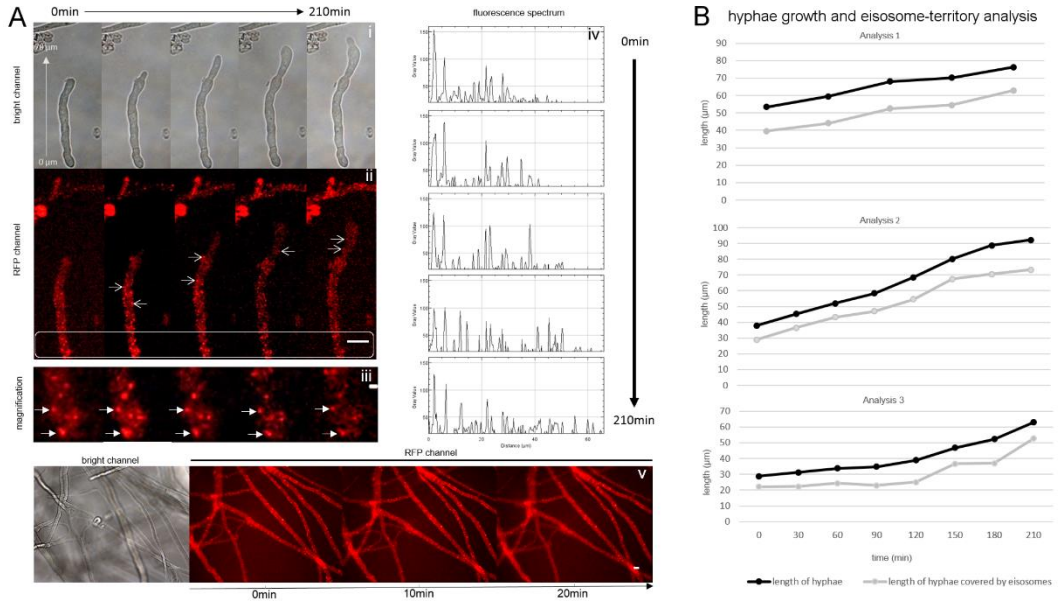

Supplementary Fig. S4. Time-lapse analysis of germinating hyphae and mature hyphae. A. Microscope captures and the fluorescence intensity profiles. **i.** Bright file of the germinating hyphae. **ii.** The LSP-1 distribution in the young germinating hyphae within 210 min. As fluorescence blenches, the intensity becomes weaker and weaker. However, there are still newly formed fluorescent spots detected (arrows direct), but with low intensity. **iii.** The magnifications of the oldest part (box region in i) of the young hypha in different capture time. The arrows show the fluorescent spots which did not change their localizations during the time-lapse analysis. **iv.** The RFP fluorescence intensity profiles analysis of the germinating hyphae. The left side of the hyphae surface was analyzed, and the long arrow shows the direction of the analysis. It showed that there were new fluorescent spots formed at the newly germinated part of the hypha tube. **v.** Eisosome distributions in the mature hyphae within 20 min. Localizations of eisosomes are not changed and no newly formed fluorescent spots were observed. **B.** The elongation of hyphae and the formation of eisosomes during time-lapse analysis (B-Analysis 1 is corresponding to A-ii and the microscope captures of B-ii and iii are not shown.). Scale bars: 10 μm.

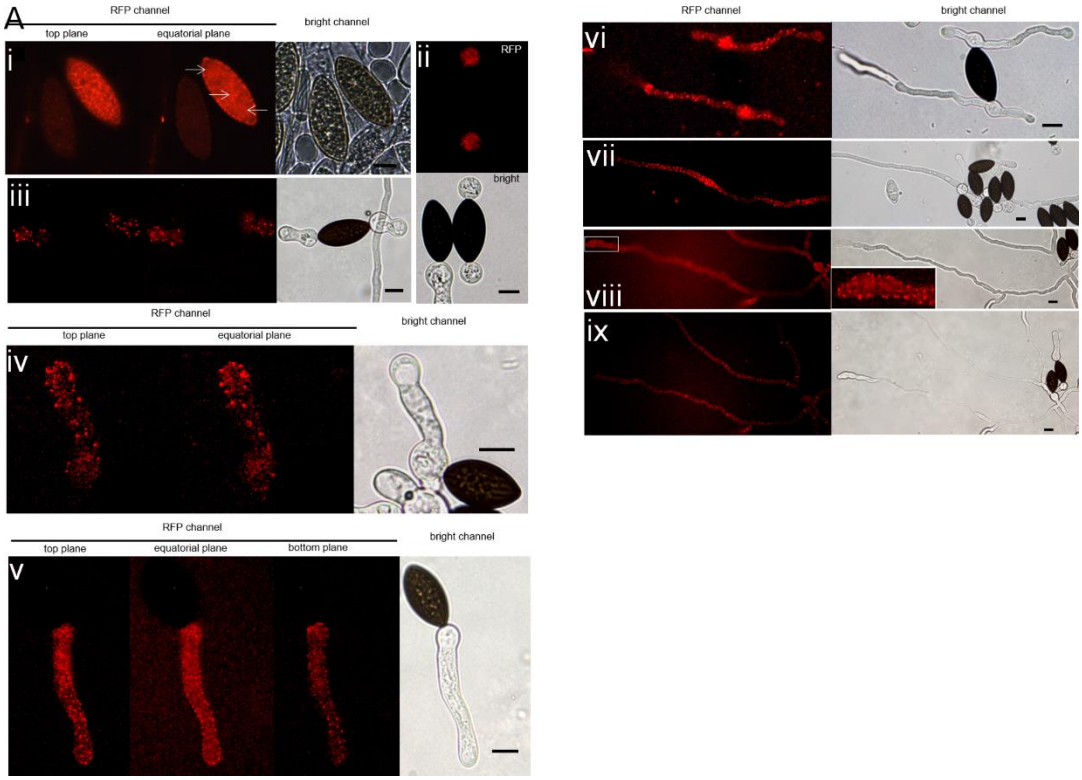

Supplementary Fig. S5. Eisosomes in ascospores and hyphae germinating from ascospores. A.i. Eisosomes locate at the cell membrane and evenly distributed in the cytoplasm of young ascospores. The arrows show fluorescent spots distributed in cytoplasm. **ii.** The germinating buds of an ascospore. Fluorescence was observed in the buds but not in the ascospore part because of melanins. **iii-ix.** The later growing stages of hyphae germinating from ascospores. **viii.** and **ix.** are captures of the same hyphae in different focus planes (viii. was focusing on the tip of the main hypha while ix. was focusing on the other part of the hyphae tube). Fluorescent spots were distributed at the whole tubes of hyphae, including the tip parts, which was very different from that in hyphae germinating from macroconidia. Scale bars: 10 μm.

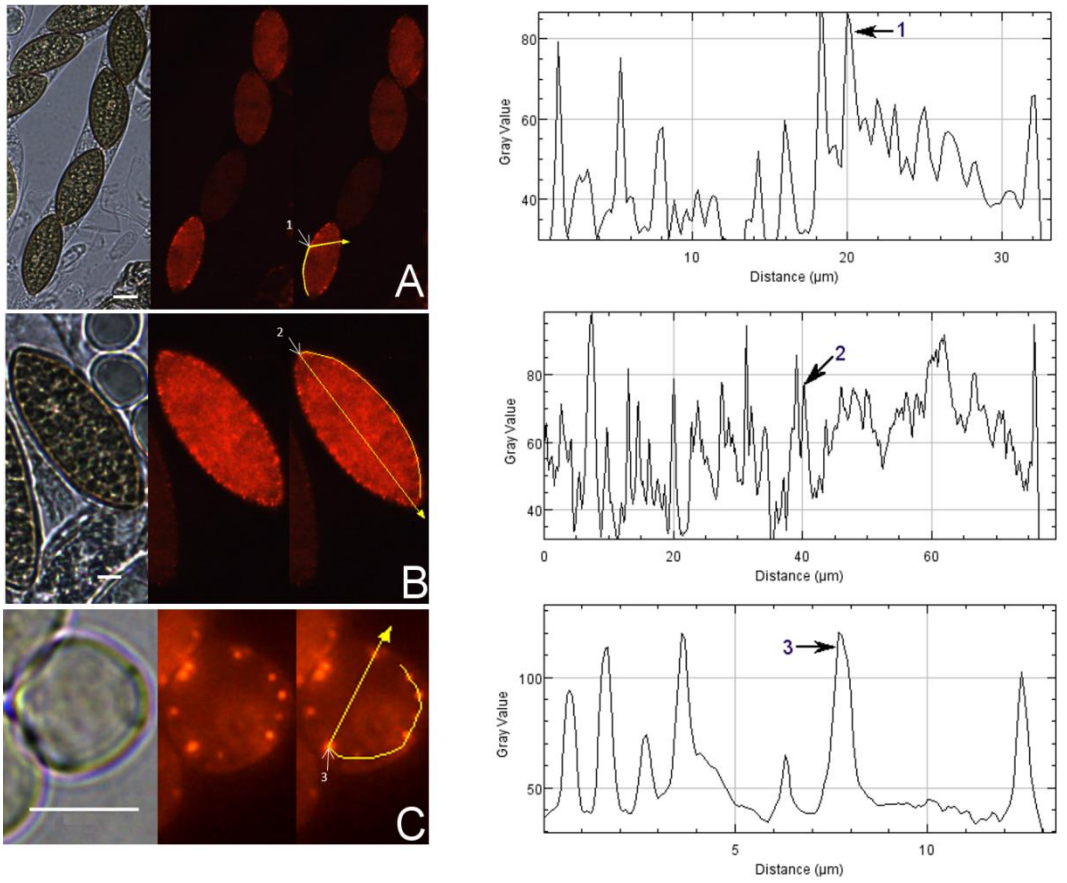

Supplementary Fig. S6. Eisosome/LSP-1 distribution in ascospores and macroconidia. Microscope captures and fluorescence intensity profiles of LSP-1::RFP in *N. crassa* ascospores and macroconidia. The arrow lines show the routes and direction of intensity profiles analysis and the numbers show the demarcation fluorescent spots between cell membrane and cytoplasm in all captures and fluorescence intensity profiles. The numbers and distance in fluorescence intensity profiles are consistent with those in the microscope captures. **A-B.** Captures of *N. crassa* ascospores. **C.** Captures of *N. crassa* macroconidia. Scale bars: 5 μm.

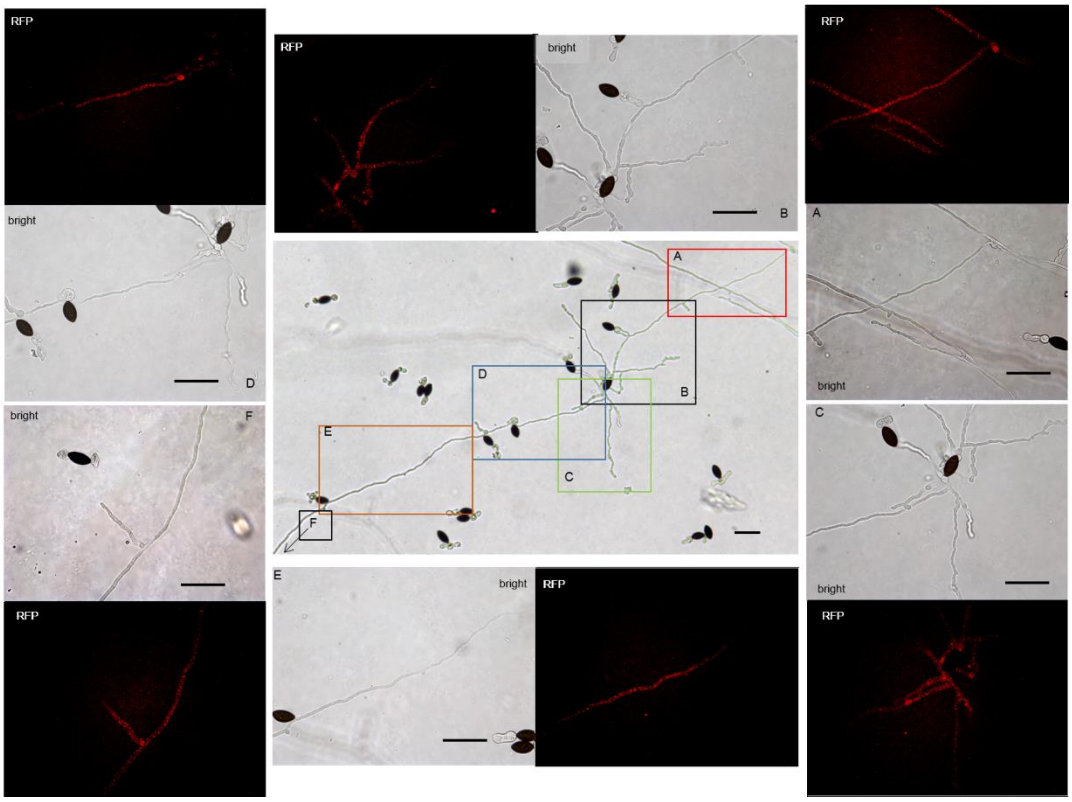

Supplementary Fig. S7. Eisosome distributions in the long-branched hyphae germinated from ascospores. A - E. The magnifications are corresponding to different parts of the hyphae (box region) according to the letter of the alphabet. **F.** The magnification of the down left hyphae part which is out of the low magnification capture. No obvious eisosome distribution differences were found at different parts of the hyphae. Scale bars: 50 μm.

Supplementary Table S1. Strains used in our research

Strain	Genotype	Source
FGSC6103	*his-3* (Y234M723) mat A	Fungal Genetics Stock Center
FGSC9716	*his-3* (Y234M723) mat a	Fungal Genetics Stock Center
NcT462	*ccg1 promoter:: lsp-1::rfp* mat a	This study
NcT475	*ccg1 promoter:: lsp-1::rfp* mat A	This study
NcT507	*lsp-1 promoter:: lsp-1::rfp* mat A	This study
NcT508	*lsp-1 promoter:: lsp-1::rfp* mat a	This study

Supplementary Table S2. Primers used in the study

Primer	Sequence	combined fragment
QY2942	5’-CCTTAATTAAGGTGAGGACGGATGAATAAGAC-3’	*N. crassa lsp-1* promoter
QY2943	5’-TTGGCGCGCCGGTGGATTAGGTAGTATTTATCGATTG-3’	*N. crassa lsp-1* promoter
AA2865	5’-GGAGACAUATGCATCGAACCTACTCCATG-3’	*N. crassa lsp-1* NCU07495
AA2866	5’-ACAAGCCUGGCAGCAACAGGCTCAGT-3’	*N. crassa lsp-1* NCU07495
FK2700	5’-GACGCCGGAGCGTCTTCGGGG-3’	pQY868 seqprimer
QY3218	5’-CACCGCCATCATCCACAAAG-3’	pQY868 seqprimer
QY3219	5’-TCGCTCTTCACCACTAACAC-3’	pQY868 seqprimer
QY3220	5’-GGAGGTGGCGGATTATGAGG-3’	pQY868 seqprimer
QY3221	5’-GCCTCATCTACAACGTCAAG-3’	pQY868 seqprimer
QY3213	5’-CGGGATCCCGATGCATCGAACCTACTCCATGCG-3’	*N. crassa lsp-1::rfp* fragment
QY3214	5’-CGGAATTCCTTGTACAGCTCGTCCATGCC-3’	*N. crassa lsp-1::rfp* fragment
QY3217	5’-GTTCCTGAAACGCAGATGTG-3’	pQY878 seqprimer
QY3218	5’-CACCGCCATCATCCACAAAG-3’	pQY878 seqprimer
QY3219	5’-TCGCTCTTCACCACTAACAC-3’	pQY878 seqprimer
QY3220	5’-GGAGGTGGCGGATTATGAGG-3’	pQY878 seqprimer
QY3221	5’-GCCTCATCTACAACGTCAAG-3’	pQY878 seqprimer

CHAPTER III

Multiple bioactivities of eisosomes and interspecific differences in *Neurospora crassa*.

Qin Yang, Frank Kempken*

Department of Botanical Genetics and Molecular Biology

Botanical Institute and Botanic Gardens

Olshausenstr. 40

24098 Kiel

Germany

Phone: +49 431 880 4274

Fax: +49 431 880 4248

* author for correspondence: fkempken@bot.uni-kiel.de

Abstract

Eisosomes are protein-containing domains in the plasma membrane in fungi and algae. The function(s) of eisosomes remains unclear. In this study, six eisosome components and five other proteins that appear to be spatially and temporally associated with eisosomes were identified in the filamentous fungus *Neurospora crassa*. These findings demonstrated interspecific differences, as the yeast eisosomal components Can1, Pkh1/2 and Fhn1 were not among the eisosomal proteins in *N. crassa*, and one new eisosomal protein (glucosamine-fructose-6-phosphate aminotransferase, gene ID: NCU07366) was found. Based on modeling and bioinformatic analysis of the identified eisosome components, an eisosomal structural model in *N. crassa* is presented. Multiple functions of eisosomes, associated with cell wall synthesis, response and signaling, transmembrane transport and actin organization are discussed.

Introduction

The biological membrane system is complex and has several critical functions for biochemical processes in living cells. It segments into coexisting compartments which enable spatiotemporal segregation and coordination of different activities within the system[1]. For example, it has been recognized for a long time that there are heterogeneous lateral compartments in the plasma membrane of all cells[2]. In fungi, plasma membrane lateral microdomains have been reported. These microdomains are named by specific marker proteins: the membrane compartment that contains Can1 (**MCC**), the membrane compartment that contains Pma1 (**MCP**) and the membrane compartment that contains Torc2 (target of rapamycin complex 2) (**MCT**)[3,4]. Eisosomes are protein complexes in fungi and algae which are located at the plasma membrane, associated with the MCC domain[5]. Eisosomes were initially proposed in the yeast *Saccharomyces cerevisiae* in 2006[6]. Currently eisosomes are described as large

cytosolic protein scaffolds that stabilize the invaginations of the integral membrane portion MCC[1]. Eisosomes have furrow shapes and consist of distinct protein compositions[7]. However, the exact composition of eisosomes remains controversial, even in *S. cerevisiae,* where eisosomes have been most studied[6]. Pil1, Lsp1 and Sur7 are the first reported eisosomal components and eisosomes are reported to be composed primarily of Pil1 and Lsp1 in *S. cerevisiae*[6]. In yeast, Pkh1 and Pkh2 regulate eisosome assembly and organization via the Pkh signaling pathway[8]. Slm1 and Slm2 are another pair of eisosomal proteins found in *S. cerevisiae.* These proteins have a BAR domain and act in actin cytoskeleton organization[5,9]. Furthermore, some proteins with unknown functions have been discovered to localize with eisosomes, including Seg1 and Ygr130c[10], Eis1 and Mdg1[9], Msc3[11].

For other fungi, only a few eisosomal proteins have been discovered so far. The eisosome compositions appears to be different in the analyzed fungi[12]*.* In *Aspergillus nidulans*, PilA, PilB and SurG were studied and described as core components of eisosomes[13]. Among them, PilA and PilB are homologs of the *S. cerevisiae* eisosomal proteins Pil1/Lsp1. SurG is a homolog of the eisosomal protein Sur7 in yeast[13]. However, in contrast to *S. cerevisiae,* Sur7 in *A. nidulans* is a core component of the eisosome[13]. The three eisosomal proteins in *A. nidulans* exhibit different characteristics between different types of cells, for example, PilA and SurG are necessary for eisosome organization in conidia, whereas in germlings of ascospores, the punctate structures are composed only of PilA, PilB is diffused in the cytoplasm and SurG is located in vacuoles and endosomes[13,14]. In addition, an Nce102 homolog was reported to be another eisosomal protein in *A. nidulans*[15]*.*

Not only the composition, but also the formation and function(s) of eisosomes remain unclear. The spatial location of the eisosome is regulated, as the polar distribution restriction found in *N. crassa* (Yang et al. Eisosomes Show Different Features in Morphologically Identical Hyphae Germinating from Sexual and Asexual Spores in

Neurospora Crassa.) was not only observed in the unicellular fungus *S. cerevisiae*[5,16], but also discovered in the filamentous fungi *A. nidulans*[13]. What is more, eisosomes are stably distributed at the cell periphery[15–17] and are always separated from each other; however, the mechanism for that is still unknown[5,11]. The functions of eisosomes have been studied in *S. cerevisiae*[18,19], *Candida albicans*[20,21], *Beauveria bassiana*[22], *Ashbya gossypii*[23] and *A. nidulans*[14,15]. Eisosomes have been reported to be involved in diverse cellular processes, such as cellular signaling[18], membrane domain formation[19], polarized growth[23], cell wall synthesis and morphogenesis[5,20], and pathogen virulence[22]. Even so, the significant function(s) of eisosomes is still poorly understood. As in *S. cerevisiae* no fitness defects were detected in cells lacking eisosomes[24], and in *A. nidulans* deletion of the core eisosomal proteins does not lead to any obvious growth defects and does not affect viability or germination of ascospores[13,14].

Neurospora crassa is a well-established model organism for genetics, biochemistry and molecular biology since it was first described by Payen in 1843[25]. The genome is about 40 megabases containing 10,000 protein-coding genes[26]. Recently, the LSP-1 protein in *N. crassa* was detected as a functional and core component of the eisosome (Yang et al. Eisosomes Show Different Features in Morphologically Identical Hyphae Germinating from Sexual and Asexual Spores in *Neurospora Crassa*.). Nevertheless, the composition of the eisosome is still poorly understood in *N. crassa.* Nor has the function(s) of eisosomes been reported in *N. crassa.* As a morphologically complex multicellular fungus, *N. crassa* has sexual and asexual life cycles with a range of cell types, which make it much more complicated than the unicellular yeast *Saccharomyces*[27,28]. Besides, in *N. crassa* there are many characteristic biological activities including hyphal fusion occurring at different stages[29], the establishment and maintenance of hyphal polarity[30] and so on, which are not found in unicellular yeasts. These make *N. crassa* a better-suited model system to deeply study the composition

and function(s) of eisosomes. Our data reveal the eisosome composition in *N. crassa* and bring new insights into the eisosome function(s).

Results

Isolation and enrichment of eisosomal proteins

To isolate eisosomes, the core eisosomal protein LSP-1 (Yang et al. Eisosomes Show Different Features in Morphologically Identical Hyphae Germinating from Sexual and Asexual Spores in *Neurospora Crassa*.) was fused with green fluorescence protein (GFP) and used as a reporter. *N. crassa* cells were ground to powder in liquid nitrogen and put into solution, centrifuged twice at different speeds to remove nuclei, organelles and intact cells in the pellet. During the isolation process, we determined that the eisosomes were in the supernatants after centrifugation by checking the GFP fluorescence with a fluorescence microscope (**Figure 1 A**). The supernatant was then loaded onto a 40-36-20% sucrose gradient for ultracentrifugation (**Figure 1 A-B**). After the ultracentrifugation six gradient fractions were taken and the eisosomes were specifically detected in the topmost fraction (**Figure 1 B**). Therefore, the first fraction was taken for further anti-GFP immunoprecipitation purification using magnetic beads. As LSP-1 is the fundamental and core component of eisosomes, the eluted fraction after the immunoprecipitation magnetic separation was enriched for eisosomal proteins. An isolation from a WT strain that expresses no GFP fused proteins was isolated and purified in the same way from the beginning and acted as a blank control in the subsequent mass spectrometry analysis, because it contains proteins nonspecifically bound to the anti-GFP immunoprecipitation magnetic beads.

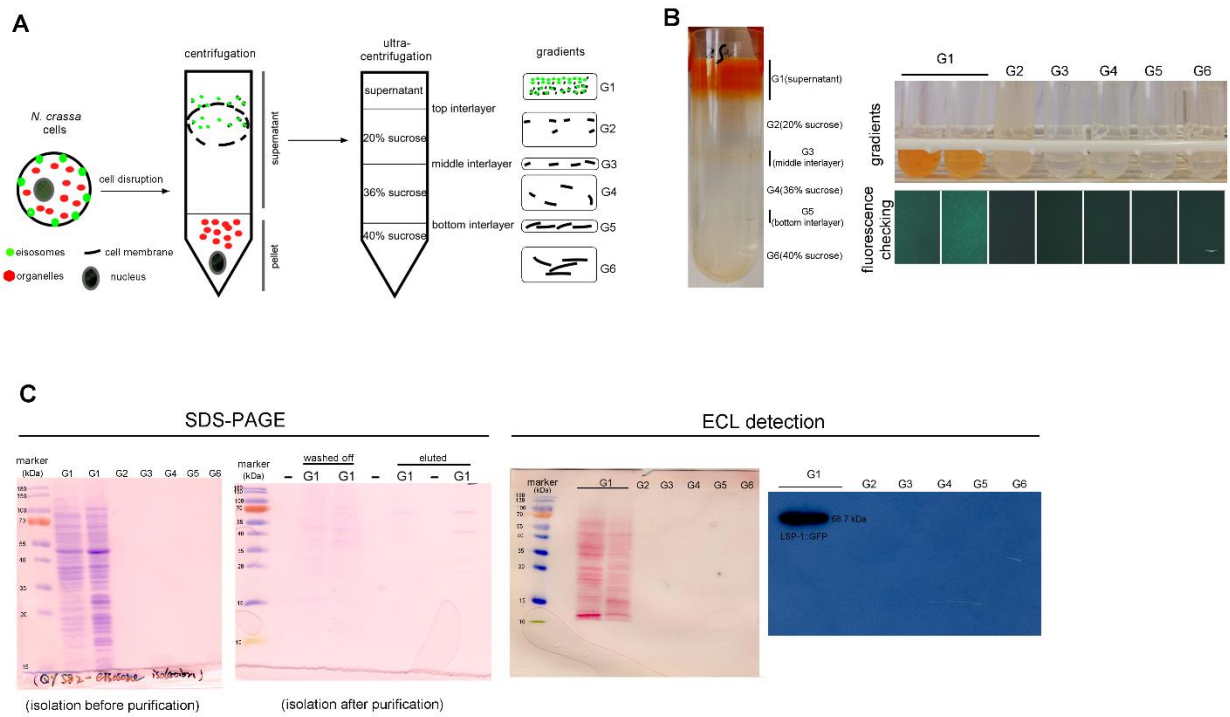

Figure 1. Isolation of eisosomes and the western blot result. A. The schematic diagram of the eisosome isolation process. Eisosomes were discovered in the supernatant after the normal centrifugation. G1 - G6 present the six gradients separated after the ultracentrifugation. **B.** The result of the eisosome isolation after the ultracentrifugation. The six fractions were transferred into six small tubes and checked under a fluorescence microscope. It seems there were two layers in the G1 fragment, so we transferred them into two tubes and found they were the same during later examinations. As the fluorescence result shown here, LSP-1::GFP was specifically detected in gradient G1. **C.** The SDS-PAGE images of the primary isolation and the enriched isolation, which reflects most of the unspecific proteins were removed after the purification. The ECL detection results reveal that proteins were successfully transferred on a nitrocellulose membrane and specific bands of LSP-1::GFP (68.7 kDa) were detected from G1 sample without any other bands. There was no band detected from G2 - G6 on films during ECL detection.

Western blot analysis

LSP-1::GFP was confirmed in the isolation by western blot (**Figure 1 C**). The signal of the fusion protein was significant strong using enhanced chemiluminescence (ECL) detection. The band exists at around 70 kDa, which is consistent of the size of LSP-

1::GFP (68.7 kDa) in theory (**Figure 1 C**). The eisosome fragments were successfully extracted in the isolation. In addition, the by-product proteins which are not combined with LSP-1 were washed away during the enrichment process (**Figure 1 C**). The SDS PAGE result showed that there were many proteins of different sizes isolated after the pull-down enrichment. The protein concentration decreased approximately fivefold after the enrichment. An anti-GFP antibody was used for the western blot. All the samples used for further study in our research were detected by fluorescence analysis and showed strong GFP signals before western blotting.

Identification of proteins from the enriched eisosomal protein fragment

Once it was confirmed that the enriched fractions contained the LSP-1::eGFP eisosomal protein, liquid chromatography-tandem mass spectrometry (LC-MS) was used to identify proteins in the purified sample. As the ultra-centrifugation could easily extract proteins whose specific gravities are similar to eisosomes and the unspecific proteins may not be completely removed after GFP pull-down, it was necessary to set up control groups. The enriched sample was analyzed as the experiment group, while the isolation without GFP pull-down was set as the conditional control, and the enriched sample from WT was used as the blank control. The nonspecifically isolated proteins which were not combined with LSP-1 were largely removed by the specific immune pull-down, whereas the eisosomal proteins were mainly retained (**Figure 1 C**). In this way, the ratio of eisosomal components was greatly increased in the enriched sample. Considering that there might be proteins apart from eisosomes nonspecifically adhering to the magnet beads during the pull-down process, the peptide hits existing in the LC-MS blank control list will all be deleted from the final eisosomal protein list despite the augmentation of their ratio. With this condition, in the comparison of the experimental group and the conditional control, we detected twenty-two (excluding LSP-1) eisosomal proteins from the LC-MS analysis (**Table 1**).

Table 1. LC-MS identification result. *

gene ID**	nomalized spectra		ratio	protein coverage	relationship to eisosomes
(FungiDB)	control	purification	(control/purified)		
NCU07495	12	611	50.9	66%	highly colocated
NCU03647	3	232	77.3	47%	highly colocated
NCU02540	12	138	11.5	54%	highly colocated
NCU02120	0	108	-	31%	related
NCU02425	1	73	73.00	30%	highly colocated
NCU05803	6	71	11.83	20%	related
NCU07366	10	71	7.10	37%	highly colocated
NCU03897	12	67	5.58	27%	related
NCU06943	12	60	5.00	37%	related
NCU02839	8	53	6.63	41%	related
NCU06544	3	51	17.00	23%	related
NCU09808	6	48	8.00	34%	related
NCU08875	4	44	11.00	20%	related
NCU08699	6	41	6.830	40%	related
NCU02207	8	41	5.13	47%	related
NCU05887	2	37	18.50	34%	related
NCU09700	4	33	8.25	32%	related
NCU08340	3	31	10.33	57%	related
NCU03102	4	28	7.00	31%	related
NCU00410	2	26	13.00	29%	related
NCU07567	3	26	8.67	28%	related
NCU09119	3	26	8.67	30%	related
NCU08920	5	25	5.00	26%	related

* protein threshold = 95%; peptide threshold = 95%; peptides contigs ≥ 5.

** The gene annotation and production are listed in Supplementary Table S1.

All of the 22 proteins were detected from the top hits with a protein threshold of 95%, peptide threshold of 95%, and more than five peptide contigs were detected in the LC-MS analysis. Additionally, the ratio of these proteins in the purification sample were at least five-fold greater than those in the conditional control. In our study, we ranked the 22 top hits (excluding LSP-1) by their normalized spectral parameter and assumed that the proteins with normalized spectra higher than 70 are core eisosomal proteins in *N. crass* (**Table 1**). In this way, we discovered six (excluding LSP-1) fundamental eisosomal proteins from the LC-MS analysis. We subsequently tested our hypothesis by dual fluorescence localization analysis. Four of the assumed core eisosomal proteins were tagged by green fluorescence protein (GFP) and individually expressed with the eisosomal reporter protein LSP-1::RFP (red fluorescence protein). We examined the colocalization of each protein with the known core eisosomal protein LSP-1 and finally confirmed that these four proteins are all fundamental eisosomal components (**Figure 2**). The dual fluorescence intensity profiles showed that the fluorescence from each protein (GFP) was perfectly colocalized with LSP-1::RFP (**Figure 2 A**). Even more intriguing, the four proteins all got extremely high Pearson's correlation coefficient values in the colocalization analysis with LSP-1, which confidently indicates that they are located in eisosomes in *N. crassa* cells (**Figure 2 A**).

Homolog analysis of eisosomal proteins

Several eisosomal proteins have been discovered since 2006[6]. Most of these are found in *Saccharomyces cerevisiae* and a few homologs of the yeast eisosomal proteins have been found in other fungi. Use bioinformatic methods, we found eleven homologs (excluding LSP-1) of eisosomal proteins in *N. crassa* (**Table 2**). Most of these matched eisosomal proteins in *S. cerevisiae,* which are all well-known eisosomal proteins but were never confirmed as eisosome components in *N. crassa*. However, it is surprising that the predicted eisosomal protein list obtained by homolog analysis

Table 2. Putative eisosomal proteins from homolog analysis.

gene and production (Gene ID from fungiDB)	GO terms (from fungiDB)	relationship to eisosomes	homolog in yeast
NCU07495 sphingolipid long chain base-responsive protein LSP1	eisosome; response to heat	highly colocated	Pil1/Lsp1
NCU02540 meiotic expression up-regulated protein 14	response to light stimulus	highly colocated	Pil1/Lsp1
NCU03647 hypothetical protein	cellular response to oxidative stress	highly colocated	Ykl050c
NCU04639 non-classical export protein (Nce102)	membrane-associating domain; membrane	highly colocated	Nce102
NCU05230 hypothetical protein	membrane-associating domain	highly colocated	Nce102
NCU04195 purine-cytosine permease FCY21	cellular component; membrane	partly colocated	Lyp1
NCU00586 non-anchored cell wall protein-6	cellular component; fungal-type cell wall	partly colocated	Sur7
NCU03571 serine/threonine protein kinase	protein phosphorylation; response to oxidative stress	unrelated	Pkh1
NCU05198 general amino acid permease	cellular component; membtane	unrelated	Lyp1/Can 1
NCU07334 uracil permease	cellular component; membtane	unrelated	Can1
NCU07754 methionine permease	cellular component; membrane	unrelated	Lyp1
NCU04809 MFS phospholipid transporter	integral component of membrane	unrelated	Fhn1
total		**12**	

hardly coincided with the LC-MS eisosomal protein list. Except for LSP-1, there were only two proteins (NCU02540 and NCU03647) that existed on both lists (**Figure 2 B**). These two proteins have been verified as core components of eisosomes in *N. crassa,* as was described above. Thus there are 20 proteins newly discovered to be associated with eisosomes (four core eisosomal proteins and 16 candidate eisosomal proteins) from the eisosome enrichment and LC-MS analysis in this study.

For the other nine putative eisosomal proteins from the homolog prediction, which did not correspond with the LC-MS identification results, more experiment evidence was needed to validate whether they were truly eisosomal proteins. We performed fluorescence trace analysis to identify their localization with eisosomes. Each of these proteins was fused with GFP and expressed individually with LSP-1::RFP. We detected two proteins (NCU04639, a homolog of Nce102; NCU05230 hypothetical protein, another homolog of Nce102) highly co-locating with LSP-1 (**Table 2, Figure 2 A-B**); two proteins partly locating with LSP-1 (**Table 2**, **Figure 2** B, **supplementary Figure 1**); four proteins not locating with eisosomes at all and there was one protein that showed no fluorescence signal (**Table 2, Figure 2** B). For every fluorescence colocalization experiment, we performed a fluorescence density profile analysis, calculated the Pearson correlation coefficient and did statistical analysis to calculate the colocalization relationship between these proteins and eisosomes separately (**Figure 2** A). In *N. crassa*, NCU04639 is the non-classical export protein (Nce102) and is a homolog of the yeast eisosomal core component Nce102. In our research, NCU04639 was determined to have specific localization with eisosomes at the cortex of *N. crassa* cells (**Figure 2 A**). The fluorescence density profile experiment showed that the GFP signals from NCU04639 and the RFP signals from eisosomes significantly overlap. The value of the Person's coefficient is 0.85 ± 0.11 (**Figure 2 A**). NCU05230 is a hypothetical protein which is homologous to the yeast eisosomal protein Nce102. NCU05230 was not among the final LC-MS identified protein list (It

was detected in the eisosome enrichment LC-MS experiment, but was eliminated by the filter parameters). The fluorescence microscopy showed that NCU05230 was densely located at eisosomes at the *N. crassa* cell membrane (**Figure 2 A**). The dual fluorescence signals from NCU05230 and LSP-1 perfectly coincide in the fluorescence density profiles. The Pearson correlation coefficient value was 0.95 ± 0.03 (**Figure 2 A**). These strongly indicate that NCU04639 and NCU05230 are fundamental eisosomal components in *N. crassa*. With regard to the two proteins partly located at eisosomes, we determined that NCU00586 is the homolog of the yeast Sur7 protein and NCU04195 is the homolog of LYP1 in *S. cerevisiae*. These two proteins all have multifarious distributions in *N. crassa* cells. The fluorescence analysis captures showed that they form spot patterns at the cell membrane and cytoplasmic pools as well as spot patterns in the cytoplasm (**supplementary Figure 1A**). The fluorescence density profile analysis showed that the GFP signals from these two proteins are not completely overlapped with the fluorescence from LSP-1::RFP(**supplementary Figure 1A**). At most of the LSP-1::RFP fluorescence profile peaks, there were co-locating GFP fluorescence profile peaks for those proteins; nevertheless, the area and the value of those peaks did not perfectly coincide with each other as the core eisosomal components' did. The Pearson's coefficient values for NCU00586 and NCU04195 were 0.32 ± 0.01, 0.23 ± 0.04 respectively (**supplementary Figure 1B**), which demonstrates that NCU00586 and NCU04195 were partly located with eisosomes but were not among the main components of eisosomes in *N. crassa*. These proteins may dynamically locate at eisosomes for their function(s) in different biological processes and dissociate from eisosomes after that. It indicates eisosomes could be dynamic complex protein structures that are involved in multiple functions.

In our research, five eisosome homologous proteins were determined not to be components of eisosomes (**Figure 2** B). It was determined that the *N. crassa* proteins NCU03571, NCU05198, NCU07334 and NCU07754 are homologs of eisosomal

proteins Pkh1, Can1/Lyp1, Can1 and Lyp1 respectively. Surprisingly, in our study, we found that these four proteins were not components of eisosomes in *N. crassa*. Their GFP signals did not overlap with the LSP-1::RFP signals in the fluorescence density profiles. As for NCU04809, it is a homolog of eisosome component Fhn1 in *S. cerevisiae.* We did not detect any significant fluorescence signals at the cell membrane from the GFP fused protein in the transformed cell.

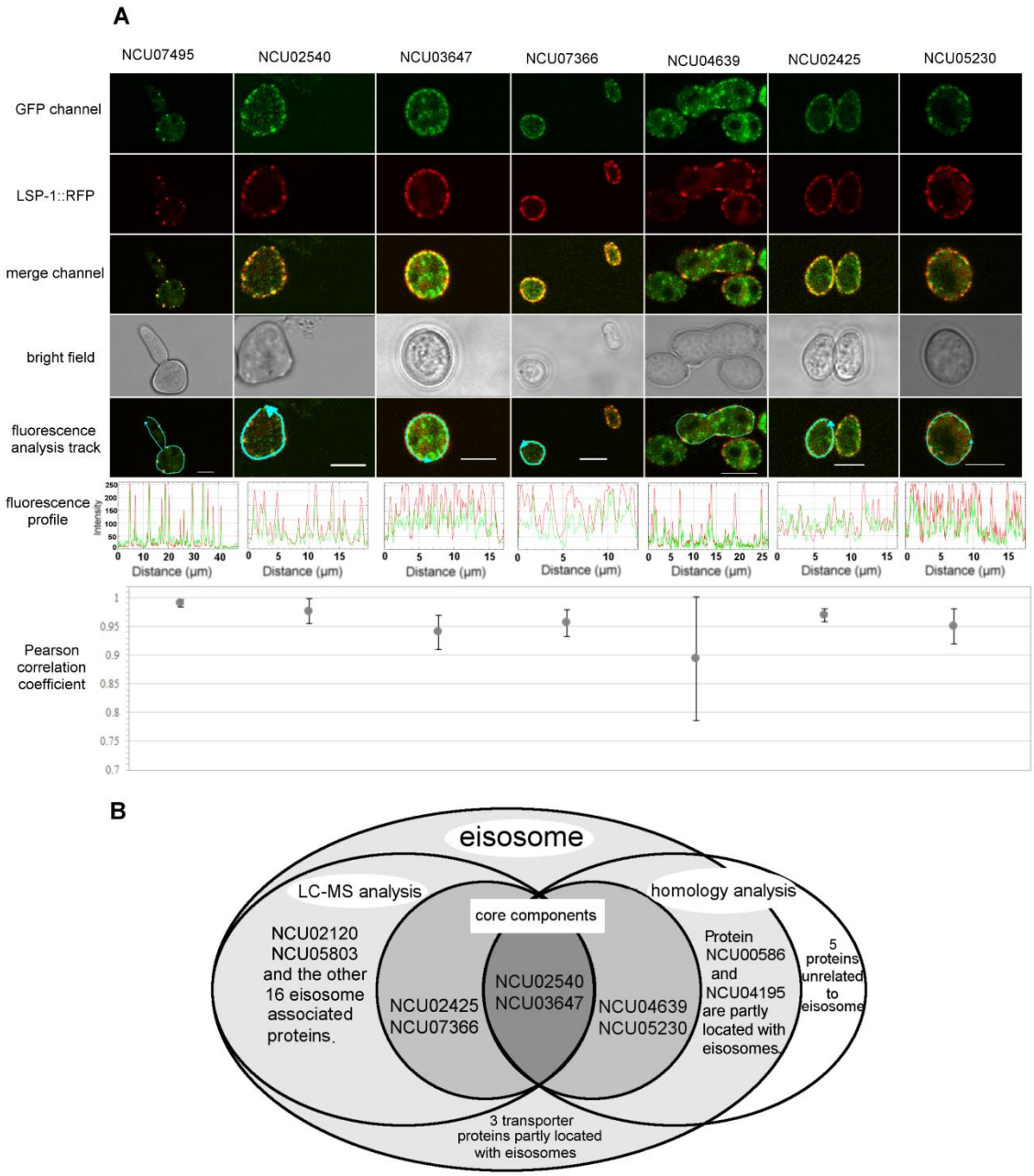

Figure 2. Localization verification of the core eisosomal proteins identified in our

study. A. The dual fluorescence colocalization analysis of LSP-1::RFP and eisosomal proteins tagged by GFP. The GFP and RFP signals merged well, which reveals that the eisosomal proteins are highly co-located with eisosomes. The fluorescence profiles and the Pearson correlation coefficients confirmed the colocalization between the eisosomal proteins identified in the current study and eisosomes. The arrow lines in the fluorescence analysis track channel shows the routes of the fluorescence density profile analysis. The Pearson correlation coefficient value is between -1 and +1, where the value closer to 1 means more positive correlation; 0 means no correlation; the value closer to -1 means more negative correlation. Mean ± SD, n ≥ three experiments, statistical analysis using one-way analysis of variance (P = 0.012, results significant). **B.** Overview of the LC-MS analysis, homolog analysis and transporter protein detection for eisosomal protein identification.

Three transporter proteins were detected to partly locate at eisosomes

In addition to the eisosomal proteins discovered from the LC-MS and the homolog analysis, we detected three transporters that partly locate at eisosomes in *N. crassa* cells (**Table 3**, **Figure 2 B**). It is well known that eisosomes and transporter proteins are all located at the cell membrane[31,32]. In order to determine whether there are connections between them, we fused GFP to some transporter proteins and performed the dual fluorescence localization analysis. NCU06352 (oligopeptide transporter 4), NCU06384 (MFS sugar transporter) and NCU01065 (ammonium transporter MEP2) were discovered to associate with eisosomes (**Table 3, supplementary Figure1**). Their colocalization statistical analysis yielded Pearson correlation coefficients of 0.33 ± 0.10; 0.35 ± 0.04 and 0.34 ± 0.08 respectively (**Table 3**, **supplementary Figure1 B**), which indicates that they all associate with eisosomes in *N. crassa* but not strongly. This relationship suggests that eisosomes may participate in transmembrane transport in *N. crassa* cells.

Table 3. Three transporter proteins partly located at eisosomes.

gene and production (Gene ID from fungiDB)	function prediction (GO terms from funfiDB)	protein length	relationship to eisosomes
NCU06352 oligopeptide transporter 4	transmembrane transport	1057 aa	partly colocated
NCU01065 ammonium transporter MEP2	cellular component; membrane	481 aa	partly colocated
NCU06384 MFS sugar transporter	integral component of membrane	532 aa	partly colocated
total	3		

Characteristics of the core eisosomal proteins

The six core eisosomal proteins identified in our study, as well as the LSP-1 protein, were analyzed with the I-Tasser and ProFunc approaches for their characteristics. The predicted protein structures are shown in **Figure 3**.

For the eisosomal marker LSP-1, the model was generated by using the templates, including 3pltA, in the PDB library without any restraints. LSP-1 contains a conserved domain which belongs to the Pil1 superfamily. The model has a filament shape (**Figure 3** A) consisting of 374 residues. It contains 16 α-helices accounting for 58.3% of the residues. The rest of the residues (41.7%) include other secondary structures such as 3_{10}-helix, beta turns and gamma turns and there is no β-sheet in the model (**Figure 3** B).

The protein NCU02540 had a high similarity to LSP-1. The model also has a filament shape (**Figure 3** A) and was mainly generated by using the template 3pltA in the PDB library. NCU02540 has the same Pil1 superfamily conserved domain as LSP-1. In contrast to LSP-1, the NCU02540 model has only four α-helices accounting for 53.7% of the 339 residues and the helices individually consist of more than 18 residues. In

the model, the remaining 46.3 % of the residues are composed of other secondary structures such as beta turns and gamma turns. There is no β-sheet in the model (**Figure 3** B).

The model of NCU03647 was constructed according to the threading template alignment including 5yz0A in PDB. It has 1062 residues with 69 helices including 52 α-helices accounting for 51.5% and 17 3_{10}-helices accounting for 4.1%. In addition, there are two β-sheets accounting for 0.3%, with 44.1% consisting of other secondary structures such as β-bulges, helix-helix interactions, beta and gamma turns (**Figure 3** B). The model has a spiral shape (**Figure 3** A).

The X-ray crystallographic structure of glucosamine-6-P synthase 2j6hA and some other structures in the PDB library served as templates without any restrains to build the model of protein NCU07366 which is a new eisosomal protein identified in our study. The model has 22 helices including 18 α-helices accounting for 30.4% and five 3_{10}-helices taking up 2.3%, (with the last α-helices and 3_{10}-helices blending into one helix) of the total 700 residues. There are 17 β-sheets which accounts for 12.1% of the residues in the model, and 55.1% of other secondary structures (**Figure 3** B). The model has an approximately dumbbell shape (**Figure 3** A).

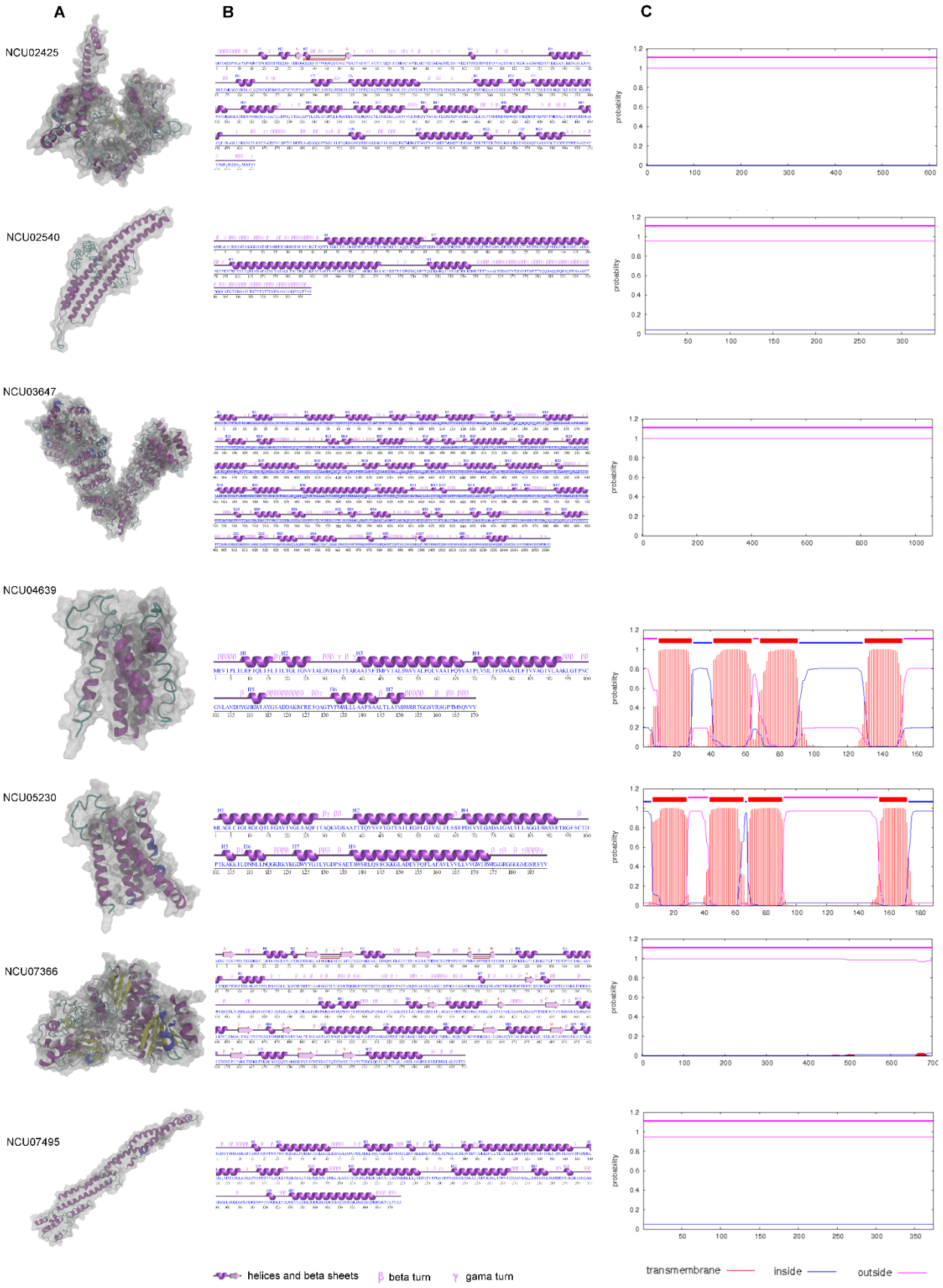

Figure 3. The modelling and characteristics analysis of eisosomal core

components. A. The column of the protein structures modelled with I-Tasser and visualized with VMD. **B.** The secondary structure characteristics of each core components. **C.** The transmembrane analysis of each core eisosomal protein.

Based on templates from the PDB entry such as 6aayA, the protein structure prediction was performed. The model of NCU02425 has a hooked shape (**Figure 3** A) and contains 20 α-helices and four 3_{10}-helices accounting for 42.4% of the total 616 residues; two short β-sheets accounting for 1% and other secondary structures accounting for 56.7% (**Figure 3** B).

NCU04639 is an eisosomal protein in the homolog analysis but was not among fragments obtained in the LSP-1 pull-down procedure. It was modeled according to the threading template alignment of X-ray real structures including the 5tjvA protein in the PDB library. The predicted model has a barrel-like shape (**Figure 3** A) with seven α-helices (including three long helices consisting of 13, 24 and 29 residues and three short helices composed of five, five, eight and nine residues) accounting for 54.7% of 170 residues. There is no β-sheet in the model and 45.3% of other secondary structures including helix-helix interactions, beta and gamma turns (**Figure 3** B). It is a transmembrane protein located at eisosomes (**Figure 3** C).

NCU05230 is the other core eisosomal protein identified from homolog analysis but missing from in the final LC-MS result. The model was generated by using known structural proteins including 4amjA and 5tjvA in the PDB library as templates. The length and shape of the model is similar to NCU04639 (**Figure 3** A). It was determined to be another transmembrane protein located at eisosomes (**Figure 3** C). The secondary structure of the NCU05230 model consists of seven α-helices accounting for 68.3% (four long α-helices respectively composed of 24, 26, 27 and 38 residues; three short ones with four, four and six residues) of 189 residues and two 3_{10}-helices accounting for 2.1%. There is no β-sheet and the other secondary structures in the

model are helix-helix interactions, beta and gamma turns accounting for 29.6% (**Figure 3** B).

Structural and functional analysis of the core eisosomal proteins

As no obvious phenotype was observed from mutants of each of the six core eisosomal proteins identified in our study, nor from mutants of the LSP-1 protein, a bioinformatic analysis was performed to predict their structural and functional characteristics.

The model of LSP-1 has a structural conservation with the *S. cerevisiae* Lsp1 protein, spectrin and actin. The protein is functional in actin filament organization and cell connection and is a cell membrane lateral component. It could have a H^+/K^+-exchanging ATPase or xenobiotic transporter activity according to the bioinformatic analysis. However, the confidence score was not high.

The structural analog analysis in the modelling shows NCU02540 protein has substantial conservation with the yeast Lsp1 protein which is an eisosomal protein but is not functional in eisosome formation. It is a lateral cell membrane component. It probably has the Na^+/K^+ transferase activity and is associated in ATP synthesis based on the functional analysis.

For protein NCU03647, six conserved protein superfamilies were detected, which are the eisosome-1 superfamily required for normal formation of eisosomes; the SMC_prok_A superfamily playing roles in organizing and segregating chromosomes for partition; the SbcC superfamily associated with DNA replication, recombination and repair; the DUF5401 superfamily having an unknown function; the Pneumo_att_G superfamily of attachment membrane glycoprotein G; and the PLN03237 superfamily for DNA topoisomerase 2. The NCU03647 protein has structural similarity with inositol 1,4,5-trisphosphate receptor and human ATR-ATRIP complex. The functional analysis

indicates it has endo-alpha-N-acetylgalactosaminidase activity and is associated with protein binding and nuclear protein transfer.

NCU07366 protein has conserved domains belonging to five superfamilies: the PLN02981 superfamily is describe as the glucosamine:fructose-6-phosphate aminotransferase; the GlmS superfamily is the glucosamine 6-phosphate synthetase containing amidotransferase and phosphosugar isomerase domains; the glmS superfamily including the glucosamine-fructose-6-phosphate aminotransferase (isomerizing); the GFAT superfamily that is found at the N-terminus of glucosamine-6P synthase, the domain catalyzes amide nitrogen transfer from glutamine to the appropriate substrate; and the SIS superfamily including the sugar Isomerase that is found in many phosphosugar isomerases and phosphosugar binding proteins. The structure alignment of the model shows that NCU07366 has a similarity with the isomerase domain of glucosamine 6-phosphate synthase. In agreement with the analog result, the functional analysis confidently verified that NCU07366 has glucosamine-6-phosphate synthase activity. In addition, the protein has a binding function that interacts with proteins or protein complexes, which well explains the colocalization of NCU07366 and eisosomes.

NCU02425 has conserved domains belongs to PH (Pleckstrin Homology) and PH-like superfamily. These superfamilies generally play roles in targeting proteins to the appropriate cellular location or in the interaction with a binding partner and are found in cytoskeletal associated molecules as well as in eukaryotic signaling proteins. The model of NCU02425 protein is similar to *Prevotella buccae* RNase and RNA binding protein at the structural level. The functional analysis was not able to assign any enzyme activity with confidence but found that it has a protein binding function as well as a function in the location establishment of cellular components. What is more, it is involved in protein-containing complexes located at the cell periphery and has roles in

cellular protein-containing complex assembly. The analysis indicated that the protein most probably establishes the localization and formation of eisosomes.

A MARVEL superfamily conserved domain was detected during the analysis of protein NCU04639. It is a membrane-associating domain usually found in lipid-associating proteins and may play roles in membrane apposition and vesicle transport. The model of NCU04639 has structural analogs such as oxidoreductase, lipid G protein coupled receptor and the cytochrome C family protein. The functional analysis showed it to be an integral component of the membrane that plays roles in the G protein-coupled receptor signaling pathway and defense response. Furthermore, it is associated with the glycosaminoglycan catabolic process, peptidoglycan and cell wall macromolecule metabolic process.

Similar to the NCU04639 protein, NCU05230 also contains a conserved domain that belongs to the MARVEL superfamily and has the same structural analogs, which reveals that these two proteins probably have similar function(s) at the plasma membrane. However, in contrast to NCU04639, NCU05230 has an oxidase analog at the structural level and appears to have adenylosuccinate lyase activity based on a confident score during the functional analysis. NCU05230 is predicted to relate to the G protein-coupled receptor signaling pathway and establishment of cellular component localization. In addition, it has a transmembrane signaling receptor function and takes part in the phosphate-containing compound metabolic process, light stimulus detection process and cellular protein modification process. It is not only predicted as an integral component, but also as a photoreceptor inner/outer segment at the plasma membrane.

Structure of eisosomes

The eisosomal core components from LC-MS and homolog analysis were analyzed by TMHMM server to detect their transmembrane location (**Figure 3** C). Interestingly, the

four proteins that combine with LSP-1, which were identified in the LC-MS analysis, show no transmembrane domains. They are all located outside of the phospholipid bilayer. In contrast, NCU04639 and NCU05230, which were identified from the homolog analysis, rather than in the LSP-1 pull-down isolation, are both transmembrane proteins. This is consistent with the protein modeling result. Each of the transmembrane proteins has four transmembrane regions. The transmembrane parts of NCU04639 are between residues 10-29, 42-64, 69-91 and 130-152 while the transmembrane areas of NCU05230 lay between residues 7-29, 44-66, 69-91 and 154-172. The beginning of protein NCU04639 is out of the membrane lipid bilayers while protein NCU05230 starts from the inside of the cell membrane. The 2nd and 3rd transmembrane areas in both proteins are of same length and the locations are similar/same. The first and last transmembrane regions of NCU04639 are three and four residues longer than NCU05230. All the above considered, in the model of the eisosome, it is clear that LSP-1 and the proteins combined with it are located on the cytosolic side of the cell membrane. They constitute the framework of the furrow structure of eisosomes while NCU04639 and NCU05230 traverse the cell membrane and are located at the furrow on the cell membrane (**Figure 4**). These differences could account for the fact that NCU04639 and NCU05230 are both eisosomal core components that can be identified by homolog analysis but cannot be enriched by the LSP-1 pull-down procedure. The eisosomal proteins that partly associate with eisosomes may periodically be temporarily colocated at eisosomes as they perform their own dynamic and special function(s). According to the structural and functional analysis results of each eisosomal core component, NCU02425 establishes the location and promotes the assembly of eisosomes and then is bound with LSP-1 (NCU07495); LSP-1 and NCU02540 grasp the cell membrane and form the furrow structures of eisosomes; NCU03647 and NCU07366 bind to LSP-1 at eisosomes on the cytoplasmic side of the cell membrane and carry out their respective functions; NCU04639 and NCU05230 are transmembrane proteins located at the furrow of

eisosomes and may have connections with NCU02540 because the later has the Na^+/K^+ transferase activity, which needs transmembrane protein domains (**Figure 4**).

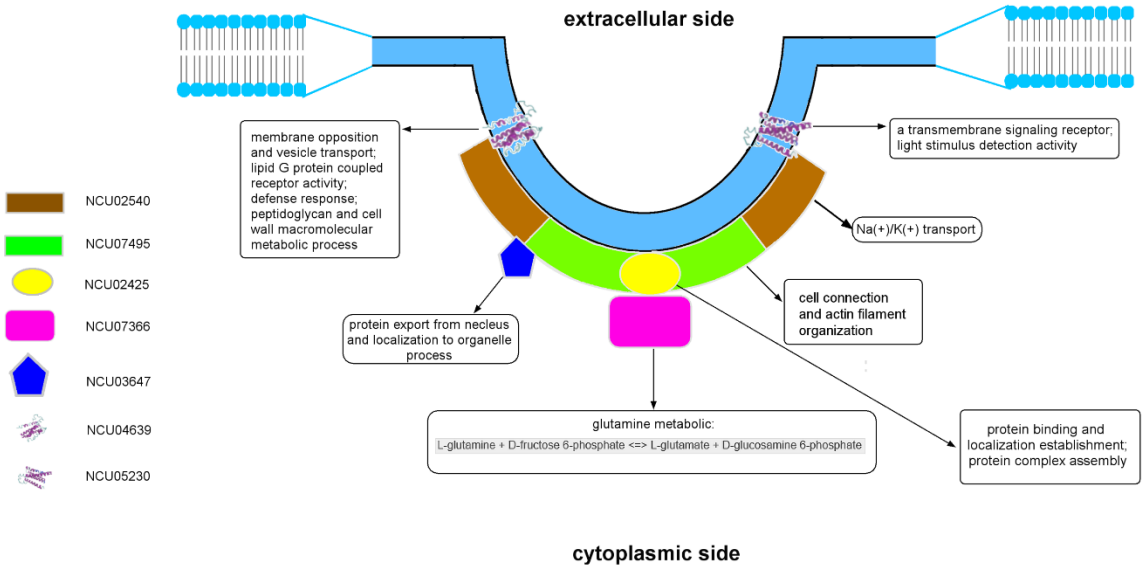

Figure 4. The model of the eisosome structure in *N. crassa*.

Discussion

In our study, we isolated the eisosomal proteins complexed to LSP-1 in *N. crassa*. The fluorescence from attached GFP conveniently and precisely reported the presence or absence of eisosomes during the isolation and enrichment. Interestingly, we found two proteins highly colocalized with eisosomes but not combined with LSP-1. This suggests that eisosomes are not a structure consisting of only one protein cluster, but rather a complex membrane domain including protein clusters, independent protein components and phospholipids.

In the LC-MS identification project, there were six prime eisosomal protein candidates that were selected with high confidence filter parameters (described in the Results section). We successfully verified that four of these are core eisosomal components in *N. crassa*. The other two proteins (NCU02120, coding a 5540 bp gene, and NCU05803,

coding an 8293 bp gene) were not tagged by GFP in the cloning experiment, but they are extremely likely to be core eisosomal proteins because their identification parameter is higher than some of the verified core eisosomal proteins. Nevertheless, we cautiously consider them as eisosome-associated proteins in our study until they are confirmed in further research.

For the two core eisosome components existing in the LC-MS analysis but not in the homolog analysis, NCU02425 has a homologous area with Slm1/2 in yeast, and NCU07366 is a new eisosome core component detected in our study. In contrast, most of the eisosomal proteins in the homolog analysis result are different than the proteins identified in the LC-MS experiment. What is more, seven of the eleven proteins identified as homologs to known eisosomal components in yeast are only partly or not at all located at eisosomes in *N. crassa* cells. One possible explanation could lie in the growth conditions during the research. Because eisosomes have dynamic compositions which are depending on different growth conditions[7,33]. From another aspect, it shows that the eisosomes in *N. crassa* are very different than those in *S. cerevisiae.* It is also confirmed that the eisosomes' compositions and assembly are different for different species, which is consistent with the published research[5,12,16]. For example, Sur7 and Slm1 were detected as two eisosomal proteins in budding yeast[6,34,35] and the Sur7 homolog was even examined as a core eisosome component in *A. nidulans*[13], whereas the detected homologs of Slm1 and Sur7 were not located in eisosomes in fission yeast[16]. Also, in our study on *N. crassa*, the Sur7 homolog was found only partly located at eisosomes. What is more, the homologs of the *S. cerevisiae* eisosomal components Can1, Pkh1/2, Lyp1 and Fhn1[18] were not at all located at eisosomes in *N. crassa*. This strongly indicate that the homolog analysis has limitations and is far from enough for eisosome composition research. We suggest a new, high throughput direction for the eisosome composition analysis that identifies

proteins in eisosome isolations by LC-MS followed by checking them through dual fluorescence analysis. (Details to be published in the near future.)

According to our study, based on the composition and structure, eisosomes could be hubs on the cell membrane, which have multiple functions associated with diverse bioactivities. For example, the eisosome component NCU03647 functions in nuclear protein transfer; NCU07366 plays roles in the glucosamine-6-phosphate (GlcN6P) synthesis process (GlcN6P is the prominent precursor in the biochemical synthesis of lipoprotein[36]); NCU04639 is associated with vesicle transport. It reveals eisosomes may have function(s) in protein modification and secretion. Furthermore, GlcN6P is an essential precursor of cell wall components chitin and peptidoglycan[37,38] and NCU04639 also play roles in the cell wall macromolecule metabolic process, which indicates that eisosomes are probably associated with cell wall synthesis. Additionally, NCU05230 and NCU04639 both have a transmembrane receptor function and the former plays roles in light stimulus detection while the latter is associated with defense response. Therefore, from our study, eisosomes appear to have function(s) in signaling pathways in *N. crassa* cells. Eisosomes may also be involved with cation transport and membrane potential, because NCU02540 is predicted to be an ion pump at the cell membrane. As for LSP-1, it has an actin filament organization activity, which demonstrates that eisosomes most probably have cytoskeleton related function(s) at the plasma membrane. Last but not the least, eisosome components NCU02425 and LSP-1 may establish the location of eisosomes on the plasma membrane.

The eisosome structure in *N. crassa* proposed in our study should be considered as a preliminary model. As eisosome composition research advances, new eisosome components in *N. crassa* are likely to be identified.

Materials and Methods

Media and growth conditions

The media and growth conditions in our study were as described previously[39].

Strains

The *N. crassa* strains used in our study are listed in **Supplementary Table S2**. The strains constructed in our study are based on the histidine auxotrophic strains FGSC #6103 and 9716 (Fungal Genetics Stock Center; Kansas City, MO, USA). The genes fused with *gfp/rfp* integrate into *N. crass* chromosomes by homologous recombination[40].

The bacterial strain *E. coli* XL1-Blue [*recA1, endA1, gyrA96, thi-1, hsdR17, supE44, relA1, lac F'proAB lacIqZΔM15 Tn10 (Tetr)*] (200249, Stratagene) was used for electroporation and chemical transformations. A *ccdB* survival *E. coli* strain [*F-mcrA Δ(mrr-hsdRMS-mcrBC) Φ80lacZΔM15 ΔlacX74 recA1 araΔ139 Δ(ara-leu)7697 galU galK rpsL (StrR) endA1 nupG fhuA::IS2*] (A10460, Invitrogen) was used for Gateway cloning.

Eisosome fragment isolation

The conidia of the LSP-1::GFP strainwere harvested and soaked in sterile water for three hours. Samples were centrifuged (Allegra X-30, Beckman Coulter) at 4000 rpm for 5 min and then the supernatants were removed. The fresh pellets were collected, and the harvested conidia were weighed. As soon as possible after weighting, the conidia were frozen in liquid nitrogen for 5 min and then stored at -80°C overnight. Samples of the frozen conidia were next ground into a fine powder in liquid nitrogen as quickly as possible using mortars and pestles. According to their fresh weight, the powders were immediately dissolved into the appropriate amount of solution buffer (5 ml/g). The dissolved samples were then centrifuged at 1000 × g for 10 min at 4°C (Avanti J-20 XP, Beckman Coulter), then the supernatants were collected and

centrifuged again at 11000 × g for 20 min at 4°C (Avanti J-20 XP, Beckman Coulter). The second supernatants were collected and put on ice. The supernatants and pellets were checked after every centrifugation using a fluorescence microscope (ECLIPSE Ci system plus INTENSILIGHT C-HGFI 130w lamp, Nikon) to make sure that the eisosome/LSP-1::GFP complexes were successfully isolated.

The gradients for ultracentrifugation were set as follows: 40% sucrose 10 ml, 36% sucrose 10 ml and 20% sucrose 12 ml. The gradients were transferred to the centrifugation tubes from the bottom (40% sucrose) to the top (20% sucrose) in a cool room and stored at 4°C for 2h. Then a maximum of 2 ml of the final supernatants were quickly loaded onto the cold gradient in the cool room. Next the tubes containing the samples and gradients were placed into centrifugation cups and centrifuged in an ultracentrifuge TST28.38 rotor at 24000 rpm for 1h at 4°C (Optima L-90K Ultracentrifuge, Beckman Coulter). After the ultracentrifugation, each fragment was carefully collected from each tube as soon as possible. The fluorescence of each fragment was checked with a fluorescence microscope (ECLIPSE Ci system plus INTENSILIGHT C-HGFI 130w lamp, Nikon) (a 40×/NA0.75 (plan fluor) objective lens was used to acquire images) and then they were stored at -80°C.

Enrichment of the isolated fragments

The isolation of eisosome fragment was enriched by using the μMACS GFP Isolation Kit (130-091-125, Miltenyi Biotec). Fifty μl of the GFP-Tag Microbeads were added from the kit to 1 ml of each protein sample. They were mixed well and were keep on ice for 30 min. The micro-columns in the kit were put on the magnet rack and then were equilibrated with 200 μl of lysis buffer. After that the protein-microbeads mixes were transferred into the equilibrated micro-columns. Next the micro-columns containing protein samples were washed four times with a total of 800 μl of washing buffer one from the kit before washing them once with 100 μl of washing buffer 2 from

the kit. The elution buffer from the kit was heated to 95°C initially. First, 20 μl of the pre-heated elution buffer was added into each micro-column and they were incubated at room temperature for 5 min. Finally the LSP-1::GFP combined proteins were eluted with 50 μl of the 95°C elution buffer.

Western blot

The protein samples were prepared and loaded onto a 5% stacking gel and 15% separating gel. After the samples were resolved by SDS-PAGE, they were transferred onto a 0.1 μm nitrocellulose transfer membrane (G161476, Whatman) under 3.5 mA/cm^2 (E835, Consort) for 30 min at room temperature. After that, the proteins were probed with an HPR conjugated mouse anti-GFP antibody (working dilution: 1:5000) (SIGMA-ALDRICH). Signals were detected by ECL detection.

LC-MS analysis

The isolated and enriched proteins were measured by the Bradford method and sent to the Max Planck Institute of Molecular Cell Biology and Genetics (Dresden, Germany) for LC-MS procedure. Peptide sequences were searched against the *N. crassa* database in FungiDB to try to match the detected spectra and identify the protein using Scaffold 4 software (Proteome Software). Strict parameters were set (protein threshold > 95%, peptide threshold > 95% with at least five peptide hits) to obtain proteins identified with high confidence. We set as controls proteins identified from the wild type strain as well as from the unpurified LSP-1::GFP isolation, and compared these with the enriched fragments to identify the eisosomal proteins.

Homolog analysis of eisosomal proteins

Eisosomes were initially reported and have been best studied in *S. cerevisiae*. Until now LSP-1 is the only confidently identified eisosomal protein in *N. crassa*. As two eukaryotic model organisms, both fungi have sequenced genomics. From the *Saccharomyces* Genome Database (SGD) we obtained the DNA and protein

sequences of eisosome components in *S. cerevisiae*. By blasting against the *N. crassa* database, some eisosomal protein homologs were detected. Other bioinformatic methods such as gene ontology (GO) analysis were also performed to identify more eisosomal protein homologs in *N. crassa*. Most of the homolog proteins have conserved domains of *S. cerevisiae* eisosomal proteins.

Molecular experiments in the study

DNA isolation and DNA amplification were performed as described previously[39,41].

Gel electrophoresis was normally performed on 1% agarose at 20 V for 20 min and then the voltage was increased to 100-120 V for 1h[41].

A NucleoSpin Gel and PCR Clean-up kit (740609.50, Macherey-Nagel) was used for gel elution.

DNA restrictions were processed using endonuclease enzymes from New England BioLabs, following the manufacturer's recommendations.

USER enzyme (M5505S, New England BioLabs), CloneJET PCR cloning Kit (K1231, Thermo scientific) and T4 ligase (M0202S, New England BioLabs) were employed for cloning experiments.

Plasmid construction

The plasmids used in our study are listed in **Supplementary Table S3**. They were constructed as described previously[39].

Plasmids pQY867 and pQY868 carry the *N. crassa lsp-1* promoter which controlled the expression of the *N. crassa lsp-1::gfp* sequence and *N. crassa lsp-1::rfp* sequence respectively.

The other plasmids individually carry *gfp* tagged genes coding LSP-1 and putative eisosomal proteins detected by the LC-MS procedure and homolog analysis. The *cfp* promoter is a strong promoter from *N. crassa* and was used to control the expression

of the potential eisosomal genes fused with *egfp/trfp* in these plasmids[42]. These putative eisosomal genes in the LC-MS and homolog analysis lists were separately amplified using the oligos listed in **Supplementary Table S4**. The *egfp/trfp* fragment was amplified as previously described[39,41].

Electroporation and selection of transformants

Electroporation of *N. crassa* conidia was carried out as described previously[43]. The induction and selection of homozygous single colonies were performed in the same way as described previously[39]. All cloning and transformation experiments were conducted in accordance with the requirements of the German gene technology law (GenTG).

Construction of dual fluorescence strains

N. crassa strains of the same mating type, which individually contain GFP and RFP were cultivated in VMM + S slants at 25°C for seven days to get enough macroconidia. The spores of each strain were harvested and washed with 1 M sorbitol. Then they were counted under a microscope and their final concentrations were made to 6.5×10^7 spores/ml. One hundred μl of each conidial sample from the GFP strains were individually mixed with the same amount of conidia from the LSP-1::RFP strain. They were incubated at 25°C for 30 min and then were pipetted into VMM + S slants. The slants were incubated at 25°C in light for five to six days, during which time the spores of both fluorescence were germinating, fusing and developing into strains with dual fluorescence proteins. The conidial spores from each dual fluorescence strain were inoculated onto VMM + S thin agar plates and were cultivated briefly or were directly checked for fluorescence under the fluorescence microscope (ECLIPSE Ci system plus INTENSILIGHT C-HGFI 130w lamp, Nikon).

Microscopy

Fungi of different genotypes were incubated on thin agar plates before microscopy.

Microscope analysis was performed with a fluorescence microscope (ECLIPSE Ci system plus INTENSILIGHT C-HGFI 130 w lamp, Nikon). 40×/NA0.75 (plan fluor), 100×/NA1.30 oil (plan fluor) objective lenses were used to acquire images. Immersion oil (Type N, Nikon) was used with the oil objective lens for observation and image acquisition. Epi-Fluorescence filter G-2E/C (TRITC), EX 540/25, DM 565, BA 605/55 was used for red fluorescence. A GigE camera (DFK 23U274, Imaging Source) was used to capture photos. The acquisition software was NIS elements D basic (Nikon). Images were captured at room temperature (22 - 25°C).

Confocal fluorescence analysis was performed using a confocal laser scanning microscope (Leica, TCS SP5) and images were captured with the Leica LAS AF Lite Software. GFP was excited with 488 nm light and emission was detected at 500-550 nm, while RFP was excited with 543 nm light and emission was detected at 590-610 nm.

During each microscope experiment, including CLSM, a blank control of WT was set to make sure there was no auto fluorescence at the experimental settings.

Fluorescence and colocalization analysis

The analysis of the fluorescence and colocalization of LSP-1 and putative eisosomal proteins was performed by ImageJ software after microscopy. The fluorescence intensity profiles of GFP and RFP at the cell membrane were determined to display the degree of overlay of these dual fluorescences, which visually indicated the localization relationship of LSP-1 and other proteins. Pearson's coefficients were calculated to indicate the statistical significance of the colocalization frequency.

Gateway cloning

In our study, we modified the Gateway method and created a one-step destination vector cloning system, which is a convenient high throughput system for *N. crassa* expression studies. First, the *N. crassa* expression vector was equipped with the *attP*-

flanked DNA fragment (**supplementary Figure S2**), then inserted the *egfp* ORF behind the *attP*-flanked DNA fragment. The modified vector was used as a donor as well as an entry vector during the one-step Gateway cloning and is shown in supplementary **Figure S2**. It contains a fragment of 1618 base pairs of *his-3* sequence for the homologous recombination induced chromosomal integrations[40].The *cfp* promoter and *arg* terminator also controlled the expression of genes between them[41]. The $attP_1$/$attP_2$ flanks were necessary for the recombination reaction between the PCR product and the vector. Between the $attP_1$/$attP_2$ flanks are the chloramphenicol fragment and *ccdB* fragment for colony selection, which would all be replaced by the target genes after the cloning. The $attB_1$ and $attB_2$ linker were added in front of the forward and reverse primers of the target genes. The PCR was performed with the high fidelity *Pwo*-DNA-Polymerase (732-3262, PeqLab). The accurately amplified fragments were directly mixed with the modified vector and the BP reactions were performed using the Gateway BP Clonase (11789020, Thermo Fisher Scientific) to generate the destination plasmids. The transformation and colony selections were described above. The destination plasmids were verified by DNA sequencing.

Protein modelling and prediction

We used I-TASSER and ProFunc servers for protein modelling, and structural and functional analysis in our study. The transmembrane prediction was performed with TMHMM2.0.

References

1. Zahumensky J, Malinsky J. Role of MCC / eisosome in fungal lipid homeostasis. 2019:1-20.

2. Leon S, Teis D. Functional patchworking at the plasma membrane. 2018;(July):2-4. doi:10.15252/embj.2018100144

3. Karotki L, Huiskonen JT, Stefan CJ, et al. Eisosome proteins assemble into a membrane scaffold. *J Cell Biol*. 2011;195(5):889-902. doi:10.1083/jcb.201104040

4. Kolláth-Leiβ K, Kempken F. The fungal MCC / eisosome complex : an unfolding story. In: Anke T, Schüffler A, eds. *The Mycota XV*. Physiology. Springer International Publishing AG 2018; 2017:119-130.

5. Douglas LM, Konopka JB. Fungal membrane organization: the eisosome concept. *Annu Rev Microbiol*. 2014;68(1):377-393. doi:doi:10.1146/annurev-micro-091313-103507

6. Walther TC, Brickner JH, Aguilar PS, Bernales S, Walter P. Eisosomes mark static sites of endocytosis. *Nature*. 2006;439(7079):998-1003. doi:Doi 10.1038/Nature04472

7. Babst M. Eisosomes at the intersection of TORC1 and TORC2 regulation. 2019;(March):543-551. doi:10.1111/tra.12651

8. Walther TC, Aguilar PS, Fröhlich F, et al. Pkh-kinases control eisosome assembly and organization. *EMBO J*. 2007;26(24):4946-4955. doi:10.1038/sj.emboj.7601933

9. Grossmann G, Malinsky J, Stahlschmidt W, et al. Plasma membrane microdomains regulate turnover of transport proteins in yeast. *J Cell Biol*. 2008;183(6):1075-1088. doi:10.1083/jcb.200806035

10. Deng C, Xiong X, Krutchinsky AN. Unifying fluorescence microscopy and mass spectrometry for studying protein complexes in cells. *Mol Cell Proteomics*. 2009;8(6):1413-1423. doi:10.1074/mcp.M800397-MCP200

11. Moreira KE, Walther TC, Aguilar PS, Walter P. Pil1 controls eisosome biogenesis. *Mol Biol Cell*. 2009;20:809–818. doi:10.1091/mbc.E08

12. Scazzocchio C, Vangelatos I, Sophianopoulou V. Eisosomes and membrane compartments in the ascomycetes : A view from *Aspergillus nidulans*. 2011;4(1):64-68. doi:10.4161/cib.4.1.13764

13. Athanasopoulos A, Boleti H, Scazzocchio C, Sophianopoulou V. Eisosome distribution and localization in the meiotic progeny of *Aspergillus nidulans*. *Fungal Genet Biol*. 2013;53:84-96. doi:10.1016/j.fgb.2013.01.002

14. Vangelatos I, Roumelioti K, Gournas C, Suarez T, Scazzocchio C, Sophianopoulou V. Eisosome organization in the filamentous ascomycete *Aspergillus nidulans*. *Eukaryot Cell*. 2010;9(10):1441-1454. doi:10.1128/EC.00087-10

15. Athanasopoulos A, Gournas C, Amillis S, Sophianopoulou V. Characterization of AnNce102 and its role in eisosome stability and sphingolipid biosynthesis. *Sci Rep*. 2015;5. doi:10.1038/srep15200

16. Kabeche R, Baldissard S, Hammond J, Howard L, Moseley JB. The filament-forming protein Pil1 assembles linear eisosomes in fission yeast. *Mol Biol Cell*. 2011;22(21):4059-4067. doi:10.1091/mbc.E11-07-0605

17. Lacy MM, Baddeley D, Berro J. Single-molecule imaging of the BAR domain protein Pil1p reveals filament-end dynamics. *Mol Biol Cell*. 2016. doi:10.1101/092536

18. Olivera-Couto A, Aguilar PS. Eisosomes and plasma membrane organization. *Mol Genet Genomics*. 2012;287(8):607-620. doi:10.1007/s00438-012-0706-8

19. Bartlett K, Gadila SKG, Tenay B, Mcdermott H, Alcox B, Kim K. TORC2 and eisosomes are spatially interdependent, requiring optimal level of phosphatidylinositol 4, 5-bisphosphate for their integrity. *J Biosci*. 2015;40(2):299-311. doi:10.1007/s12038-015-9526-4

20. Foderaro JE, Douglas LM, Konopka JB. MCC / eisosomes regulate cell wall synthesis and stress responses in fungi. *J Fungi*. 2017;1(Mcc):1-18. doi:10.3390/jof3040061

21. Alvarez FJ, Douglas LM, Konopka JB. The Sur7 protein resides in punctate membrane subdomains and mediates spatial regulation of cell wall synthesis in *Candida albicans*. *Commun Integr Biol*. 2009;2(2):76-77. doi:10.1091/mbc.E08-05-0479.76

22. Zhang LB, Tang L, Ying SH, Feng MG. Two eisosome proteins play opposite roles in autophagic control and sustain cell integrity, function and pathogenicity in *Beauveria bassiana*. *Environ Microbiol*. 2017;19(5):2037-2052. doi:10.1111/1462-2920.13727

23. Seger S, Rischatsch R, Philippsen P. Formation and stability of eisosomes in the filamentous fungus *Ashbya gossypii*. *J Cell Sci*. 2011;124(10):1629-1634. doi:10.1242/jcs.082487

24. Moseley JB. Eisosomes. *Curr Biol*. 2018;28(8):R376-R378. doi:10.1016/j.cub.2017.11.073

25. Roche CM, Loros JJ, McCluskey K, Glass NL. *Neurospora crassa*: Looking back and looking forward at a model microbe. *Am J Bot*. 2014;101(12):2022-2035. doi:10.3732/ajb.1400377

26. Galagan JE, Calvo SE, Borkovich KA, et al. The genome sequence of the filamentous fungus *Neurospora crassa*. *Nature*. 2003;422(6934):859-868. doi:10.1038/nature01554

27. Seale T. Life cycle of *Neurospora crassa* viewed by scanning electron microscopy. *J Bacteriol*. 1973;113(2):1015-1025.

28. Bistis GN, Perkins DD, Read ND. Different cell types in *Neurospora crassa*. *Fungal Genet Rep*. 2003;50(1):17-19. doi:10.4148/1941-4765.1154

29. Fleißner A, Simonin AR, Glass NL. Cell fusion in the filamentous fungus, *Neurospora crassa*. *Methods Mol Biol*. 2008;475:21-38. doi:10.1007/978-1-59745-250-2_2

30. Riquelme M, Yarden O, Bartnicki-Garcia S, et al. Architecture and development of the *Neurospora crassa* hypha - a model cell for polarized growth. *Fungal Biol*. 2011;115(6):446-474. doi:10.1016/j.funbio.2011.02.008

31. Coronas-serna JM, Fernández-acero T, Molina M, Cid VJ. A humanized yeast - based toolkit for monitoring phosphatidylinositol 3 - kinase activity at both single cell and population levels. 2018;5(12):545-554. doi:10.15698/mic2018.12.660

32. Douglas LM, Wang HX, Keppler-ross S, Dean N, Konopka JB. Sur7 promotes plasma membrane organization and is needed for resistance to stressful conditions and to the invasive growth and virulence of *Candida albicans*. *MBio*. 2012;3(1):1-12. doi:10.1128/mBio.00254-11.Editor

33. Appadurai D, Gay L, Moharir A, et al. Plasma membrane tension regulates eisosome structure and function. Bassereau P, ed. *Mol Biol Cell*. December 2019:mbc.E19-04-0218. doi:10.1091/mbc.E19-04-0218

34. Busto J V., Elting A, Haase D, et al. Lateral plasma membrane compartmentalization links protein function and turnover. *EMBO J*. 2018:e99473. doi:10.15252/embj.201899473

35. Malinsky J, Opekarová M. New insight into the roles of membrane microdomains in physiological activities of fungal cells. In: *International Review of Cell and Molecular Biology*. Vol 325. Elsevier Inc.; 2016:119-180. doi:10.1016/bs.ircmb.2016.02.005

36. Zakiev ER, Sobenin IA, Sukhorukov VN, Myasoedova VA, Ivanova EA, Orekhov AN. Carbohydrate composition of circulating multiple-modified low-density lipoprotein. *Vasc Health Risk Manag*. 2016;12:379-385. doi:10.2147/VHRM.S112948

37. Bulik DA, Olczak M, Lucero HA, Osmond BC, Robbins PW, Specht CA. Chitin synthesis in *Saccharomyces cerevisiae* in response to supplementation of growth medium with glucosamine and cell wall stress. *Eukaryot Cell*. 2003;2(5):886-900. doi:10.1128/EC.2.5.886-900.2003

38. Li Y, Zhou Y, Mac Y, Li X. Design and synthesis of novel cell wall inhibitors of *Mycobacterium tuberculosis* GlmM and GlmU. *Carbohydr Res*. 2011;346(13):1714-1720. doi:10.1016/j.carres.2011.05.024

39. Kollath-Leiß K, Bönniger C, Sardar P, Kempken F. BEM46 shows eisosomal localization and association with tryptophan-derived auxin pathway in *Neurospora crassa*. *Eukaryot Cell*. 2014;13(8):1051-1063. doi:10.1128/EC.00061-14

40. Margolin BS, Freitag M, Selker EU. Improved plasmids for gene targeting at the *his-3* locus of *Neurospora crassa* by electroporation. *Fungal Genet Reports Vol*. 1997;44.

41. Mercker M, Kollath-Leiß K, Allgaier S, Weiland N, Kempken F. The BEM46-like protein appears to be essential for hyphal development upon ascospore germination in *Neurospora crassa* and is targeted to the endoplasmic reticulum. *Curr Genet*. 2009;55(2):151-161. doi:10.1007/s00294-009-0232-3

42. Temporini ED, Alvarez ME, Mautino MR, Folco HD, Rosa AL. The *Neurospora crassa cfp* promoter drives a carbon source-dependent expression of transgenes in filamentous fungi. *J Appl Microbiol*. 2004;96(6):1256-1264. doi:10.1111/j.1365-2672.2004.02249.x

43. Kumar A, Kollath-Leiß K, Kempken F. Characterization of bud emergence 46 (BEM46) protein: Sequence, structural, phylogenetic and subcellular localization analyses. *Biochem Biophys Res Commun*. 2013;438(3):526-532. doi:10.1016/j.bbrc.2013.07.103

Acknowledgments

Qin Yang appreciates financial support from the China Scholarship Council.

We appreciate the support from Dr. John Van der Meer for the copy-edit assistance of the manuscript.

Author Contributions

F.K. conceived the study. Q.Y. carried out the experiments, analyzed the data and drafted the paper.

Additional Information

Competing Interests: The authors declare that they have no competing financial or nonfinancial interests.

Supplementary Materials

Supplementary Table S1. genes and their productions in LC-MS result

gene ID (from FungiDB)	gene production
NCU07495	sphingolipid long chain base-responsive protein LSP1
NCU03647	hypothetical protein
NCU02540	meiotic expression up-regulated protein 14
NCU02120	hypothetical protein
NCU02425	PH domain-containing protein
NCU05803	translational activator
NCU07366	glucosamine-fructose-6-phosphate aminotransferase
NCU03897	RNA binding effector protein Scp160
NCU06943	SIK1
NCU02839	T-complex protein 1
NCU06544	protein kinase C-like protein
NCU09808	dynamin-1
NCU08875	Cullin binding protein CanA
NCU08699	bli-4 protein
NCU02207	T-complex protein 1 subunit beta
NCU05887	oxidoreductase
NCU09700	T-complex protein 1 subunit beta
NCU08340	ADP-ribosylation factor 1
NCU03102	40S ribosomal protein S11
NCU00410	eukaryotic release factor 1
NCU07567	T-complex protein 1 subunit theta
NCU09119	ATP synthase subunit gamma
NCU08920	ATP-binding cassette sub-family F member 2

Supplementary Table S2. strains used in our research

Strain	Genotype	Source
FGSC6103	*his-3* (Y234M723) mat A	Fungal Genetics Stock Center
FGSC9716	*his-3* (Y234M723) mat a	Fungal Genetics Stock Center
QY127-4	*NCU04809::gfp*	This study
NcT462	*lsp-1::rfp* mat a	This study
NcT475	*lsp-1::rfp* mat A	This study
NcT463	*NCU06384::gfp*	This study
NcT464	*NCU03571::gfp*	This study
NcT465	*NCU07334::gfp*	This study
NcT466	*NCU01065::gfp*	This study
NcT467	*lsp-1::gfp*	This study
NcT468	*NCU04195::gfp*	This study
NcT469	*NCU06352::gfp*	This study
NcT470	*NCU05198::gfp*	This study
NcT471	*NCU00586::gfp*	This study
NcT474	*NCU07754::gfp*	This study
NcT510	*NCU05230::gfp*	This study
NcT511	*NCU04639::gfp*	This study
NcT512	*NCU02540::gfp*	This study
NcT515	*NCU07754::gfp*	This study
NcT516	*NCU03647::gfp*	This study
NcT517	*NCU02425::gfp*	This study
NcT518	*NCU07366::gfp*	This study

Supplementary Table S3. plasmids used in the study

plasmid	inserted fragment
pAS827	*NCU05198::gfp*
pMF844	*NCU00586::gfp*
pAA846	*NCU07495::gfp*
pCE847	*NCU07754::gfp*
pBS848	*NCU06384::gfp*
pQY849	*NCU06352::gfp*
pQY853	*NCU07334::gfp*
pQY854	*NCU03571::gfp*
pQY855	*NCU04809::gfp*
pQY856	*NCU01065::gfp*
pQY857	*NCU04195::gfp*
pQY882	*NCU03647::gfp*
pQY883	*NCU07366::gfp*
pQY884	*NCU02425::gfp*
pQY885	*NCU05230::gfp*
pQY887	*NCU04639::gfp*
pQY888	*NCU02540::gfp*
pQY860	*N. crassa lsp-1 promoter*
pQY867	*lsp-1 promoter::NCU07495::gfp*
pQY868	*lsp-1 promoter::NCU07495::rfp*

Supplementary Table S4. primers used for the amplification of aim genes in our study

primer	sequence	combined fragment
FK2654	5’- GGAGACAUGGCGCGCCATGTTGTCAACCGGAGTGGAC -3’	*NCU05198*
FK2655	5’- ACAAGCCUAAAAAGCCAATCCAAAACCCATTCGAG -3’	*NCU05198*
MF2867	5’- GGAGACAUATGAACAAATCTCGTAAGTTGAT -3’	*NCU00586*
MF2868	5’- ACAAGCCUGTAGTCATCCTTGACCCT -3’	*NCU00586*
QY3213	5’- CGGGATCCCGATGCATCGAACCTACTCCATGCG -3’	*NCU07495*
QY3214	5’- CGGAATTCCTTGTACAGCTCGTCCATGCC -3’	*NCU07495*
JG2838	5’- GGAGACAUATGGGCACCGACACAAAAGGG -3’	*NCU07754*
JG2839	5’- ACAAGCCUGTGTATAGCTCCGTAACTGCCG -3’	*NCU07754*
JG2832	5’- GGAGACAUATGGGTTACACCACTCTCTGG -3’	*NCU06384*
JG2833	5’- ACAAGCCUAACACGCTCGCTATGAAAAGACTG -3’	*NCU06384*
QY2890	5’- GGAGACAUATGACGCCTGACCGAGATAGG -3’	*NCU06352*
QY2891	5’- ACAAGCCUCCAAACATCAGGCCCAAACCTTC -3’	*NCU06352*
QY2898	5’- GGAGACAUATGGCAGAGAAACTCAGCGCC -3’	*NCU07334*
QY2899	5’- ACAAGCCUGACAATCTTGCTGTCATCTGCACC -3’	*NCU07334*
QY3069	5’- TTGGCGCGCCATGAACGGAGACTTCAGCCTGT -3’	*NCU03571*
QY3070	5’- CCCAAGCTTAAAAGCAGCCCCCAACCCAT -3’	*NCU03571*
QY2914	5’- GGAGACAUATGTTCGGATTCGGCCAGCG -3’	*NCU04809*
QY2915	5’- ACAAGCCUCTGAGCAGGACTTACCTTCTTC -3’	*NCU04809*

QY2916	5’- GGAGACAUATGTCGTCCGGCCCCGTTGAA -3’	*NCU01065*
QY2917	5’ ACAAGCCUGACCTGCTTCTCAGGGTCCCT --3’	*NCU01065*
QY2912	5’- GGAGACAUATGGTGACCCAAAGTGACGAC -3’	*NCU04195*
QY2913	5’- ACAAGCCUTCGCCCACTAATCTTCTTCTCC -3’	*NCU04195*
QY3203	5’- AAAAAGCAGGCTATGGTCTCATCTACTGCGCTTACG -3’	*NCU03647*
QY3204	5’- AGAAAGCTGGGTATCCTCCTTATCAAAATTCTCCG -3’	*NCU03647*
QY3209	5’- AAAAAGCAGGCTATGTGGTACGTTAAAGAGAACCT -3’	*NCU07366*
QY3210	5’- AGAAAGCTGGGTCTCCACAGTCACCGACTTG -3’	*NCU07366*
QY3201	5’- AAAAAGCAGGCTATGATGACCGCTAGATCTCC -3’	*NCU02425*
QY3202	5’- AGAAAGCTGGGTCACTAAGCGGGGAAACGG -3’	*NCU02425*
QY3034	5’- GGAGACAUATGCTCGCCGGTTTATGTATC -3’	*NCU05230*
QY3035	5’-ACAAGCCUAACATACGACCTCGACCCCA-3’	*NCU05230*
QY3036	5’- GGAGACAUATGGAAGTGATACCCCTCATC -3’	*NCU04639*
QY3037	5’- ACAAGCCUGACGACCACCTGTGACAT -3’	*NCU04639*
QY3032	5’- GGAGACAUATGTGAGTTAGCCCACATGTAATC -3’	*NCU02540*
QY3033	5’- ACAAGCCUAACAGCAGTTGTCTGCACC -3’	*NCU02540*
QY2942	5’- CCTTAATTAAGGTGAGGACGGATGAATAAGAC -3’	*N. crassa lsp-1 promoter*
QY2943	5’-TTGGCGCGCCGGTGGATTAGGTAGTATTTATCGATTG-3’	*N. crassa lsp-1 promoter*

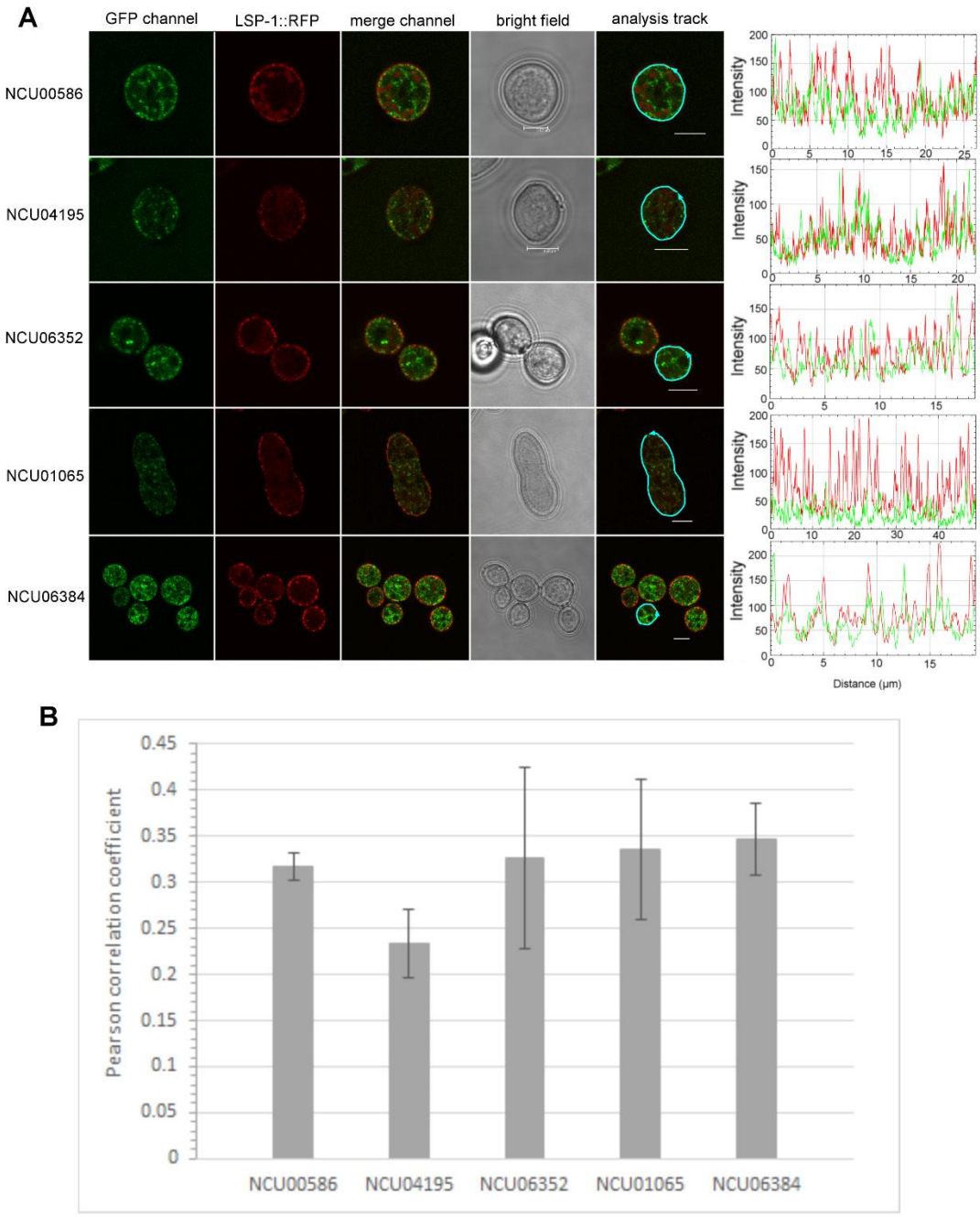

Supplementary Figure S1. Localization verification of the eisosome associated proteins identified in our study. A. The dual fluorescence colocalization analysis of LSP-1::RFP and eisosome associated proteins tagged by GFP. **B.** The Pearson correlation coefficients on the colocalization between the eisosome associated proteins and eisosomes.

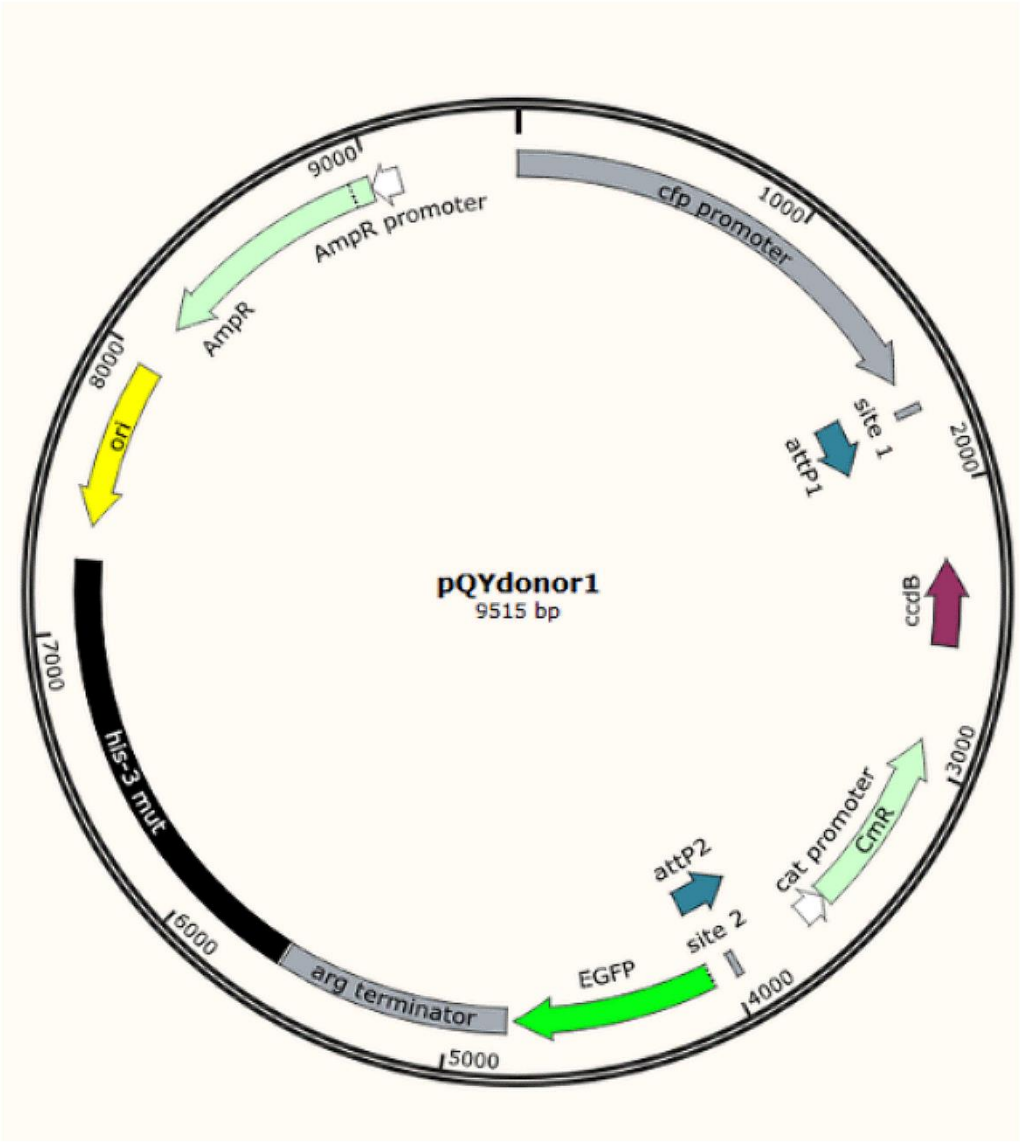

Supplementary Figure S2. The *N. crassa* expression vector used in the research.

CHAPTER IV

The cytoskeleton regulates the formation and distribution of eisosomes in *Neurospora crassa*

Qin Yang,[a] Frank Kempken[a,#]

[a]Department of Botanical Genetics and Molecular Biology

Botanical Institute and Botanic Gardens

Olshausenstr. 40

24098 Kiel

Germany

Phone: +49 431 880 4274

Fax: +49 431 880 4248

[#] author for correspondence: fkempken@bot.uni-kiel.de

Abstract

Eisosomes are stable protein complexes at the plasma membrane, with distribution patterns similar to actin patches. Their formation and how their locations are determined remain unclear. The current study discovered that the formation and distribution of eisosomes are regulated by the cytoskeleton. A disassembly of either the F-actin or the microtubules leads to eisosome localization at hyphal tips in *Neurospora crassa*, and treatment with a high concentration of the microtubule-inhibitor benomyl results in the production of filamentous eisosome patterns. The defect of the cytoskeleton caused by the disassembly of microtubules or F-actin leads to an increased formation of eisosomes.

Importance

Eisosomes have stable fluorescence patterns similar to actin patches; however, the relationships between eisosomes and the cytoskeleton have never been closely examined. The current study has established that an intact cytoskeleton is necessary for the normal localization of eisosomes. The absence of microtubules or F-actin causes eisosomes to become localized at the germ tube tips as well as at mature hyphal tips. In addition, the phenotype and overexpression of eisosomes during benomyl and latrunculin B inhibitions suggest that eisosomes help counteract the defects/cell death caused by cytoskeleton disassembly. Furthermore, eisosomes were observed to attach at the cell membrane and move with the elongation of actively growing hyphal tips. These observations bring a new insight into eisosomes, in that they appear to be capable of maintaining hyphal shape in the absence of the cytoskeleton.

Observations

Low-temperature cultivation inhibits hyphal elongation but does not influence the distribution of eisosomes.

Eisosomes have been reported to show different features during hyphal elongation in *Neurospora crassa* (*N. crassa*) (Yang et al. Eisosomes Show Different Features in Morphologically Identical Hyphae Germinating from Sexual and Asexual Spores in *Neurospora Crassa*. *Microbiological Research*, under review.). They are normally formed in macroconidial spores and the mature parts of hyphae germinated from macroconidia, whereas they are normally absent from the tips of these hyphae. In this study hyphal elongation in *N. crassa* was inhibited by various means to investigate the relationships between eisosome formation and hyphal elongation.

Low-temperature growth slows down all biological processes in *N. crassa* cells and represses the elongation of hyphae. In our study, *N. crassa* cultures at 8°C showed an obvious inhibition of hyphal elongation, while the distribution of eisosomes had no significant changes (**Figure 1**). The *N. crassa* colonies elongated 0.03 ± 0.06 cm at 8°C for 20 hours while at 20°C they elongated 1.08 ± 0.08 cm, and at 25°C 1.98 ± 0.14 cm under cultivation conditions that were the same apart from temperature and for the same duration (**Figure 1**). Despite the growth rate differences, the eisosome distribution in these *N. crassa* colonies exhibited the same features. For this study, red fluorescence protein (RFP) was used to tag the eisosomal core protein LSP-1 and thus indicate the localization of eisosomes. Our data show that the hyphal elongation inhibition caused by the low temperature had no influence on eisosome distribution (**Figure 1**). In colonies from the low-temperature treatment, as well as normal cultures, most of the fluorescent spots were detected in macroconidia, whereas the older hyphal parts (i.e. further away from the hyphal tips) usually had more fluorescent spots. In addition, there were no fluorescent spots observed at hyphal tips of these colonies. Thus, while the eisosome formation rates were repressed by low-temperature

cultivation, the distribution mechanism of eisosomes was not affected.

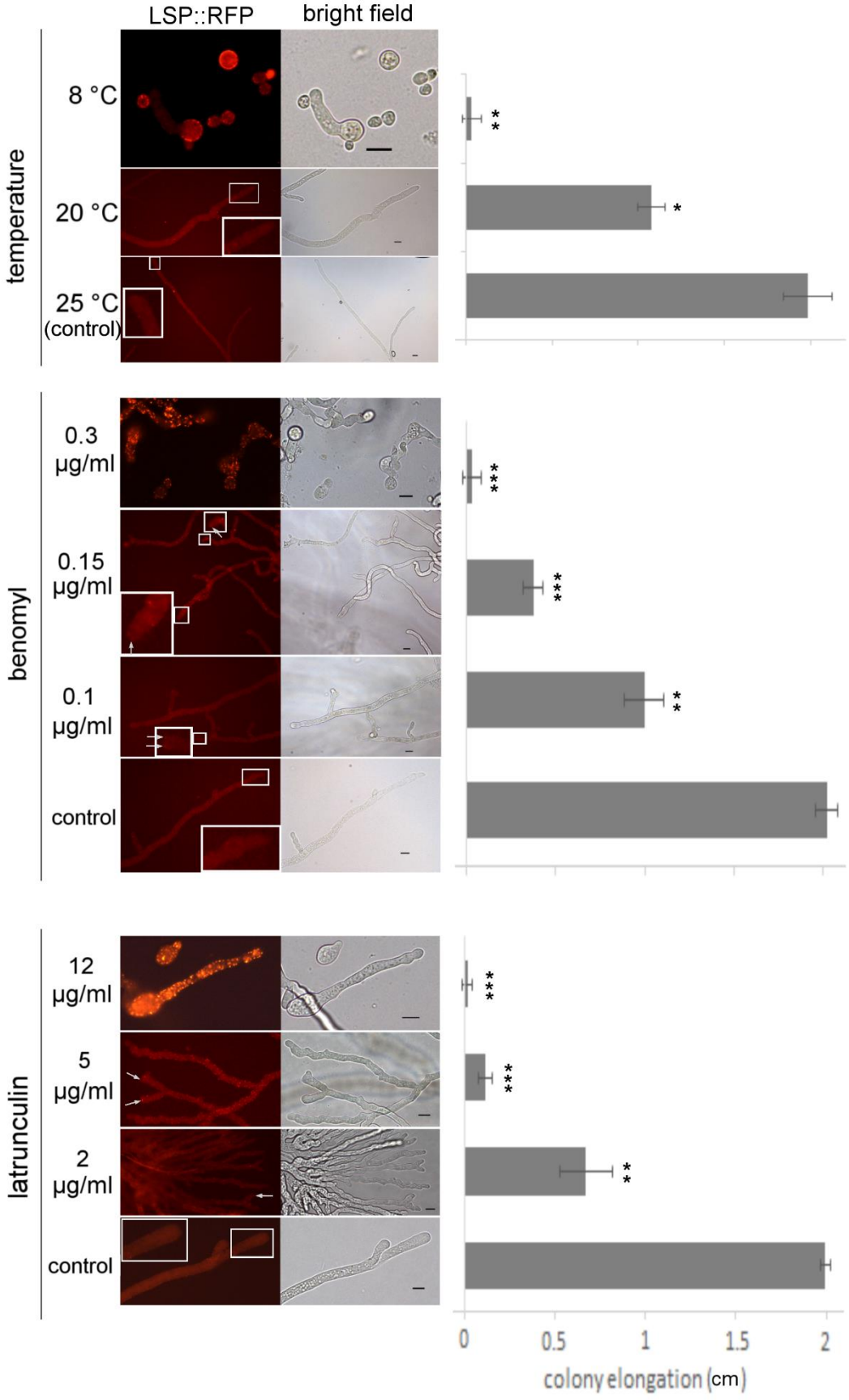

Figure 1. Hyphal elongation inhibition test using different factors. The *N. crassa* strain expressing LSP-1::RFP was cultivated at 25°C for 20h with different inhibitor treatments. The fluorescent protein tagged eisosomal core component LSP-1 was used to show the distribution and formation of eisosomes. Importantly, the background fluorescence of *N. crassa* cells in the RFP channel was negligible in our setup. The frames are the magnification of some hyphal tips and arrows indicate the fluorescent spots at the tips. They were applied to show the fluorescence details at the hyphal tips, because there were no fluorescent spots at hyphal tips in the controls and the low-temperature treatment, while there were brighter fluorescent spots at hyphal tips with the higher concentrations of benomyl and latrunculin B. The colony growth is shown on the right of each group. Mean ± SD, n = 3 experiments, statistical analysis using one-way analysis of variance (ANOVA, $P_{temperature} = 1.13 \times 10^{-6}$, $P_{benomyl} = 3.80 \times 10^{-9}$, $P_{latrunculin\ B} = 4.82 \times 10^{-9}$) with paired t-tests of each concentration/temperature and the control. Single asterisk represents $P < 0.05$, double asterisk represents $P < 0.01$, triple asterisk represents $P < 0.001$. Scale bar: 10 µm.

Benomyl changes the distribution and phenotype of eisosomes.

Benomyl has effects on microtubes/tubulin[1–3] and inhibits fungal germ tube elongation[4]. In our study, we inoculated *N. crassa* macroconidial samples on medium containing benomyl at different concentrations (0 – 0.3 µg/ml) to examine the relations between hyphal germination/elongation and eisosome distribution. The macroconidia were from a *N. crassa* strain expressing LSP-1::RFP in order to show the localization of eisosomes, since LSP-1 has been verified as a primary eisosomal component in *N. crassa* (Yang et al. Eisosomes Show Different Features in Morphologically Identical Hyphae Germinating from Sexual and Asexual Spores in *Neurospora Crassa*. *Microbiological Research*, under review.). The fungi were cultivated at 25°C for 20 hours and exhibited increased elongation suppression with increasing concentration of benomyl. The colonies growing on the medium with 0.1 µg/ml benomyl were observed to have an elongation of 1.00 ± 0.11 cm; with 0.15 µg/ml benomyl, the colonies grew 0.37 ± 0.06 cm after 20h; and using medium containing 0.3 µg/ml

benomyl, the colonies were observed to elongate only 0.03 ± 0.05 cm, whereas colonies of the control grew 2.02 ± 0.06 cm on the medium without any benomyl under the same conditions (**Figure 1**). Among the hyphae growing on the 0.1 µg/ml benomyl medium, eisosomes were detected at some hyphal tips, which was different from the control group, but the fluorescent spots at the hyphal tips were weaker than those in the older hyphal sections (**Figure 1**). The distribution of eisosomes in the macroconidial spore bodies as well as in proximal regions of the hyphae did not show any obvious differences with the control and there were still some hyphal tips without eisosomes. Considering all, the eisosome distribution changes were not distinct under low benomyl concentration. In the medium with 0.15 µg/ml benomyl, eisosomes were observed to distribute to most of the *N. crassa* hyphal tips, but the sizes and the density of the fluorescent spots remained smaller and weaker than those in other sections of those hyphae (**Figure 1**). When the benomyl concentration reached 0.3 µg/ml, the elongation of germination tubes was strongly inhibited and eisosomes were observed at the vast majority of the germination tube/hyphal tips (**Figure 1**). The difference was very significant compared to the control group. Some fluorescent spots at these hyphal tips were even bigger and brighter than normal.

In addition to the eisosome distribution changes, interesting eisosome phenotypes were observed in the high concentration (0.3 µg/ml) benomyl inhibition experiments (**Figure 2**). The fluorescence from LSP-1::RFP formed into linear structures, rather than the normal dotting distribution, in many of the strongly inhibited germinating macroconidia and germination tubes. The structure of the linear eisosomes was much bigger, and their fluorescence densities were much stronger. In addition, the filamentous phenotype tended to be found in conidial anastomosis tubes (CAT). This observation suggests that hyphal elongation and hyphal fusions are strongly related to eisosome formation and eisosome distribution via microtubules/tubulins. Considering that these are new observations, we believe that these data will add significant insights

for eisosome formation and function studies.

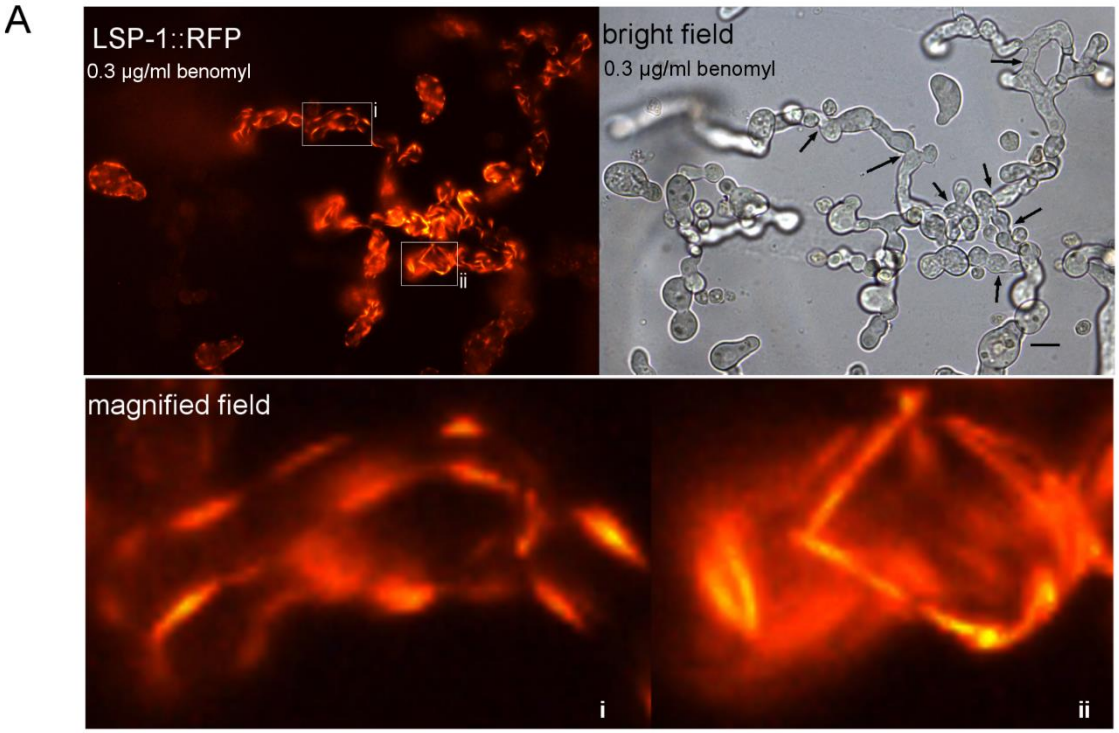

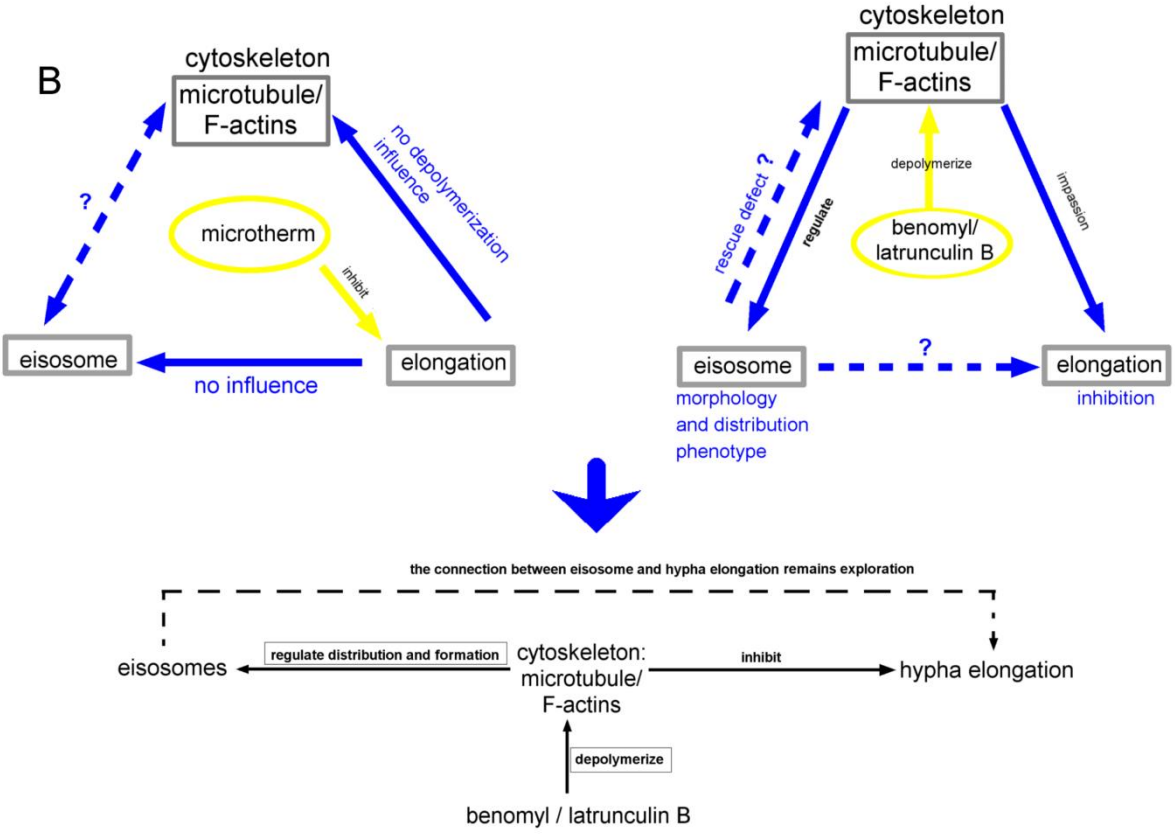

Figure 2. The filamentous eisosome phenotype caused by high concentration benomyl and the strategy of our research. A. The benomyl treatment (0.3 μg/ml) caused obvious filamentous eisosome formation phenotype. It trended to occur at the conidial anastomosis tubes (CATs). The background of *N. crassa* cells in RFP channel in our setup was negligible. **i-ii** are magnifications of the box areas, which show shape, location and fluorescence intensity details about the filamentous eisosomes. Black arrows point out the junction site of CATs. Scale bar: 10 μm. **B.** The relationships of cytoskeletons, eisosomes and hyphal elongation studied from our research. It could simply describe the conclusions of our research in a more direct and more visible way.

Latrunculin B influences the distribution of eisosomes in hyphal tips.

Latrunculin B blocks actin polymerization, which disrupts the actin cytoskeleton, inhibits hyphal elongation and leads to swelling of hyphal tips in *N. crassa*[5–8]. Eisosomes have been discovered to be absent from hyphal tips of geminated macroconidia (Yang et al. Eisosomes Show Different Features in Morphologically Identical Hyphae Germinating from Sexual and Asexual Spores in *Neurospora Crassa*. *Microbiological Research*, under review.) (**Video S1**). In the current study, a *N. crassa* strain expressing LSP-1::RFP was grown on 0 μg/ml ,2 μg/ml, 5 μg/ml, and 12 μg/ml latrunculin B medium in order to examine the connection between hyphal elongation and eisosome distribution at hyphal tips in *N. crassa*.

The fungi in each group were cultivated at 25°C. After a 20 h-cultivation, the inhibition of hyphal elongation and the swelling of hyphal tips were more obvious at the higher concentrations of latrunculin B. In the control group (no latrunculin B in the medium), the *N. crassa* colonies grew 1.99 ± 0.03 cm during the 20 h cultivation and the hyphae appeared normal (**Figure 1**). On the medium with 2 μg/ml of latrunculin B, the *N. crassa* colony growth was 0.67 ± 0.15 cm after the same cultivation time. Many moderate long branches were formed at hyphal tips, but the swelling of the tips was not obvious (**Figure 1**). In the 5 μg/ml latrunculin B group, the growth of *N. crassa* colonies was obviously inhibited to only 0.12 ± 0.04 cm and there were more but shorter branches

at most of the hyphal tips (**Figure 1**). The swelling of hyphal tips was very evident and frequently observed at this concentration of latrunculin B. Finally, on the plates containing 12 µg/ml of latrunculin B, the *N. crassa* colony growth was almost completely inhibited, with growth of just 0.02 ± 0.03 cm (**Figure 1**). Under the microscope, it was clearly evident that the germination of macroconidia and hyphal elongation were severely inhibited. Only un-germinated macroconidia and short hyphae were observed. At this high concentration of latrunculin B with strong elongation inhibition, there were fewer hyphal branches (as compared with the number of hyphal branches in treatments with lower latrunculin B concentrations in the medium). The swelling of hyphal tips was more pronounced than in the other groups, which made it difficult to distinguish between the conidial spore bodies and hyphal tips under the microscope.

The latrunculin B treatment resulted in eisosomes accumulating at hyphal tips (**Figure 1**). When there was 2 µg/ml latrunculin in the medium, eisosomes begin to appear at the hyphal tips; however, eisosomes were observed in only a few hyphal tips. In contrast to the low concentration benomyl treatment, for latrunculin B low concentration treatment, the fluorescent spots at hyphal tips were usually bigger and brighter than those of the other parts along the hyphae. As the latrunculin B concentration increased up to 5 µg/ml, many of the hyphal tips had eisosomes. The fluorescent spots along these hyphae were obviously bigger and brighter than those in the blank control and those in the low latrunculin B concentration treatments. On the medium with 12 µg/ml latrunculin B, eisosomes were observed in numerous hyphal tips, however, quite a few hyphae remained without eisosomes at their tips. The fluorescent spots along the hyphae in this group were much brighter than those in the control groups.

Actin patches and cables have been described to assemble at hyphal tips and to form caps at the tips of germ tubes in *N. crassa*[6], which are the regions without eisosomes.

In addition, actin rings precede septum formation but eventually dissipate as the septum matures[6], while eisosomes were evident at the mature septum. It appears that F-actins regulate the localization of eisosomes: under normal growing conditions eisosomes tend to localize in stable sections without F-actins, whereas are absent in the active hyphal tips having F-actins. Nevertheless, when hyphal extension was inhibited by benomyl, where F-actin organization should not be much altered at hyphal tips[7], eisosomes were observed at the inactive hyphal tips.

Eisosomes attach to the cell membrane and move with the elongation of actively growing hyphae

Eisosomes have been described as stable and static structures at the cell membrane[9,10]. In our study, eisosomes were observed to move with the elongation of actively growing hyphae (**Video S2**). The movement occurred in the section near the hyphal tip but was not observed in the mature hyphal areas, and the relative positions of these eisosomes did not obviously change. At the beginning of **Video S2** (the bright field video section), the cytoplasmic streaming is clearly observed in the actively growing hypha and other hyphae. Nevertheless, the movement only occurred in the rapidly elongating hyphae, while the eisosomes in non-growing hyphae were static. These observations indicate that the movement of eisosomes was not caused by cytoplasmic streaming but rather occurred at the cell membrane. In another words, eisosomes were attached to the cell membrane and moved with the membrane extension. The hyphal tips and sections near the tips are important for hyphal growth. It has been demonstrated that pressure is a driving force for hyphal elongation. Localized incorporation of vesicles and cell wall materials creates the characteristic tip growing form, and regulation of wall extensibility is a key element that controls the hyphal expansion rates[11]. Eisosomes have been shown to function in cation transport, which is related to cell pressure. They have also been found to be associated with

vesicle transport and cell wall synthesis (Yang et al. Multiple bioactivities of eisosomes and interspecific differences in *Neurospora crassa*, in preparation.). From the evidence above, it appears that eisosomes must have functions during hyphal elongation, such as maintaining hyphal shape, and hydrostatic pressure and thus regulate the rate of hyphal expansion.

Conclusion

The formation and distribution of eisosomes are not affected by hyphal elongation but are regulated by the cytoskeleton (microtubule and F-actins) (**Figure 2** B). Low-temperature cultivation inhibited hyphal elongation but did not change the distribution of eisosomes. In addition, there was no obvious change in phenotype of eisosomes resulting from the low-temperature treatment. When the cytoskeleton components (microtubule and F-actins) were blocked by benomyl or latrunculin B, eisosomes were observed to localize at the hyphal tips.

Apart from the distribution observations, it was found that microtubules and F-actin influence the formation and phenotype of eisosomes. The disassembly of microtubules leads to an abnormal stripe-shaped fluorescence of eisosomes and the inhibition of F-actin results in bigger and brighter fluorescent spots of eisosomes.

These observations indicate that eisosomes have connections with the cytoskeleton or could be a component of the cytoskeleton at the plasma membrane. Eisosomes are stable structures at the cell membrane and the fluorescence observations of them are quite similar to actin patches. What is more, eisosomes tend to form in stable sections of hyphae and may act as attachment sites at the plasma membrane (**Video S2**), which suggests that eisosomes have roles similar to the cytoskeleton in hyphal shape maintenance. Microtubules and F-actin are the main components of the cytoskeleton, and are important to hyphal shape maintenance and polar growth. Their disassembly

leads to higher expression of eisosomes, which could be a stress or rescue response to the cytoskeleton defect.

Eisosomes were not regulated by hyphal elongation but may play roles in hyphal regulation (**Figure 2** B). They may help maintain the shape of growing hyphae, regulate cell pressure via cation transport, and adjust the expansion rates. However, this conclusion needs confirmation and more direct evidence.

Materials and Methods

Strains

The *N. crassa* strains used in our study were derived from the histidine auxotrophic strains FGSC #6103 and 9716 (Fungal Genetics Stock Center; Kansas City, MO, USA). Two strains: NCT 507 and 508 were used in our study, which expressed LSP-1::RFP fusion protein. We constructed the two strains by transferring a *his-3* homologous recombination vector which carries the *lsp-1::rfp* fragment into the receptor strains. The coding sequence of the fused protein was integrated with the chromosomes at the his-3 loci by the 1618 base-pair homologous recombination area[12].

Media and growth conditions

In our study, the constructed *N. crassa* strains were grown using Vogel's minimal medium with 2% sucrose (4621.1, ROTH) (VMM + S) [13] while the *His*-3^{-} *N. crassa* strains FGSC #6103 and 9716 were grown on Vogel's minimal medium with sucrose with 0.02% histidine (H5659-25G, SIGMA-ALDRICH) (VMM + S + His). The transformed colonies were grown and selected on Vogel's minimal medium with 1% sorbose (4028.1, ROTH), 0.05% glucose (6887.1, ROTH), and 0.05% fructose (4981.1, ROTH) (VMM + SGF) medium. For microscope analysis, samples of the fungi were grown and checked on thin agar plates. *N. crassa* strains were cultivated at 25°C

normally, but for low-temperature analysis, conidia were cultivated on thin agar at set temperatures.

Chemical treatment

We treated *N. crassa* with fungal inhibitors benomyl (45339, Sigma-Aldrich) and latrunculin B (L5288, Sigma-Aldrich) to detect the connections between hyphal elongation and eisosome distribution at hyphal tips. Benomyl and latrunculin B were dissolved in DMSO (dimethyl sulfoxide) and stored as 1 mg/ml and 4 mg/ml stocks each. They were added into VMM + S medium respectively to get the working concentrations during the benomyl and latrunculin B experiments. For the controls of these 2 inhibitor treatments, fungi were respectively treated with DMSO under the same concentrations used in the highest working concentrations of benomyl and latrunculin B experiments. In all these experiments, DMSO was used less than 0.5% (v/v) in the medium.

Microscopy

Fungi were incubated on thin agar plates. At different time points, fungi in different developmental stages were cut out of the plates. The thin agar sections with fungi were transferred to optical slides and were investigated by microscopy. The analysis could get clear captures when the spores were covered by sterile cover slips. Perithecia were collected with a needle and squashed on the slides by the cover glass before the microscopic analysis.

A fluorescence microscope (ECLIPSE Ci system plus INTENSILIGHT C-HGFI 130w lamp, Nikon) was used for the microscope analysis in our study. We used a 40×/NA0.75 (plan fluor) objective lens to acquire images. The red fluorescence was detected with an Epi-Fluorescence filter G-2E/C (TRITC), EX 540/25, DM 565, BA 605/55 and images were captured by using an A GigE camera (DFK 23U274, Imaging

Source) at room temperature (22 - 25°C). Acquisition software NIS elements D basic (Nikon) was used for the microscope.

Fluorescence and localization analysis

ImageJ software was used to perform the fluorescence analysis of the eisosome distribution. The figures in our study were created with ImageJ software.

Acknowledgments

Qin Yang appreciates financial support from the China Scholarship Council and appreciates the support from Dr. John Van der Meer for the copy-edit assistance of the manuscript.

Author contributions

Frank Kempken conceived the project. Qin Yang prepared the samples, performed the experiments, analyzed the data, and wrote the manuscript.

References

1. Kawaratani Y, Matsuoka T, Hirata Y, Fukata N, Nagaoka Y, Uesato S. Influence of the carbamate fungicide benomyl on the gene expression and activity of aromatase in the human breast carcinoma cell line MCF-7. *Environ Toxicol Pharmacol*. 2015;39(1):292-299. doi:10.1016/j.etap.2014.11.032

2. Horio T, Oakley BR. The role of microtubules in rapid hyphal tip growth of *Aspergillus nidulans*. *Mol Biol Cell*. 2005;16(2):918-926. doi:10.1091/mbc.E04-09-0798

3. Roberts CA, Miller JH, Atkinson PH. The genetic architecture in *Saccharomyces cerevisiae* that contributes to variation in drug response to the antifungals benomyl and ketoconazole. *FEMS Yeast Res*. 2017;17(3):1-11. doi:10.1093/femsyr/fox027

4. Temperli E, Roos UP, Hohl HR. Germ tube growth and the microtubule cytoskeleton in *Phytophthora infestans*: Effects of antagonists of hyphal growth, microtubule inhibitors, and ionophores. *Mycol Res*. 1991;95(5):611-617. doi:10.1016/S0953-7562(09)80075-0

5. Silverman-Gavrila LB, Lew RR. Regulation of the tip-high [Ca2+] gradient in growing hyphae of the fungus *Neurospora crassa*. *Eur J Cell Biol*. 2001;80(6):379-390. doi:10.1078/0171-9335-00175

6. Berepiki A, Lichius A, Shoji JY, Tilsner J, Read ND. F-actin dynamics in *Neurospora crassa*. *Eukaryot Cell*. 2010;9(4):547-557. doi:10.1128/EC.00253-09

7. Heath IB, Gupta G, Bai S. Plasma membrane-adjacent actin filaments, but not microtubules, are essential for both polarization and hyphal tip morphogenesis in *Saprolegnia ferax* and *Neurospora crassa*. *Fungal Genet Biol*. 2000;30(1):45-62. doi:10.1006/fgbi.2000.1203

8. Czymmek KJ, Bourett TM, Shao Y, DeZwaan TM, Sweigard JA, Howard RJ. Live-cell imaging of tubulin in the filamentous fungus *Magnaporthe grisea* treated with anti-microtubule and anti-microfilament agents. *Protoplasma*. 2005;225(1-2):23-32. doi:10.1007/s00709-004-0081-3

9. Olivera-Couto A, Aguilar PS. Eisosomes and plasma membrane organization. *Mol Genet Genomics*. 2012;287(8):607-620. doi:10.1007/s00438-012-0706-8

10. Douglas LM, Konopka JB. Fungal membrane organization: the eisosome concept. *Annu Rev Microbiol*. 2014;68(1):377-393. doi:doi:10.1146/annurev-micro-091313-103507

11. Lew RR. How does a hypha grow? The biophysics of pressurized growth in fungi. *Nat Rev Microbiol*. 2011;9(7):509-518. doi:10.1038/nrmicro2591

12. Margolin BS, Freitag M, Selker EU. Improved plasmids for gene targeting at the *his-3* locus of Neurospora crassa</i> by electroporation. 1997;44.

13. Davis RH. *Neurospora*: contributions of a model organism. *Oxford Univ Press*. February 2000. doi:10.1017/s0016672301215080

Supplemental Material

Video S1. Eisosomes were absent from hyphal tips germinating from macroconidia. It is a Z-Stack video of 2 macroconidia producing hyphae (in the middle). All sections of these hyphae were scanned during the microscopy and there were no fluorescent spots (eisosomes) at the hyphal tips at any focal level. Arrows indicate the fluorescent spots that appear in different hyphal sections. Scale bar is shown at the beginning (bright field) of the video.

Video S2. Eisosomes in an actively growing hypha. The bright field start of this video clearly shows the cytoplasmic flows in the actively growing hypha and other inactive hyphae. Arrows point to the eisosomes, which were moving with the elongation of the actively growing hypha. The asterisk indicates the hyphal tip.

Videos are available under the following link:

https://drive.google.com/drive/folders/1RtC-J-qz-7RVaSrqK51Nhk3QjK7Kf6Uy?usp=sharing

General Discussion and Perspective

Research on eisosomes has been going on for 14 years (Walther *et al*, 2006). Eisosomes have been studied in many model organisms such as *S. cerevisiae*, and *A. nidulans.* Currently, in the well-established model fungus *N. crassa*, eisosomes are poorly understood. To learn more about eisosomes, this thesis focuses on the study of the distribution, composition, functions, and the regulation of eisosomes in *N. crassa*. This thesis provides new insights into eisosomes and helps us get a better understanding.

LSP-1 is an eisosomal marker in *Neurospora crassa*

In *N. crassa*, LSP-1 is a homologue of the primary eisosomal protein Pil1/Lsp1 (Vangelatos *et al*, 2010). However, this conclusion was drawn from the phylogenetic tree prediction and had not been confirmed by experimental approaches. In this thesis, LSP-1 has been observed for the first time to localize to the furrow-like invaginations at the plasma membrane of *N. crassa* cells. The co-localization of LSP-1 and eisosomes was also confirmed by our yeast complementary study. LSP-1 protein was recognized as an eisosomal marker and used in the study of eisosomes in *N. crassa* carried out in this work.

The core eisosomal protein Pil1 is one of the most highly expressed proteins in *S. cerevisiae* (Moseley, 2018). The expressions of its protein homologue, LSP-1 in *N. crassa*, promoted by the *lsp-1* promoter and by the strong promoter *ccg-1* (Freitag *et al*, 2004) were found to be equally strong in this work. It appears that the expression or assembly of LSP-1 during the formation of eisosomes is a key step. Additionally, it also indicates that the overexpression of LSP-1 caused by the experimental methods does not distort eisosome studies.

The studies on eisosomes in *Neurospora crassa* provide new understandings at the compositional and functional level

To date, most of the eisosomal associated proteins have been identified in *S. cerevisiae.* Based on homology analysis, some eisosome related proteins have been discovered in other fungi, such as in *A. nidulans* (Vangelatos *et al*, 2010; Scazzocchio *et al*, 2011). In this work, eisosomal fragments in *N. crassa* were enriched. The fluorescence from attached GFP (green fluorescent protein) precisely reported the presence or absence of eisosomes during the isolation and enrichment, and the western blot results confirmed the validity/success of the enrichment. The enriched eisosomal fragments were then analyzed by an LC-MS approach, which is efficient for identifying the components of eisosomes. Some of the *S. cerevisiae* eisosomal protein homologues are not co-localized with eisosomes in *N. crassa*, and at least one protein is newly recognized to be a key component of eisosomes in *N. crassa*. In addition, three transporter proteins were found partly co-localized with eisosomes, which suggests that eisosomes are dynamic complexes and presumably play roles in nutrient transporter regulation in *N. crassa*. Currently, eisosomes are broadly accepted as dynamic structures in spite of their immobility on the plasma membrane of *S. cerevisiae* cells (Douglas & Konopka, 2014; Moseley, 2018), due to the fact that the Pil1 protein has been found to exchange dynamically at the tips of eisosomes (Lacy *et al*, 2017). In addition, resent research has described eisosomes as the harbors of nutrient transporters (Appadurai *et al*, 2019). Eisosomes were found to trap or release nutrient transporters according to different growth conditions (Appadurai *et al*, 2019). It provides evidence of the dynamic composition of eisosomes, and that the dispersion of the eisosomal protein homologues and eisosomes in *N. crassa* are presumably a result of the growth conditions.

There is not much information available on the functional roles of eisosomes in filamentous fungi. Protein modelling data based on the sequence-to-structure-to-

function paradigm of the key components of eisosomes in *N. crassa* were used for functional predication in this thesis. According to the modelling analysis of the key components of eisosomes in *N. crassa*, eisosomes appear to have functions relating to Na^+/K^+ transport, glucosamine-6-phosphate synthesis, cell wall synthesis, signaling and defense response, and actin filament organization. Eisosomes have been reported to participate in cell wall synthesis in *C. albicans* (Alvarez *et al*, 2008; Wang *et al*, 2011), and *B. bassiana* (Zhang *et al*, 2017), and are associated with signaling and stress response in *S. cerevisiae* (Douglas & Konopka, 2014; Yoshikawa *et al*, 2009; Young *et al*, 2002). Intriguingly, during the silico analysis in this work, LSP-1 was found to have an annotation of a cell connection function, which is consistent with a recent study where eisosomes have been described to play roles in cER (cortical endoplasmic reticulum) and plasma membrane contacts (Qi *et al*, 2020). According to the protein modelling results in this study, eisosomes are assumed to be associated with ion transport, and glucosamine-6-phosphate synthesis. Glucosamine-6-phosphate is a precursor of glycosylation, it indicates eisosomes could presumably have a function in protein secretion and plasma membrane reorganization. N-acetylglucosamine, a derivative of Glucosamine-6-phosphate, is a component of fungal cell walls, which appears to explain that eisosomes are important in fungal cell wall synthesis (Alvarez *et al*, 2008; Wang *et al*, 2011; Zhang *et al*, 2017). In addition, both modelling analysis and experimental studies have shown that eisosomes are related to actin filament organization, because it was found in this work that the inhibition of actin filaments in *N. crassa* leads to a strong distribution defect for eisosomes.

The modelling of eisosomal key components in *Neurospora crassa* brings new insights into the structure of eisosomes

Although some key components have been identified in *S. cerevisiae* (Walther *et al*, 2006; Douglas & Konopka, 2014), *A. nidulans* (Vangelatos *et al*, 2010;

Athanasopoulos *et al*, 2013), and some other fungi (Douglas *et al*, 2013; Wang *et al*, 2016; Zhang *et al*, 2017; Moreira *et al*, 2012; Kabeche *et al*, 2011). The functions and significance of eisosomes at the cellular level are not clear. On one hand, eisosomes have been found to play roles in a wide range of biological processes (Olivera-Couto & Aguilar, 2012; Bartlett *et al*, 2015). However, the deletions of the primary eisosomal components do not lead to any obvious decrease in cellular fitness or growth fitness in many fungi, such as *S. cerevisiae* (Moseley, 2018; Olivera-Couto & Aguilar, 2012), *A. nidulans* (Vangelatos *et al*, 2010), and *Schizosaccharomyces pombe* (Kabeche *et al*, 2011). The deletions only caused defects in the formation or morphology of eisosomes (Olivera-Couto & Aguilar, 2012; Walther *et al*, 2006; Athanasopoulos *et al*, 2013; Vangelatos *et al*, 2010). On the other hand, in some other fungi, such as the pathogenic fungi *C. albicans* and *B. bassiana,* the absence of eisosomal proteins influenced cell wall synthesis and morphogenesis and led to defects in pathogenic virulence (Alvarez *et al*, 2008; Wang *et al*, 2011; Bernardo & Lee, 2010; Douglas *et al*, 2012; Zhang *et al*, 2017). The reason(s) of the differences at the functional level is unknown. According to the protein modelling analysis based on the sequence-to-structure-to-function paradigm in this work, some eisosomal proteins were found to have annotations of functions on the assembly and localization of eisosomes; whereas other eisosomal components were found to have functional annotations on cellular processes. This study brings up a new assumption: eisosome complexes are presumably composed of structural components and functional components. The structural components of eisosomes are constant, fixed proteins, whereas the functional components are variable, comprising different proteins, depending on growth conditions or developmental requirements. Deletions of the structural components result in defects limited to eisosomes, for example, the formation of eisosomes or morphological phenotypes of eisosomes (Olivera-Couto & Aguilar, 2012; Walther *et al*, 2006; Athanasopoulos *et al*, 2013; Vangelatos *et al*, 2010). Those defects influence the functional proteins of eisosome domains but cannot completely

remove the functional proteins from eisosomes. As a result, the functions of eisosomes cannot be fully blocked and in turn the fungal growth fitness might not be discernibly affected. Nevertheless, the deletion of the functional components of eisosome domains cause defects at the cellular level, affecting diverse bioactivities (Moseley, 2018; Qi *et al*, 2020; Colou *et al*, 2019; Appadurai *et al*, 2019; Zhang *et al*, 2017), polarized growth (Seger *et al*, 2011), pathogenicity (Alvarez *et al*, 2008; Wang *et al*, 2011; Bernardo & Lee, 2010; Douglas *et al*, 2012; Zhang *et al*, 2017), and perhaps some other biological processes.

The assembly of eisosomes

There is not much available information on the assembly processes of eisosomes in filamentous fungi and studying the structure-assembly of eisosomes in a well-studied filamentous fungus could be of high importance. Based on the modelling analysis of key eisosomal proteins presented here, a hypothesis about the assembly and structure of eisosome complexes is proposed. The NCU02425 protein initiates the formation of eisosomes at the plasma membrane, establishes the localization of eisosomes, and then attracts the LSP-1 and NCU02540 proteins at the appropriate cellular location. Because the NCU02425 protein has a conserved domain which belongs to PH (Pleckstrin Homology) superfamily. The PH superfamily plays roles in targeting proteins to the appropriated cellular location. In addition, during the modelling analysis, NCU02425 protein had a functional annotation of the location establishment of cellular components. The LSP-1 and NCU02540 proteins both had banana shapes and BAR (Bar-Amphiphysin-Rvs) domains (Lacy *et al*, 2017; Kabeche *et al*, 2011, 2015; Moseley, 2018) in the silico analysis. It is assumed that after being bound by NCU02425, LSP-1 and NCU02540 assemble into filaments of the half-pipe-shaped shells (Karotki *et al*, 2011; Lacy *et al*, 2017) (Figure **1**). The long filaments could bind the plasma membrane and promote the formation of curvatures with their BAR

domains (Foderaro *et al*, 2017; Karotki *et al*, 2011; Olivera-Couto *et al*, 2011; Ziółkowska *et al*, 2011; Zimmerberg & McLaughlin, 2004; Grossmann *et al*, 2008). NCU03647 appears to be another protein required for eisosome formation, because it has a conserved domain of eisosome-1 superfamily which is a prerequisite for the normal formation of eisosomes. NCU07366 is a new eisosomal component that was identified in *N. crassa* in this work. This protein is recognized to be a key eisosomal component. NCU04639 and NCU05230 are two tetraspanins, and do not appear to be involved with eisosomal formation according to the silico analysis. Nevertheless, the NCU05230 protein presumably localizes at the plasma membrane in advance of the formation of eisosomes, due to the fact that NCU05230 has an annotation of function in the establishment of cellular component localization.

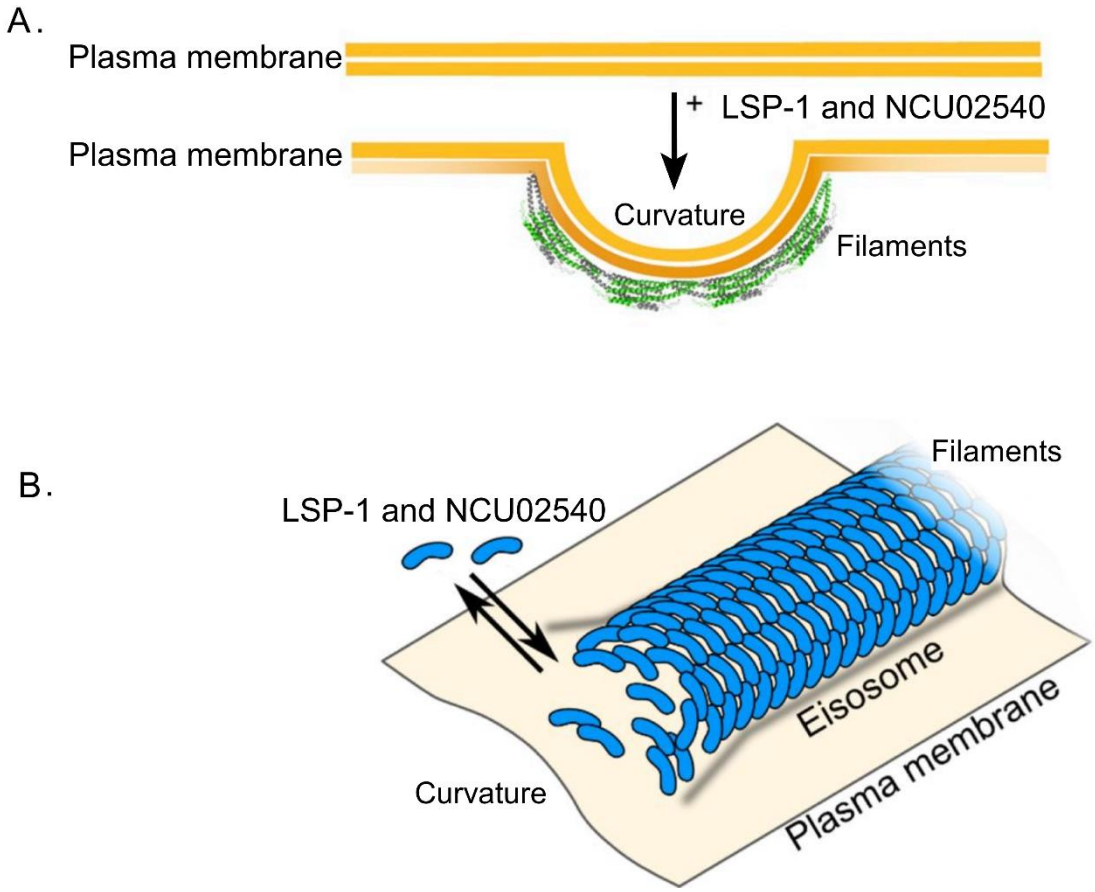

Figure 1. Model of the filaments of half-pipe-shaped shells in eisosomes. Adapted from drawing works of Karotki et al, 2011; Lacy et al, 2016. **A.** The filaments of LSP-1 and NCU02540 bind the plasma membrane and promote the formation of curvatures with their BAR domains (Karotki et al, 2011). **B.** A magnified model of the half-pipe-shaped shell filaments composed of the LSP-1 and NCU02540. The filaments are dynamically in an assembly and disassembly balance (Lacy et al, 2017).

The formation and distribution of eisosomes are regulated

The studies on the formation and distribution of eisosomes in *N. crassa* reported here, provide more interesting data than those for the unicellular model fungus *S. cerevisiae.* Eisosomes have distributional restrictions in *N. crassa* and show polar distributions during different developmental stages. Previously, it was recognized that the levels of mRNAs encoding eisosomal proteins are tenfold higher in spores than in hyphae in the filamentous fungus *Ashbya gossypii* (Seger *et al*, 2011). This suggests that the formation and localization of eisosomes are under control of unknown pathways, which is another research topic in need of investigation to obtain a better understanding of eisosomes. To date, the relationships between eisosomes and cytoskeletons remain unclear. On one hand, eisosomes were not directly related to cytoskeletons. For example, the Pil1 filaments in eisosomes appear to be independent of the actin and microtubule cytoskeletons (Kabeche *et al*, 2011), and the immobility of eisosome domains does not appear to be related to a direct connection between eisosomes and F-actin or microtubules (Kabeche *et al*, 2011; Malinska, 2004; Foderaro *et al*, 2017). On the other hand, eisosomes appear to have strong connections with cytoskeletons. In *C. albicans,* the deletion of the functional eisosomal component Sur7 led to incorrect localization of actin, while the deletion the primary eisosomal components Pil1 and Lsp1 caused defects in actin organization and morphogenesis (Wang *et al*, 2016). Furthermore, Pil1 has even been described as a novel component of the cytoskeleton in *S. pombe* (Kabeche *et al*, 2011). In this work, the regulation of the distribution of

eisosomes was explored from the relationship(s) between eisosomes and cytoskeletons. In contrast to the previous study in which the filaments composed of Pil1 were described to be independent of the actin and microtubule cytoskeletons (Kabeche *et al*, 2011), the LSP-1 in *N. crassa* is found to be associated with cytoskeletons in this work. The eisosomal distribution was found to have strong defects caused by the disassembly of F-actin and microtubules. The data indicate that F-actin and microtubules influence the localization of eisosomes. Furthermore, microtubules even clearly influence the formation of eisosomes. These data provide new insights and research directions regarding regulation of the formation and distribution of eisosome complexes.

Current situation and outlooks for research on eisosomes

To date, a complete list of eisosomal proteins does not yet exist. On one hand, the composition of eisosomes has interspecific differences in fungi. On the other hand, eisosome complexes presumably have dynamic components according to different growth conditions. Given these two situations, comparative and high throughput protein localization analysis approaches, which could be applied to different species of fungi, would be needed to fully study the composition of eisosomes. The workload would be heavy, but it would provide important data for the functional and structural studies of eisosomes.

From the perspective of cell biology, it is important to understand the structures of cellular complexes. Currently, the structure of eisosome domains remains poorly understood. Eisosomes have been observed to be furrow-like invaginations of the fungal plasma membrane at the morphological level, and hypothetical structures of these eisosomes are proposed in *N. crassa* in this study and in *S. cerevisiae* in previous studies (Foderaro *et al*, 2017; Ziółkowska *et al*, 2012; Babst, 2019).

Nevertheless, protein structural analysis approaches such as X-ray diffraction, Nuclear Magnetic Resonance (NMR), and Cryo-electron microscopy (Cryo-EM) are needed to establish the actual structures of eisosomal complexes. Such studies will help to further understand the interactions between eisosomal components, and the assembly of eisosome complexes, and will contribute to the discovery of the exact structure of eisosomes. Even so, the difficulties associated with the purification of plasma membrane proteins will need to be overcome first.

Establishing the function(s) of eisosomes is the ultimate goal of studies on these complexes. It is also the most challenging and intriguing part of eisosome studies. In some fungi, such as *S. cerevisiae* and *A. nidulans*, deletions of the primary eisosomal components did not to lead to any defects in growth or morphological fitness (Olivera-Couto & Aguilar, 2012; Walther *et al*, 2006; Athanasopoulos *et al*, 2013; Vangelatos *et al*, 2010). In some other fungi, such as the pathogenic fungi *C. albicans* and *B. bassiana,* the absence of eisosomal proteins influenced cellular processes and led to defects in pathogenic virulence (Alvarez *et al*, 2008; Wang *et al*, 2011; Bernardo & Lee, 2010; Douglas *et al*, 2012; Zhang *et al*, 2017). This difference raises questions about the importance of eisosome domains to cell growth and cellular bioactivities, as well as the major or most significant function(s) of eisosomes. However, the evidence supporting many of the proposed functions remains indirect and more work is needed to gather the data that would answer the questions.

Compared with the composition and function(s) of eisosomes, the regulation pathways behind the formation and localization of eisosomes, the interactions between eisosomes and other cellular structures, and the applied studies searching for effective treatments against the pathogenic fungi through eisosomes are even less known and still need to be better studied and understood.

With the on-going developments, innovative research approaches will be applied to the study of eisosomes. As complex domains at the plasma membrane, fully understanding the significant function(s) of eisosomes as complete structures might be the primary goal of new studies. Additionally, new eisosomal components might be identified and the structure of eisosomes will probably become fully established. The regulation pathway(s)/mechanism(s) behind the formation and distribution of eisosomes will be further identified in the future, which will help us understand how eisosomes assemble at the plasma membrane.

It is hypothesized in this thesis that there are more microdomains at the cell membrane than we have recognized to date. These microdomains must be significantly important for the multiple functions of the cell membrane; thus, the continuing study of the cell membrane domains would be of great interest. Understanding, in detail, the microdomains of and at the plasma membrane is a worthy challenge to help us further understand the biological activities in a living cell. Studies on eisosome complexes could be the key to that understanding.

References

Alvarez FJ, Douglas LM, Rosebrock A & Konopka JB (2008) The Sur7 protein regulates plasma membrane organization and prevents intracellular cell wall growth in *Candida albicans*. **19:** 5214–5225

Appadurai D, Gay L, Moharir A, Lang MJ, Duncan MC, Schmidt O, Teis D, Vu TN, Silva M, Jorgensen EM & Babst M (2019) Plasma membrane tension regulates eisosome structure and function. *Mol. Biol. Cell***:** mbc.E19-04-0218

Athanasopoulos A, Boleti H, Scazzocchio C & Sophianopoulou V (2013) Eisosome distribution and localization in the meiotic progeny of *Aspergillus nidulans*. *Fungal Genet. Biol.* **53:** 84–96

Babst M (2019) Eisosomes at the intersection of TORC1 and TORC2 regulation. *Traffic* **20:** 543–551

Bartlett K, Gadila SKG, Tenay B, Mcdermott H, Alcox B & Kim K (2015) TORC2 and eisosomes are spatially interdependent, requiring optimal level of phosphatidylinositol 4, 5-bisphosphate for their integrity. *J. Biosci.* **40:** 299–311

Bernardo SM & Lee SA (2010) Candida albicans SUR7 contributes to secretion, biofilm formation, and macrophage killing. *BMC Microbiol.* **10:** 133

Colou J, N'Guyen GQ, Dubreu O, Fontaine K, Kwasiborski A, Bastide F, Manero F, Hamon B, Aligon S, Simoneau P & Guillemette T (2019) Role of membrane compartment occupied by Can1 (MCC) and eisosome subdomains in plant pathogenicity of the necrotrophic fungus Alternaria brassicicola. *BMC Microbiol.* **19:** 295

Douglas LM & Konopka JB (2014) Fungal membrane organization: the eisosome concept. *Annu. Rev. Microbiol.* **68:** 377–393

Douglas LM, Wang HX, Keppler-ross S, Dean N & Konopka JB (2012) Sur7 promotes plasma membrane organization and is needed for resistance to stressful conditions and to the invasive growth and virulence of *Candida albicans*. *MBio* **3:** 1–12

Douglas LM, Wang HX & Konopka JB (2013) The MARVEL domain protein Nce102 regulates actin organization and invasive growth of *Candida*. *MBio* **4:** 1–12

Foderaro JE, Douglas LM & Konopka JB (2017) MCC / eisosomes regulate cell wall synthesis and stress responses in fungi. *J. Fungi* **1:** 1–18

Freitag M, Hickey PC, Raju NB, Selker EU & Read ND (2004) GFP as a tool to analyze the organization, dynamics and function of nuclei and microtubules in *Neurospora crassa*. *Fungal Genet. Biol.* **41:** 897–910

Grossmann G, Malinsky J, Stahlschmidt W, Loibl M, Weig-Meckl I, Frommer WB, Opekarová M & Tanner W (2008) Plasma membrane microdomains regulate turnover of transport proteins in yeast. *J. Cell Biol.* **183:** 1075–1088

Kabeche R, Baldissard S, Hammond J, Howard L & Moseley JB (2011) The filament-forming protein Pil1 assembles linear eisosomes in fission yeast. *Mol. Biol. Cell* **22:** 4059–4067

Kabeche R, Howard L & Moseley JB (2015) Pil1 cytoplasmic rods contain bundles of crosslinked tubules. *Commun. Integr. Biol.* **8:** 1–6

Karotki L, Huiskonen JT, Stefan CJ, Ziółkowska NE, Roth R, Surma MA, Krogan NJ, Emr SD, Heuser J, Grünnewald K & Walther TC (2011) Eisosome proteins assemble into a membrane scaffold. *J. Cell Biol.* **195:** 889–902

Lacy MM, Baddeley D & Berro J (2017) Single-molecule imaging of the BAR-domain protein Pil1p reveals filament-end dynamics. *Mol. Biol. Cell* **28:** 2251–2259

Malinska K (2004) Distribution of Can1p into stable domains reflects lateral protein segregation within the plasma membrane of living *S. cerevisiae* cells. *J. Cell Sci.* **117:** 6031–6041

Moreira KE, Schuck S, Schrul B, Fröhlich F, Moseley JB, Walther TC & Walter P (2012) Seg 1 controls eisosome assembly and shape. *J. Cell Biol.* **198:** 405–420

Moseley JB (2018) Eisosomes. *Curr. Biol.* **28:** R376–R378

Olivera-Couto A & Aguilar PS (2012) Eisosomes and plasma membrane organization. *Mol. Genet. Genomics* **287:** 607–620

Olivera-Couto A, Grana M, Harispe L & Aguilar PS (2011) The eisosome core is composed of BAR domain proteins. *Mol. Biol. Cell* **22:** 2360–2372

Qi A, Ng E, Yunn A, Ng E, Qi A, Ng E, Yunn A, Ng E & Zhang D (2020) Plasma membrane furrows control plasticity of ER-plasma membrane furrows control plasticity of ER-PM contacts. *CellReports* **30:** 1434-1446.e7

Scazzocchio C, Vangelatos I & Sophianopoulou V (2011) Eisosomes and membrane compartments in the ascomycetes : A view from *Aspergillus nidulans*. *Communicative & Integrative Biology* **4:** 64–68

Seger S, Rischatsch R & Philippsen P (2011) Formation and stability of eisosomes in the filamentous fungus *Ashbya gossypii*. *J. Cell Sci.* **124:** 1629–1634

Vangelatos I, Roumelioti K, Gournas C, Suarez T, Scazzocchio C & Sophianopoulou V (2010) Eisosome organization in the filamentous ascomycete *Aspergillus nidulans*. *Eukaryot. Cell* **9:** 1441–1454

Walther TC, Brickner JH, Aguilar PS, Bernales S & Walter P (2006) Eisosomes mark static sites of endocytosis. *Nature* **439:** 998–1003

Wang HX, Douglas LM, Aimanianda V, Latgé J-P & Konopka JB (2011) The *Candida albicans* Sur7 protein is needed for proper synthesis of the fibrillar component of the cell wall that confers strength. *Eukaryot. Cell* **10:** 72–80

Wang HX, Douglas LM, Veselá P, Rachel R, Malinsky J & Konopka JB (2016) Eisosomes promote the ability of Sur7 to regulate plasma membrane organization in *Candida albicans*. *Mol. Biol. Cell* **27:** 1663–1675

Yoshikawa K, Tanaka T, Furusawa C, Nagahisa K, Hirasawa T & Shimizu H (2009) Comprehensive phenotypic analysis for identification of genes affecting growth under ethanol stress in *Saccharomyces cerevisiae*. *FEMS Yeast Res.* **9:** 32–44

Young ME, Karpova TS, Brügger B, Moschenross DM, Wang GK, Schneiter R, Wieland FT & Cooper JA (2002) The Sur7p family defines novel cortical domains in *Saccharomyces cerevisiae*, affects sphingolipid metabolism, and is involved in sporulation. *Mol. Cell. Biol.* **22:** 927–934

Zhang LB, Tang L, Ying SH & Feng MG (2017) Two eisosome proteins play opposite roles in autophagic control and sustain cell integrity, function and pathogenicity in *Beauveria bassiana*. *Environ. Microbiol.* **19:** 2037–2052

Zimmerberg J & McLaughlin S (2004) Membrane curvature: How BAR domains bend bilayers. *Curr. Biol.* **14:** 250–252

Ziółkowska NE, Christiano R & Walther TC (2012) Organized living: formation mechanisms and functions of plasma membrane domains in yeast. *Trends Cell Biol.* **22:** 151–158

Ziółkowska NE, Karotki L, Rehman M, Huiskonen JT & Walther TC (2011) Eisosome-driven plasma membrane organization is mediated by BAR domains. *Nat. Struct. Mol. Biol.* **18:** 854–856

Acknowledgements

First and foremost, I would like to thank my supervisor Prof. Dr. Frank Kempken. Thank you for giving me the opportunity of doing my PhD in your lab. Your professional guidance and inspirations motivated me to think out of the box and helped me move forwards when I met difficulties and obstacles in my research projects. Your insights were the lighthouse that gave me directions on my route to become a scientist and paved ways for my personal growth. Your great support and encouragements made me become more confident and provided me with the momentum to finish this work.

I am also very grateful for the help and support from the exam committee! Thank you for your professional judgements on this work.

I would also like to dedicate my sincere gratitude to Prof. Dr. John P van der Meer for helping me copy edit my manuscripts. I learned a great deal from you. Your deep passion for science as well as your work ethic often inspire me and showed me the true value of dedication, perseverance and enthusiasm.

A big thank you to all of the present and past members of our lab: Hanna Schmidt, Krisztina Kollath-Leiß, Stefanie Grüttner, Hossein Emami, Abhishek Kumar, Puspendu Sardar, and Pradeep Phule. During the last four years, you gave me a lot of support and we've had a lot of interesting discussions. I feel very lucky to have met you and it was great working with you!

A special thank to my family and my wife Danni, who supported me whole-heartedly and inspired me to be a better version of myself. You were my cornerstone. Without you, I wouldn't have been the person that I am today.

Another big thank goes to Mr. Cay Kruse from the Center of Microscopy (Zentrale Mikroskopie im Biologiezentrum der Christian-Albrechts-Universität zur Kiel) for the support of various microscopic technologies, I learnt a lot form you. Thank you for your detailed explanation. It helped me a lot and was a great boost for my research, as I was then able to capture, record and analyse the experiment results by myself.

I want to also thank everyone who has helped me throughout my life. It's your favors that have kept me going on.

Declaration

I, **Qin Yang**, hereby declare that:

- apart from my supervisor’s guidance, the content and design of my dissertation is the product of my own work. Specific aspects of my thesis were supported by my colleagues; their contribution is specified in detail in ‘Author’s Contributions'.

- The thesis has not been submitted elsewhere partially or wholly as part of a doctoral degree to another examine body but indicated parts of the thesis have been submitted for publishing.

- The thesis has been prepared subject to the Rules of Good Scientific Practice of the German Research Foundation.

- My academic degrees have never been withdrawn.

Signature: _____